FINAL TECHNICAL REPORT
(2003)

CONTRACT N° : FIKW-CT-2000-00035

PROJECT N° :

ACRONYM : ACTAF

TITLE : Aquatic Chemistry and Thermodynamics of Actinides and Fission Products Relevant to Nuclear Waste Disposal

PROJECT CO-ORDINATOR: Forschungszentrum Karlsruhe GmbH (FZK)

PARTNERS :
Forschungszentrum Rossendorf (FZR)
Paul Scherrer Institut (PSI)
Royal Institute of Technology (KTH)
Universitat Politecnica Catalunya (UPC)
Kobenhavn Universitet (KU)
Enterpris Ltd, (EP)
Centro de Investigaciones Energéticas, Medioambientales y Tecnológicas (CIEMAT)

REPORTING PERIOD : FROM 01.09.2000 TO 31.08.2003

PROJECT START DATE : 01.09.2000 DURATION : 3 years

Date of issue of this report : 23.04.2004

Project funded by the European Community under the 'EURATOM' Programme (1998-2002)

Forschungszentrum Karlsruhe
in der Helmholtz-Gemeinschaft

Aquatic Chemistry and Thermodynamics of Actinides and Fission Products Relevant to Nuclear Waste Disposal (ACTAF)

Final Report

23.04. 2004

This document has been prepared by Forschungszentrum Karlsruhe GmbH, Institute for Nuclear Waste Disposal (INE) under the terms of the European Commission Contract No. FIKW-CT-2000-00035

Authors: Reinhardt Klenze, Horst Geckeis

1. Table of Contents 5

2. Executive Summary 7

3. Objectives and Strategic Aspects 9

4. Synthesis Report 10

5. Scientific and Technical Description of the Results 16

5.1 Work-package 1: Thermodynamics of aquatic actinides: Experiments to improve the database of unknown or uncertain data 16

5.1.1 Solubility, colloid formation, hydrolysis and carbonate complexation of tetravalent actinides 17

5.1.2 Complexation of actinides with small organic ligands 22

5.1.3 Complexation with minor ligands 26

5.1.4 Redox behaviour of actinides 27

5.1.5 Computational actinide chemistry 29

5.2 Work-package 2: Thermodynamics of solid-water interface reactions (sorption phenomena) 31

5.2.1 Sorption of uranium and plutonium onto iron metal oxides 32

5.2.2 Sorption of Eu(III), Cm(III) and U(VI) onto clay minerals 35

5.2.3 Sorption of U(VI) onto rock-forming mineral phases 42

5.2.4 Spectroscopic study on surface interaction mechanism for actinides 46

5.3 Work-package 3: Thermodynamics of secondary phase formation 50

5.3.1 Formation of solid solutions of actinides with calcite 51

5.3.2 Formation of solid solutions of radionuclides with barite, phosphate minerals and CSH phases 60

6. Assessment of Results and Conclusions 67

7. ANNEX 70

7.1 List of contact persons of the partner organisations 70

7.2 Glossary 71

7.3 List of ACTAF publications 72

7.4 Copies of original ACTAF publications (separate document)

2. Executive Summary

Objectives
The project aims to improve the scientific basis for the assessment of performance and safety in waste management. It is providing fundamental knowledge about the behaviour of actinides and fission products in natural aquatic systems. The project focuses on key areas where further research is essential, including: i) understanding of the mechanisms that govern the interaction of actinides and fission products in natural aquatic systems; ii) closing existing gaps in the available thermodynamic database; and iii) reducing uncertainties in currently used thermodynamic constants.

Challenges to be met
The investigations were focus on the following key issues:

Thermodynamics of aquatic actinides. To eliminate the most serious deficiencies in the thermodynamic database for the actinides, the following chemical reactions have been studied: hydrolysis and complexation of tetravalent ions, ternary complex formation, phosphate complexation and the redox behaviour of actinides.

*Thermodynamics of solid-water interface reaction :*To provide a thermodynamic basis for the quantification of sorption reactions of actinide ions onto mineral phases, the reactions at the solid-water interface have been studied for mineral phases such as goethite, magnetite, alumina, silica, clay and rock-forming minerals. A spectroscopic study on the sorbed species was aimed to provide molecular-level process understanding for the validation of thermodynamic sorption models.

Thermodynamic properties of secondary solid phases. The formation of secondary solid phases is considered to be one of the key processes for the immobilisation of radionuclides in the environment, but is not well understood jet. To develop basic understanding of the incorporation mechanism of actinides into the bulk matrix the study is focussed on calcite as a model mineral. In a addition other relevant secondary phases such as phosphates have been included in this study.

To tackle the challenging problems classical wet-chemistry methods were combined with various laser and synchrotron based spectroscopic speciation tools. Quantum chemical methods have been proven as very powerful and reliable to predict the properties of actinide complexes.

Achievements

In all the working fields notable progress has been achieved during the project, which is documented in a high number of original publications. Only few highlights are summarized below.

A notable breakthrough has been achieved filling serious gaps in the database for the solubility, hydrolysis and carbonate complexation of tetravalent actinides, necessary to predict the geochemical behaviour of e.g., plutonium. The understanding of actinide complexation with small organic ligands, which may serve as model compound for natural organic matter, has been substantially increased using various spectroscopic methods and theoretical approaches. Computational methods have been applied for the first time to chemical problems related to nuclear waste disposal. It is envisaged that these tools will play an important role for future investigations on the coordination chemistry and thermodynamic of actinides in natural aquatic systems.

The cooperation of different laboratories with expertise in either spectroscopic actinide speciation or profound experience in modelling surface sorption reactions provided an improved understanding of actinides interaction at the mineral/groundwater interface. Mechanistic insight into the sorption of U(VI) on iron oxides including surface enhanced redox reactions has been achieved as well as the elucidation of the speciation of trivalent actinides sorbed onto alumina and clay minerals. The first application of the grazing incidence X-ray absorption spectroscopy (GIXAFS) and TRLFS represents a huge step forward towards the spectroscopic characterisation of surface sorbed actinides at even trace concentration level. For the prediction of the U(VI) sorption onto rock minerals (phyllite and granite), a 'composite' model has been parameterised successfully using sorption data derived for the mineralogical rock constituents.

The combination of wet chemical methods, surface analysis and spectroscopic techniques available in the different laboratories of the project partners helped in improve the basic understanding of solid solution formation of trivalent actinides with calcite, which was studied as model mineral phase. Two different actinide species could be identified by laser spectroscopy, at least one of them is incorporated into the bulk structure. Based on a comprehensive set of sorption data obtained by coprecipitation experiments the solid solution formation was modelled for various charge compensation mechanisms. A number of mechanisms and possible species could be excluded. Thus a big step forward to the understanding of the underlying processes was made, even if a final model consistent with all sorption and spectroscopic results is still missing. Important results have also been obtained for the solid solution formation of radionuclides with other mineral phases, such as barite, phosphates and calcium silicate hydrates (CSH). The latter secondary phase is formed by cement degradation. The results gained in the ACTAF project indicate that inclusion in secondary phases can lead to a strong actinide retention in the repository or the surrounding geosphere.

3. Objectives and Strategic Aspects

Socio-economic objectives. Maintaining and improving a competitive European industry is requiring stable energy policies within the community. The strategic relevance of this project is directly related to present and future energy policies within Europe. A pre-requisite for political decisions, is a clear idea of the possible energy options available, their technical feasibility, cost, environmental impact and public acceptance. Nuclear energy will be one of these options only if Europe is able to maintain a high level of expertise and competence on nuclear energy and safety, and if public acceptance of waste disposal can be obtained. Assessment of the long-term safety of nuclear waste disposal must be based on scientific understanding of the key safety-determining processes. The focus of the ACTAF project is on issues of this type. The scientific community provides, through open publication and peer review, an independent forum for discussion, verification and validation of scientific results. This is of key importance for confidence building and acceptance both within the scientific community and in the community at large.

The present project involves co-operation between four large research institutes, several universities and a SME. In addition to being an efficient organisation for multi-disciplinary work, this network is providing young scientists with the possibility to use state-of-the-art equipment, which is not generally available, and to get accustomed to present problem-solving approaches on an international basis. This will not only broaden their technical competence, but should also foster their scientific development by co-operation with scientists from other cultures and by exposure to different scientific environments and traditions.

Large scale socio-economic systems need be accepted by the majority of the community. Well-executed and presented scientific basis for nuclear waste management is a prerequisite for public acceptance of nuclear energy and thereby for political decisions. The ACTAF project is improving discussion of future energy options on a factual basis.

Scientific/technological objectives.

The objectives of the ACTAF project are to improve the geochemical basis for the performance assessment of nuclear waste and spent fuel disposal by experiments and model development. The project is directly linked to performance assessment.

The ACTAF project will provide a fundamental understanding of key processes that will help to demonstrate the technical feasibility of geological disposal of radioactive waste and spent fuel. By investigating the basic physico-chemical processes to be expected in the various barrier systems, the project will provide data useful for the selection of management strategies. Safety and performance assessment models may be simplistic in the sense that detailed molecular features of the system must be lumped together into operational parameters. Therefore, it is of particular importance that the simplifications are based on the scientific understanding of the underlying phenomena and estimates are given for the uncertainties in the simplifications. The project will provide such scientific justification for the use of resulting approximate operational parameters that are directly relevant to repository safety assessment studies.

This project will enhance the existing international co-operation in ongoing database activities, e.g. the NEA-Thermodynamic Database or the Sorption Forum Project. In contrast to these activities, the project includes a very strong experimental component, as well as direct interactions between experimentalists and modellers. The research project is aimed at nuclear waste issues. Due to its generic nature the results are useful also in other contexts, and in particular when addressing other types of environmental problems.

4. Synthesis Report

Introduction

The project started 01.09.2000 and had a duration of three years. The present report comprises the results obtained within the full project duration. Earlier obtained achievements reported in two progress reports (01.09.2000-31.08.2001 and 01.09.2001 – 31.08.2001) are included.

Research on actinide chemistry has been already subject of previous EU research programmes as e.g. MIRAGE (European Network on the Migration of Radionuclides through the Geosphere, 1983-1995). The importance of gaining insight into the geochemistry of fission products and actinides and to create quantitative data sets within European cooperation networks is considered high. The ACTAF project is a direct consequence of a preceding concerted action entitled "Joint European Thermodynamic Database for Environmental Modelling - JETDEM" and published in the Nuclear Science and Technology series under EUR 1913 1EN (Kim, et al. 2000). Within JETDEM a number of requirements and open questions have been identified. These requirements are related to the needs of generating a consistent thermodynamic database for actinide and fission product geochemistry and the understanding of fundamental geochemical aspects appropriate to be used for the performance and safety assessment in nuclear waste disposal.

ACTAF aims to improve the scientific basis for the assessment of performance and safety in waste management. It is providing fundamental knowledge about the behaviour of actinides and fission products in natural aquatic systems. The project focuses on key areas where research is essential, including: i) understanding of the mechanisms that govern the interaction of actinides and fission products in natural aquatic systems; ii) closing existing gaps in the available thermodynamic database; and iii) reducing uncertainties in currently used thermodynamic constants. Investigations focus on the following key issues: the thermodynamics of aquatic actinide ions, the interaction of actinides and fission products at the solid/aqueous solution interface, and the thermodynamics of secondary solid phases.

The state-of-the-art with respect to thermodynamic data of actinides as was identified by the JETDEM concerted action is summarized in Fig. 1 (Kim et al., 2000; Kim, 1999). Among the actinide ions, knowledge was poor for ternary complexes, interface reactions, solid solutions and all processes of ions in the tetravalent oxidation state. As also shown in this figure, considerable progress has been made in all these previous problem areas by the ACTAF project.

The following final report provides an overview on the achieved results broken into the individual work packages. It should, however, be noted that details on the scientific output is rather available from the published papers. The ACTAF group produced an unforeseen number of publications in peer-reviewed international journals. A compilation of these papers is printed as an Annex to the present Final Report in a separate volume. It has to be furthermore mentioned that a part of the thermodynamic data developed during the present project has been already implemented into an update of the international OECD, NEA thermodynamic data base (Guillaumont et al., 2003).

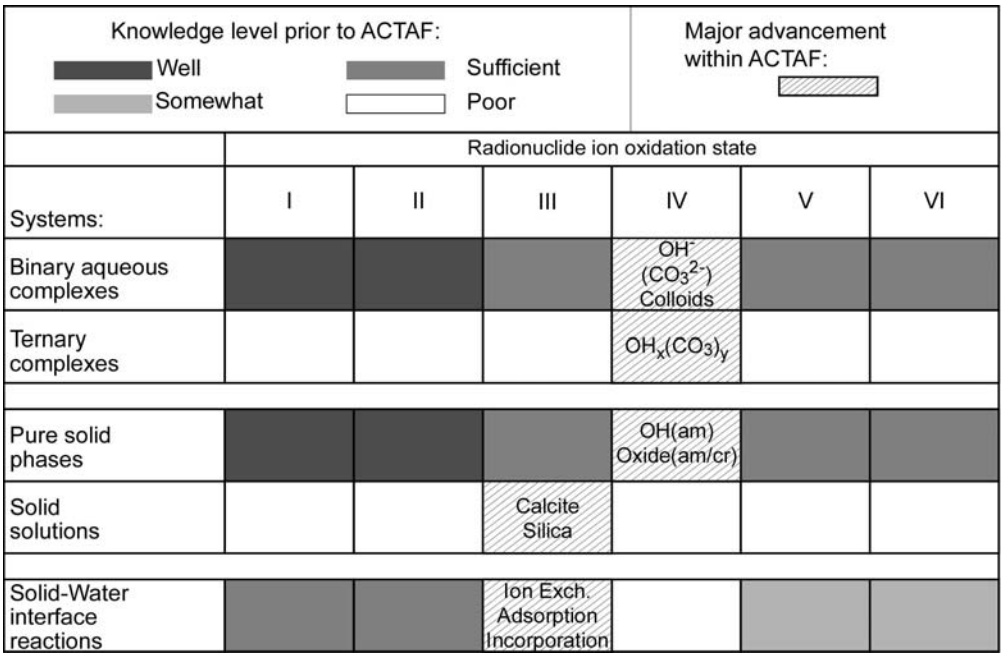

Fig. 1: Comparison of knowledge level prior to and after the ACTAF project. Description of the situation prior to the ACTAF project was elucidated within the JETDEM project and summarized by Kim et al, 2000 and Kim, 1999.

Description of work

According to the key issues the project is structured into three work packages:

Thermodynamics of aquatic actinides

To eliminate the most serious deficiencies in the thermodynamic database for the actinides, the following chemical reactions are being studied: hydrolysis and complexation of the tetravalent ions, formation of ternary complexes, complexation with phosphate, and actinide redox behaviour. To tackle these problems, classical wet-chemistry methods are combined with highly sensitive laser spectroscopic tools. In co-operation with theoretically oriented groups out-side the ACTAF consortium semi-empirical and more direct theory-based methods for the prediction of chemical behaviour in actinide systems are being developed and applied.

Thermodynamics of solid-water interface reactions

To provide a thermodynamic basis for the quantification of sorption reactions of actinide ions onto mineral phases, the reactions at the solid-water interface are being studied by a combination of classical wet-chemistry and direct speciation methods. The species of U(VI), Cm(III) and Ln(III) at the solid-water interface for simple model mineral phases (e.g., alumina, silica, goethite, magnetite, illite, etc) are being characterised and quantified by e.g., laser fluorescence spectroscopy (TRLFS) and X-ray absorption fine structure spectroscopy (EXAFS). Based on this molecular-level process understanding, appropriate thermodynamic sorption models will be developed. A composite approach is generated for the description of U(VI) sorption to natural rock.

Thermodynamic properties of secondary solid phases

The formation of secondary solid phases is considered to be one of the key processes for the immobilisation of radionuclides in the environment. The mechanisms by which a radionuclide is bound to a mineral are of fundamental importance and at present, not well understood. To

develop basic process understanding and data for the impact of secondary solid phase generation, the study is focussed on calcite and the phosphate minerals. As an important secondary phase generated during cement corrosion hydrated Ca-silicate phases (CSH) have also been considered. Surface sensitive spectroscopic and nanoscopic techniques are being used in combination with wet-chemistry and radioanalytical methods.

The main achievements of the ACTAF project are summarised below for each of the work packages. According to the ACTAF working plan the work packages are further subdivided into tasks. As however, the achieved results in the various research areas are not distributed evenly, the tasks have been rearranged with respect to the original working plan.

Work package 1: Thermodynamics of aquatic actinides: Experiments to improve the database of unknown or uncertain data

Solubility, colloid formation, hydrolysis and carbonate complexation of tetravalent actinides. The activities within the ACTAF project were focussed on experiments to improve the database on these reactions, which are most important with regard to the geochemical modelling of Th(IV), U(IV), Np(IV), and Pu(IV) in natural aquatic systems. Classical experimental methods (solubility studies, ultrafiltration, X-ray diffraction, absorption spectroscopy) were applied as well as modern techniques like laser-induced photoacoustic spectroscopy (LIPAS), laser-induced breakdown detection (LIBD) and X-ray absorption fine structure (XAFS) spectroscopy. As an outcome of the systematic experimental approach, a complete set of hydrolysis constants and solubility products for crystalline and amorphous oxide/hydroxides of tetravalent Th, U, Np and Pu have deduced, which have been included in the most recent update of the OECD/NEA thermochemical data base (Guillaumont et al., 2003).

The investigations have shown that the solubility of Actinide(IV) hydroxides can be increased by 3 - 4 orders of magnitude due to the contribution from colloid formation. Such colloids are found to remain stable up to investigation periods of 400 days, indicating that they might be stable or at least long-time metastable species. The quantification and modelling of the total solubility (including stable or metastable eigencolloids) is not only relevant for the tetravalent actinides but is also of particular interest for the geochemical evaluation of oxide/hydroxide colloids of Fe, Al, and Si, which are known to act as potential carriers for actinide migration. Quantum mechanical calculations on the $Th(OH)_4$ structure give a strong indication that formation of oligomers (i.e. the tetrameric $Th(OH)_4$) is energetically favored over that of the monomer.

Progress has also been made towards an appropriate geochemical modelling of tetravalent actinides in carbonate solution. The careful evaluation of different sets of experimental data, revealed the predominant existence of the ternary hydroxo carbonate species $Th(OH)(CO_3)_4^{5-}$ and $Th(OH)_2(CO_3)_2^{2-}$ and less important $Th(OH)_2(CO_3)(aq)$, $Th(OH)_3(CO_3)^-$ and $Th(OH)_4(CO_3)^{2-}$ under a wide pH and carbonate concentration range. These data can be taken as a basis for the thermodynamic modeling of tetravalent actinide solubility in presence of carbonate.

Complexation of actinides with small organic ligands. A clear step forward has been made in the understanding of the interaction of actinides with small organic ligands, such as α-hydroxo carboxylic acids, which are of relevance regarding the complexation properties of natural organic matter and wood degradation products. Even at pH <3 strong complexes can be formed through coordination with the α-hydroxy groups. Combination of various spectroscopic methods revealed the importance of steric arrangement of the functional groups acting as complexing ligands and allowed the derivation of a number of thermodynamic

complexation data. Also in this task, the use of up to date spectroscopic data as the fs-Time resolved laser fluorescence spectroscopy (TRLFS) and X-Ray absorption spectroscopy (EXAFS) proved as valuable tools to tackle such problems.

Complexation with minor ligands. The fact that in natural systems uranium, thorium and REE are frequently found enriched in phosphate minerals explains the importance to understand actinide interaction with phosphate. The complexation constants derived for the phosphate and arsenate complexation of U(IV) and U(VI) are certainly helpful to describe the uranium behaviour in abandoned uranium mine sites. But the data provided in this task represent also a valuable brick for the modelling of actinide behaviour in a nuclear repository system supplied with e.g. hydroxoapatite as a backfill material.

Redox behaviour of actinides. **T**he redox chemistry of mainly uranium (1) during dissolution of spent fuel and (2) in interaction with iron from container material was the content of studies in this subtask. Dissolution rates of UO_2 have been derived in the presence of H_2O_2 as a radiolysis product. The influence of groundwater carbonate concentrations has been considered of minor importance. Reduction of U(VI) by iron corrosion products appears to be quite dependent on the presence of H_2 overpressure which is assumed to exert a synergistic effect. The experimental data may be helpful to understand as well the influence of H_2 on the groundwater corrosion of spent fuel. H_2 overpressure is supposed to be largely inhibiting the dissolution of uranium from UO_2 and spent fuel.

Mechanistic understanding on the underlying redox processes are quite scarce. A first insight is provided by quantum mechanical calculations looking at the structure of intermediate U(VI) $-OH^-$-Fe(II) complexes occurring during the reduction of U(VI) by Fe(II).

Computational actinide chemistry. As already mentioned above, theory computational methods (molecular modelling) are implemented into the geochemical investigations of nuclear waste disposal problems. The studies provided precise structural information on the actinide interaction with inorganic and organic ligands relevant in groundwater systems close to nuclear waste repositories. Such information can be used to develop or to validate thermodynamic models especially there where where chemical species are not directly accessible by spectroscopic methods. Improved methods have been developed to describe solution chemical thermodynamics with a much better accuracy than any method developed so far. Accuracies of predictions are 10 kJ/mol, or better. The results indicate that quantum chemical methods provide not only insight into the microscopic basis of macroscopic thermodynamics, but also a useful test of empirical estimation methods.

<u>Work package 2:</u> Thermodynamics of solid-water interface reactions (sorption phenomena)

The work performed within this work package was focussed on various mineral phases such as iron oxide/hydroxides, alumina, silica, clay minerals and rock constituents. The first three of the following tasks were addressed to derive a comprehensive set of experimental data and to deduce sound thermodynamic data in terms of a state-of-the-art surface complexation model. Within the last task spectroscopic methods were applied to test whether the surface complexation models presently available are appropriate to describe the interface reaction of highly charged actinide ions correctly.

U(VI) and Pu(IV) onto magnetite and goethite. Both mineral phases are important constituents either of corrosion products tentatively generated in a nuclear repository or rock and sediments in the far field of a disposal site. The data are described by fully parameterised state of the art surface complexation models. Under anaerobic conditions a slow reduction of

U(VI) to U(IV) is observed in the presence of magnetite. Experiments on Pu sorption to both oxides were much more difficult to interpret due to redox and colloid formation processes.

Eu(III) and U(VI) onto Na-illite. The illite is considered to be the mineral phase dominating the sorption of radionuclides in clay rocks which are discussed as appropriate host rock for a nuclear waste repository. A combined non-electrostatic ion exchange and surface complexation model was developed to describe the experimental data. The speciation for both surface sorbed metal ions is followed by spectroscopic speciation methods. EXAFS obtained at pH = 5 and 6 for sorbed U(VI) verify the existence of inner-sphere complexes and the absence of polynuclear species. Eu(III) speciation is spectroscopically investigated covering the complete pH range from 3 to 13 by TRLFS using the chemical homologue Cm(III) as a fluorescence probe. Emission spectra and fluorescence lifetimes are compatible with the surface complexation model in so far as with increasing pH ternary surface complexes like $\equiv$S-O-Eu/Cm(III)$(OH)_x^{(2-x)}$ are formed. Even though the quantitative interpretation of spectroscopic data is not yet complete, it is clear that the basis of the sorption model is supported by the independent spectroscopic information. The approach of combining chemical sorption data with independent spectroscopic information is found to be indispensable for the development of surface complexation data on a high confidence level.

U(VI) onto phyllite and granite. Both rocks may play a relevant role in retention of actinides in nuclear repository and abandoned mine areas. The approach applied used surface complexation constants obtained for the rock constituents, i.e. pure mineral phases, to predict successfully the sorption onto the whole rock. In the case of phyllite it turned out that ferrihydrite generated as a secondary phase under oxidizing conditions dominated the U(VI) sorption, while for the granite no alteration is observed within the time period of the experiments. Both the concepts discussed above, (1) quantification sorption to the isolated mineral which dominates the sorption in the natural rock, and (2) the composite approach appear to be appropriate approaches to tackle the problem of creating thermodynamic sorption data for natural rock. The growing availability of spectroscopic information on the structure and chemical nature of sorbed species is considered as an important validation tool for such concepts and have to be developed further.

Spectroscopic speciation of interface reaction of Cm(III). The speciation of Cm(III) sorbed onto model mineral phases such as silica, alumina and aluminosilicates has been studied by TRLFS. It was found that TRLFS is a versatile tool to characterise and quantify the sorbed species at the mineral/water interface at trace level concentration range. Various sorption mechanism such as ion exchange in clay interlayers, specific adsorption at functional groups or incorporation into the bulk structure, could be distinguished. Furthermore, the formation of ternary hydroxo complexes of the sorbed Cm(III) with increasing pH could be traced. To gain more detailed information on the influence of the surface heterogeneity and of the surface potential on the interaction of the actinides with the surface, sorption reactions have been studies with different planes of α-alumina single crystals. Various spectroscopic and microscopic methods, such as TRLFS, GI-XAFS, XPS, AFM and non-linear IR spectroscopy were applied to elucidate the interface reactions in this model system. First successful experiments reveal that the crystal plane influences the structure and extend of actinide sorption. As such, these investigations provide indispensable prerequisites for the development of sorption model approaches.

<u>Work package 3:</u> Thermodynamics of secondary phase formation

The originally planned work was focussed on calcite and phosphate minerals. Both solids are found in nature with considerable contents of REE and natural actinides and are known to form solid solutions. Calcite has been used as a well characterised model mineral phase with

good crystallisation properties. During the project phase other mineral phases such as barite and calcium silicate hydrates have been included in the study.

Formation of solid solutions of actinides with calcite. The scientific approach again comprises wet chemical coprecipitation studies, spectroscopic speciation of interacted actinides and geochemical modelling efforts. Atomic Force Microscopy has been additionally applied to gain insight into the influence of sorbed trace elements on the crystal surface structure. Eu(III) and Cm(III) have been chosen as representatives of the trivalent actinides because of their favoured spectroscopic properties. The spectroscopic results revealed that the two species are sorbed to the calcite. The first one is incorporated in the bulk structure without any water, whereas the second one, which is partly hydrated could be a surface complex. Carefully performed coprecipitation experiments proved the strong interaction of actinides with calcite and provided comprehensive sorption data. The essential question for modelling of the experimental results is to identify the mechanism of charge compensation. A number of mechanisms and possible species could be excluded. A big step forward to the understanding of the underlying processes was made. Efforts are ongoing to clarify open questions and then to come to a thermodynamic model consistent with spectroscopically identified species.

Formation of solid solutions of radionuclides with other mineral phases. Incorporation of REE into phosphates and trivalent actinides into CSH phases is also concluded from experimental data. The understanding on the underlying mechanisms has been increased considerably during the project. However, the development of a consistent solid solution model is also in these systems still underway.

References

Guillaumont, R., Fanghänel, Th., Fuger, J., Grenthe, I., Neck, V., Palmer, D.A., Rand, M.H. OECD, NEA-TDB (2003): Update of the Chemical Thermodynamics of Uranium, Neptunium, Plutonium, Americium and Technetium, Chemical Thermodynamics, Vol. 5, Elsevier, Amsterdam.

Kim, J.I. (1999): Is the thermodynamic approach appropriate to describe natural dynamic systems? (Status and limitations). Proceedings of Euradwaste'99 : 5th European Commission Conf.on Radioactive Waste Management and Disposal and Decommissioning, Luxembourg, Nov. 15-18, p. 227-242, EUR 19143 EN.

Kim, J.I., Fanghänel, Th., Regan, L., Nitsche, H., Brendler, V., Grenthe, I., Glaser, F., Bruno, J., Saxena, S. (2000): Joint European Thermodyamic Database for Environmental Modelling –JETDEM, European Commission, Contract F14W-CT96-0029, Final Report, EUR19131 EN

5. Scientific and technical performance

5.1 Work-package 1:

Thermodynamics of aquatic actinides: Experiments to improve the database of unknown or uncertain data

Summary of the specific project objectives

To eliminate the most serious deficiencies in the thermodynamic database for the actinides, the following chemical reactions are being studied: hydrolysis and complexation of the tetravalent ions, formation of ternary complexes, complexation with phosphate, and actinide redox behaviour. To tackle these problems, classical wet-chemistry methods are combined with highly sensitive laser spectroscopic tools. In co-operation with theoretically oriented groups out-side the ACTAF consortium semi-empirical and more direct theory-based methods for the prediction of chemical behaviour in actinide systems are being developed and applied.

Structure of the work-package and contributing partners

5.1.1 Solubility, colloid formation, hydrolysis and carbonate complexation of tetravalent actinides (FZK, FZR)

5.1.2 Complexation of actinides with small organic ligands (KTH, FZR)

5.1.3 Complexation with minor ligands (FZR, KTH)

5.1.4 Redox behaviour of actinides (UPC, KTH)

5.1.5 Computational actinide chemistry (KTH, UPC)

5.1.1 Solubility, colloid formation, hydrolysis and carbonate complexation of tetravalent actinides

Introduction

The activities within this subtask were focussed on the hydrolysis reaction of Th(IV), U(IV), Np(IV) and Pu(IV) combining classical solubility measurements with new spectroscopic techniques and theoretical approaches. Of special interest is the influence of colloid formation on solubility data. Further experiments were focussed on the formation of mixed hydroxo-carbonato complexes of Th(IV). The work was performed by FZK and FZR.

The literature on the solubility and hydrolysis of tetravalent actinide ions was critically reviewed by FZK at commencement of the project [1]. See results are summarized in Table 1.1.Hydrolysis constants were selected preferentially from experimental studies, where the interference of colloid formation was to be excluded. Unknown formation constants of mononuclear complexes were estimated by an empirical correlation from known constants of other actinide ions applying a new semi-empirical electrostatic model [2]. Based on the known and estimated hydrolysis constants, the solubility products of $An(OH)_4(am)$ or $AnO_2 \cdot xH_2O(am)$ were calculated from experimental solubility data, using SIT for ionic strength correction. The derived comprehensive set of thermodynamic constants for the solubility and hydrolysis of Th(IV), U(IV), Np(IV) and Pu(IV) establish an important guideline for the experimental work within the ACTAF project.

Experimental studies were performed particularly with Th(IV) but also with U(IV), Np(IV), and Pu(IV). The redox-stable Th(IV) is used as surrogate to investigate the solubility behaviour and stability of An(IV) oxides/hydroxides, the influence of eigencolloid formation on the solubility and to identify and quantify the predominant aqueous species in the ternary system An(IV)-OH-CO_3. Classical experimental methods (solubility studies, ultrafiltration, X-ray diffraction, absorption spectroscopy) were applied as well as modern techniques like laser-induced photoacoustic spectroscopy (LIPAS), laser-induced breakdown detection (LIBD) and X-ray absorption fine structure (XAFS) spectroscopy. The results obtained within the project are summarized below. A recent summary was presented at Migration´3 [3].

Table 1.1 Selected thermodynamic constants for An(IV) hydrolysis species, solid oxides and hydroxides at 25 °C [1]

	Th(IV)	U(IV)	Np(IV)	Pu(IV)
$\log K^0_{sp}$				
$AnO_2(cr)$	-54.2 ± 1.3	-60.9 ± 0.4	-63.7 ± 4.8	-64.0 ± 1.2
$An(OH)_4(am)$ / $AnO_2 \cdot xH_2O(am)$	-47.0 ± 0.8	-54.5 ± 1.0	-56.7 ± 0.5	-58.5 ± 0.7
$\log K^0_{s(14)}$ (exper.)	-8.5 ± 0.6 [b)]	-8.5 ± 1.0 [b)]	-9.0 ± 1.0 [b)]	-10.4 ± 0.5 [b)]
$\log \beta^0_{11}$	11.8 ± 0.2	13.6 ± 0.2	14.5 ± 0.2	14.6 ± 0.2
$\log \beta^0_{12}$	22.0 ± 0.6	26.9 ± 1.0 [a)]	28.3 ± 0.3	28.6 ± 0.3
$\log \beta^0_{13}$	31.0 ± 1.0	37.3 ± 1.0 [a)]	39.2 ± 1.0 [a)]	39.7 ± 0.4
$\log \beta^0_{14}$	38.5 ± 1.0 [b)]	46.0 ± 1.4 [b)]	47.7 ± 1.1 [b)]	47.5 ± 0.5 48.1 ± 0.9 [b)]

a) Estimated

b) From experimental solubility data in neutral to alkaline solutions:
$\log K^0_{s(14)} = \log [An(OH)_4(aq)] = \log K^0_{sp}(AnO_2 \cdot xH_2O(am)) + \log \beta^0_{14}$

Solubility of amorphous Th(IV) hydroxide

The solubility of amorphous Th(IV) hydroxide at pH 3.0 - 13.5 and the aqueous speciation at pH < 4 were investigated in 0.5 M NaCl and 25°C (see Fig. 1.1) [4]. The LIBD was used to monitor the initial colloid formation during the coulometric titration of 10^{-2} - 10^{-5} M thorium solutions in the pH range of 2.7 - 4.5. The accurate solubility limit determined by this method is comparable with data measured from experiments at undersaturation conditions with an X-ray amorphous solid precipitated at higher pH and dried at room temperature. Based on the known hydrolysis constants reviewed in [1], the solubility product is calculated to be log $K°_{sp}$ = - 47.8 ± 0.3 (converted to I = 0 with the SIT) (FZK).

Influence of colloid formation on solubility

LIBD and EXAFS studies have shown that the solubility measured for amorphous Th(IV) hydroxide can be increased by 3 - 4 orders of magnitude due to the contribution from colloid formation (see Fig. 1.1) [4, 5]. LIBD and ultrafiltration studies on colloidal Th oxide/hydroxide dispersions [6] demonstrated that neither the colloidal thorium concentration nor the mean particle size changed noticeably after 100 - 400 days, indicating that these colloids might be stable or at least long-term metastable species. Moreover, pH changes measured as a function of time indicated that, after about 2 weeks, freshly prepared Th(IV) hydroxide colloid dispersions approach a steady state, where the Th(IV) colloids are in equilibrium with ionic species [6]. The question is open whether there is also an equilibrium between colloids and solid hydroxide phases. Establishment of such type of colloidal equilibrium could explain the scattering Th(IV) solubility data frequently observed in the literature. The examination of such processes is of cardinal relevance for the selection of appropriate solubility data for nuclear disposal safety assessment calculations. Available thermodynamic databases hitherto do not consider colloidal species. The quantification and modelling of the total solubility (including stable or metastable eigencolloids) requires further investigation in the future. The question whether colloidal oxide/hydroxide species formation can be described by thermodynamic equilibria is not only relevant for the tetravalent actinides but is also of particular interest for the geochemical evaluation of oxide/hydroxide colloids of Fe, Al, and Si, which are known to act as potential carriers for actinide migration (FZK).

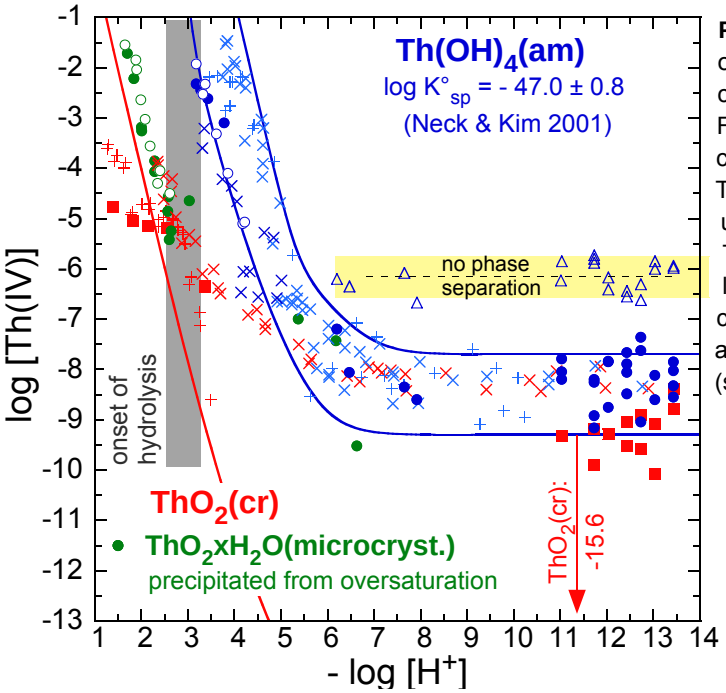

Fig. 1.1: Experimental and calculated solubility of ThO_2(cr), ThO_2xH_2O(mcr), $Th(OH)_4$(am) and colloidal $Th(OH)_4$(am) in 0.5 M NaCl at 25°C. Filled symbols: solubility data; open circles: coulometric LIBD titration; on microcrystalline ThO_2.[6]; filled squares: ThO_2 from undersaturation [7]; open triangles: colloidal $Th(OH)_4$(am) (without phase separation). The lines are calculated for I=0.5 M with hydrolysis constants and solubility products for crystalline and amorphous Th oxide/hydroxides phases (see. Tab. 2.1)

Solubility of crystalline thorium dioxide

The solubility of thorium oxides of different degree of crystallinity was investigated at 25°C (see Fig. 1.2) [7]. The dissolution of bulk crystalline ThO_2(cr) is a very slow process and the Th(IV) concentrations measured after one year in solutions at pH 1 - 3 do not represent equilibrium data. Coulometric titration of thorium nitrate solutions in the low pH range of 1.5 - 2.5 in 0.5 M HCl-NaCl solution resulted in the formation of $ThO_2 \cdot xH_2O$(mcr) particles agglomerating to a microcrystalline precipitate. The solubility of this solid, which is in equilibrium with Th^{4+}(aq), was measured from oversaturation experiments [7] and also by using the titration method combined with LIBD detection [7, 8]. A solubility product of log $K°_{sp}$ = - 53.2 ± 0.4 was obtained, close to the thermochemical value for crystalline ThO_2(cr) and about 6 orders of magnitude lower than that of X-ray amorphous Th(IV) hydroxide or hydrous oxide. The differences in the solubility products can either be explained as an effect of the particle size or as the different solubility of the different solid phases. Above the onset of Th(IV) hydrolysis at pH > 2.5, the dissolution of microcrystalline $ThO_2 \cdot xH_2O$(mcr) becomes irreversible. In near-neutral to alkaline solutions, the measured thorium concentrations approach those of amorphous $Th(OH)_4$(am). Similar results are obtained for undersaturation experiments with crystalline ThO_2(cr) in 0.5 M NaCl-NaOH solutions, indicating that the solubility is not controlled by the bulk crystalline solid but by layers of amorphous phases formed at the solid surface.

Characterization of all Th oxide/hydroxide solid phases has been performed by EXAFS and XANES at the Th L3 edge [5]. The microcrystalline $ThO_2 \cdot xH_2O$(s) phase shows a clearly different EXAFS spectrum compared to the anhydrous crystalline ThO_2(cr) and the amorphous oxide $ThO_n(OH)_{4-2n} \cdot xH_2O$(am), whereas the spectra of the colloids at -log $[H^+]$ = 3.7 and the amorphous oxide exhibit very similar structures. In the XANES regime a noteworthy decrease of the intensity of the white line with increasing particle size is observed. This effect is the subject of a theoretical study (FZK).

Hydrolysis of U(IV)

The hydrolysis of U(IV) was studied by UV/Vis and laser-induced photoacoustic spectroscopy (LIPAS or LPAS) experiments. No changes of the spectral properties in the visible wavelength range have been found for the first hydrolysis product of U(IV). Nevertheless it was possible to derive the formation constant for the first hydrolysis step using the decrease of the absorption of the solution between 620 nm and 690 nm. The formation constant for the reaction

$$U^{4+} + H_2O \leftrightarrows U(OH)^{3+} + H^+$$

was found to be log K = -1.64 ± 0.07 at ionic strength I = 2.0 M and to be log K = -1.53 ± 0.13 at ionic strength I = 0.5 M. (FZR)

Solubility, hydrolysis and colloid formation of Np(IV)

The solubility and hydrolysis of Np(IV) have been investigated by UV/Vis/NIR spectroscopy and LPAS [9]. LPAS spectra of Np(IV) in acid solution could be obtained for the 723 nm absorption band down to $2 \cdot 10^{-7}$ M Np(IV) concentration using $DClO_4/D_2O$ instead of protonated electrolyte to reduce background absorption. No change of the spectral shape was found in the range -log $[H^+]$ = 0 to 2.5 and -log $[D^+]$ = 1. However, a sudden decrease of intensity was observed above a pH threshold. LIBD measurements confirmed the formation of colloids at the threshold. Varying the Np(IV) concentration between 10^{-3} and 10^{-6} M from spectroscopic and LIBD results the solubility product of $Np(OH)_4$(am) was determined to be log K'_{sp} = -54.4 ± 0.4 in 0.1 M $HClO_4$-$NaClO_4$ and log $K°_{sp}$ = -56.5 ± 0.4 (converted to I = 0

with the SIT) [9], which is consistent with the value of log $K°_{sp}$ = -56.7 ± 0.5 selected in [1]. The dominating solution species over the pH range is $Np(OH)_2^{2+}$ and thus no change of the spectra is to be expected. (FZK)

Solubility, hydrolysis and colloid formation of Pu(IV)

LIBD, LPAS and absorption spectroscopy at [Pu] = 10^{-3} - 10^{-6} M in 0.5 M NaCl-HCl (pH 0.3 - 2) have been applied to study the hydrolysis and polymerisation of Pu(IV) up to colloid formation during careful titration by dilution with pH-neutral NaCl solution. Similar as in the study with Np(IV) [9] the solubility, log [Pu(IV)] vs. - log [H^+] at the onset of colloid formation, decreases with a slope of about -2. The preliminary solubility product derived from these data (log $K°_{sp}$ = -59.0), is somewhat lower than the value of -58.5 ± 0.7 calculated in [1] from the widely scattered solubility data reported for $Pu(OH)_4$(am). The extremely strong tendency of Pu(IV) towards polynucleation and colloid formation, even at low pH, is confirmed by EXAFS and XANES measurements at the Pu L3 edge. The spectra of a 16.1 mM Pu(IV) solution in 0.4 M HCl and of 1 mM Pu(IV) solutions in 0.5 M HCl-NaCl (- log [H^+] = 0.6 - 1.4), compared to those of 1 mM $Pu(IV)_{aq}$ in 1 M $HClO_4$ and a solid $Pu(OH)_4$(am) precipitate, clearly show the predominance of Pu(IV) polymers. (FZK)

Solubility and complexation of Th(IV) in carbonate solution

The formation of hydroxo-carbonate complexes was investigated by solubility experiments with $Th(OH)_4$(am) in $NaHCO_3$-Na_2CO_3-NaOH-NaCl solution (I = 0.5 M, 22°C) [10]. The concentrations of OH^- and CO_3^{2-} were varied in wide ranges by performing three series of closed system experiments at constant total carbonate concentrations of [HCO_3^-] + [CO_3^{2-}] = 0.1, 0.04 and 0.015 M, (-log [H^+] = 8.5 - 13.5) and two series of open system experiments under CO_2 partial pressures of 1.0 and 0.1 bar (-log [H^+] = 4.5 - 7.5). The simultaneous evaluation of the different sets of experimental data show that $Th(OH)(CO_3)_4^{5-}$ and $Th(OH)_2(CO_3)_2^{2-}$ are the most important complexes predominant under these conditions. Further significant contributions are coming from $Th(OH)_2(CO_3)$(aq), $Th(OH)_3(CO_3)^-$ and $Th(OH)_4(CO_3)^{2-}$. The formation constants, converted to I = 0 with the SIT and combined with the solubility product of log $K°_{sp}$ = - 48.7 ± 0.3 [4], are calculated to be log $β°_{114}$ = 35.8 ± 0.3, log $β°_{122}$ = 37.0 ± 0.4, log $β°_{121}$ = 30.7 ± 0.4, log $β°_{131}$ = 38.5 ± 0.6 and log $β°_{141}$= 40.7 ± 0.5. The evaluation of the experimental data gave no significant values for the pure carbonate complexes (the formation of the limiting complex $Th(CO_3)_5^{6-}$ requires carbonate concentra-

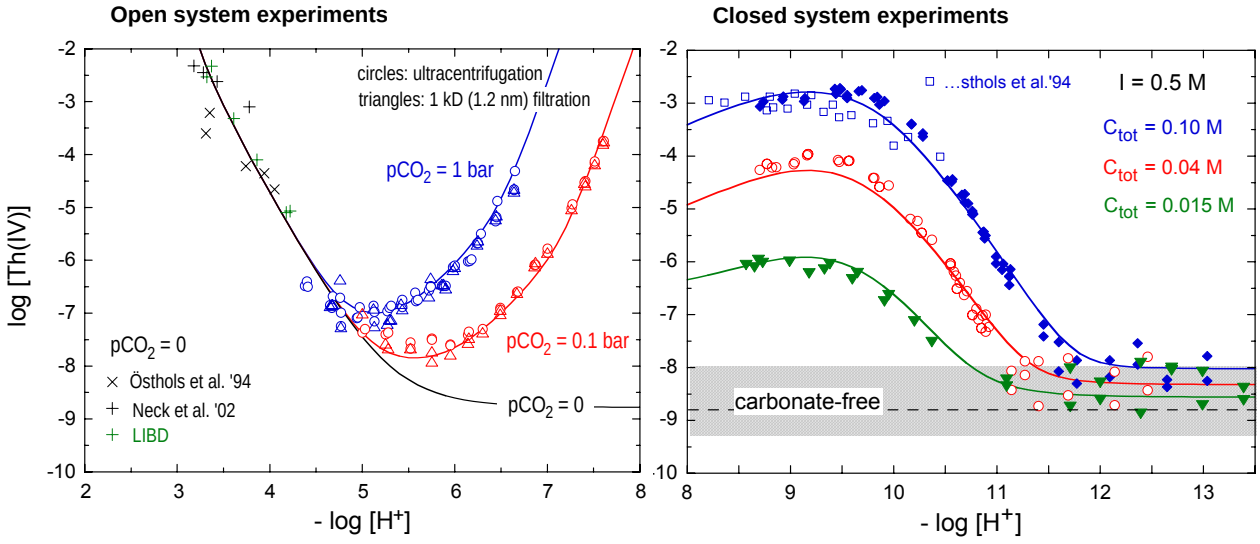

Fig. 1.2: Solubility of ThO_2xH_2O(am) in carbonate solution: Open system and closed system experiments at I = 0.5 M and 22°C compared to the solubility in carbonate-free solution [10].

tions considerably above 0.1 M) and other ternary complexes. Only upper limits could be derived for their formation constants. (FZK)

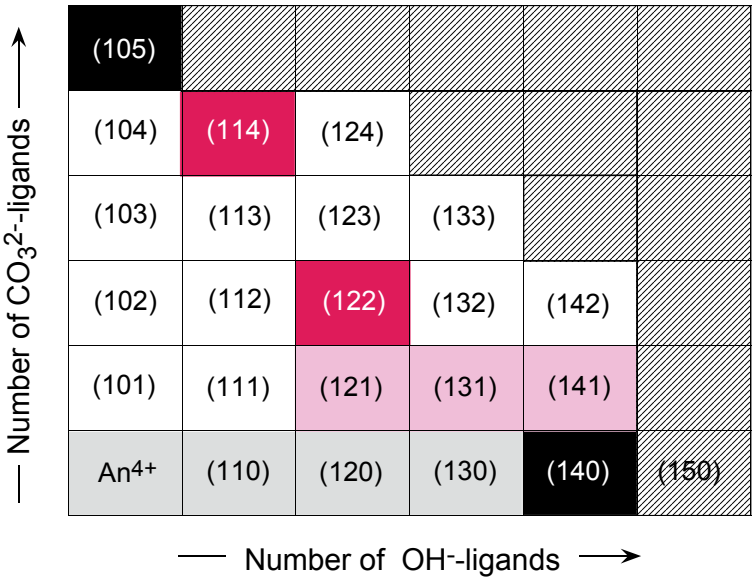

Fig. 1.3: Possible mononuclear complexes (1yz) = $An(OH)_y(CO_3)_z^{4-y-2z}$: Dark colored squares indicate predominant complexes in neutral and alkaline solution (ternary complexes in red). Less important but quantified complexes are shown in light red. These data form a base for the thermodynamic modeling of tetravalent actinide solubility in presence of carbonate [10].

5.1.2 Complexation of actinides with small organic ligands

Introduction

The activities in this subtask have addressed the complexation of U(VI), Np(V) and An/Ln(III) by various small organic ligands especially in alkaline solutions, which may favour the formation of ternary complexes. The studies apply both spectroscopic techniques as well as computational methods to gain chemical and structural information. Formation of various ternary complexes are investigated as they are supposed to be of major importance in multi component natural systems. The primary goal of this work besides derivation of thermodynamic data is to improve the scientific understanding of actinide chemistry in laboratory systems and to assess their relevance for natural conditions. Contributions came from KTH, FZR and FZK.

The rationale for this work package is to provide a theoretical and experimental basis for the estimation of equilibrium constants of actinides with the multitude of ligands present in ground and surface water systems. Special consideration has been taken to the formation of ternary complexes that in addition to the organic ligand also contains inorganic ligands like hydroxide and fluoride. The data cover the pH range 4 – 8.5 commonly encountered in ground and surface waters, but also highly alkaline conditions such as those resulting in the near-field of nuclear repositories containing cement. By using fundamental information on the coordination chemistry (coordination geometry / coordination number) and the preferred donor atoms it is possible to estimate both the stoichiometry and bonding modes of ligands based on information on the functional groups that they contain, such a theory based approach is much more rational than "brute force" methods where one makes attempts to do experimental studies of all conceivable ligands. Ligands containing α-hydroxy carboxylate functional groups with variable steric positions within the molecule are investigated. These ligands are assumed to represent the complexing moieties relevant in natural systems as soils or ground or surface water humic matter or wood degradation products. An array of experimental methods has been used to support these conclusion, conventional potentiometry, laser induced fluorescence spectroscopy, extended X-ray absorption spectroscopy (EXAFS) and nuclear magnetic resonance spectroscopy (NMR). The theory-based method often makes it possible to identify the ligands that are of dominating importance in safety and performance assessment.

Complex formation with hexa-valent and pentavalent actinides, MO_2^{2+}, MO_2^{+}

UO_2^{2+} was used as a model ion and the experimental studies were made using small ligands like α-hydroxy-carboxylates [11]. At low pH (less than 2.5) the α-hydroxy-carboxylates form fairly weak complexes in which only the carboxylate group is coordinated. At pH>3 very strong complexes are formed through deprotonation of the α-hydroxy group. Hence even small amounts of these ligands have a large effect on the speciation (KTH, FZR).

To study the role of phenolic and carboxylic groups in complexation reactions with U(VI), various carboxyphenolic acids were investigated spectroscopically, exploiting the fluorescence properties of uranium and also the organic ligand if possible. All reaction constants referred to later in this section were determined at an ionic strength of 0.1 M $NaClO_4$ (FZR).

Interaction with 2,3-dihydroxybenzoic acid as a ligand does not influence the fluorescence spectrum of uranium. This means that only the non-complexed uranium emits photons. The complex formation therefore can be studied by observing the decreasing fluorescence

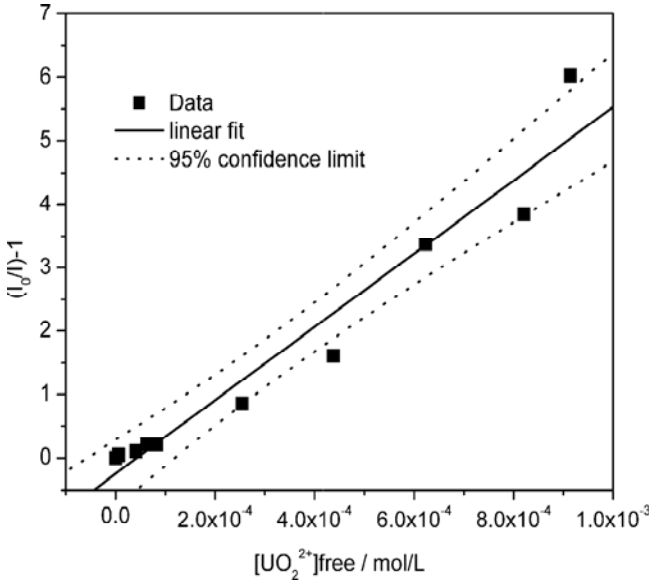

Fig. 1.4: Static quenching of the intensity of the 2,3-dihydroxybenzoic acid by free UO2+ (Stern-Volmer plot). From the linear relationship a formation constant for the 1:1 complex is derived [12].

intensity with increasing complex formation [12, 13, 14](see Fig. 1.4). Additionally to this static fluorescence quenching a dynamic quench effect of the protonated ligand on the fluorescence of uranium was observed. The dynamic quench effect can by estimated by fluorescence lifetime measurements. So both the complex formation and the dynamic quench effect can be determined. A one to one complex formation between uranium and 2,3-dihydroxybenzoic acid was thus established. Studies as function of pH also proved that two protons are released from the ligand during the complex forming reaction. The complex formation constant is calculated to be log K = -3.99 ± 0.44. From the fluorescence properties of the ligand a formation constant of log K = -3.11 ± 0.16 was derived. The agreement between both methods is acceptable. However, we have to take into consideration excited state reactions of the ligand, when the complex formation is studied by the fluorescence properties of the ligand. As the release of two protons during the complex formation was observed, the reaction may be written as:

$$C_6H_3(OH)_2COOH + UO_2^{2+} \leftrightarrows C_6H_3(OH)(O)COO(UO_2) + 2\,H^+$$

The complex formation of uranium(VI) with 2,5-dihydroxybenzoic acid in a pH range 2.5 – 4.5 was observed. Besides the static fluorescence quench effect caused by the complex formation, a dynamic fluorescence quench effect caused by the protonated ligand (self quenching) and by the non-complexed uranium appeared. The fluorescence lifetime of the ligand was determined to be 5.7 ns []. Formation of a one to one complex is derived. The number of released protons was less than 1 (0.62 ± 0.12). The complex formation constant was calculated to be log K = 0.92 ± 0.38 and a complexing reaction:

$$C_6H_3(OH)_2COOH + UO_2^{2+} \leftrightarrows C_6H_3(OH)_2COO(UO_2)^+ + H^+$$

was assumed. In the pH range 2.5 to 4.5, the formation constants not corrected for the proton release increase from log K = 2.36 to log K = 3.68. The study of the complex formation based on the fluorescence properties of the metal ion (uranyl) yields comparable results with log K ~ 3.8. However the dependence on pH is negligible. The difference between both methods may be caused again by excited state reactions of the ligand. Further studies are necessary to explain this effect.

Studies of the complex formation with 2,6-dihydroxybenzoic acid were carried out using the fluorescence properties of the uranyl ion. The deprotonation of the carboxyl group is at pH > 2.5 already complete. The formation constant for the reaction:

$$C_6H_3(OH)_2COO^- + UO_2^{2+} \leftrightarrows C_6H_3(OH)_2COO(UO_2)^+$$

was found to be log $\beta_{11} = 3.85 \pm 0.29$.

In addition to the above acids with two carboxylic groups, also the complex formation between uranyl ions and 3-hydroxybenzoic acid and 4-hydroxybenzoic acid were investigated. The experiments relied on both potentiometric and spectroscopic titrations. The complex gross stability constants thus determined for 3-hydroxybenzoic acid and 4-hydroxybenzoic acid were 3.14 ± 0.05 and 2.81 ± 0.07, respectively.

Finally, the complex formation of Np(V) with 2,3-dihydroxybenzoic acid was studied by fs-TRLFS using the fluorescence properties of the organic ligand. At pH < 5.0 a one to one complex formation was found. At higher pH values the results leads to the conclusion that a two to one complex is formed. The preliminary complex formation constants are calculated to be log $K_{11} = 3.33 \pm 0.04$ and log $K_{21} = 6.92 \pm 0.03$.

Organic ligands undergo upon excitation excited state reactions. These excited state reactions do not influence the complex formation with the metal ion. However, the change in the protonation / deprotonation of the ligand in the excited state leads to differences in the fluorescence signal of the ligand used for the calculation of the formation constants. This difference seems to be very small in the case of extreme fast and complete transfer reactions (as 2,x-dihydroxybenzoic acids), when only one form can be observed. In the case of slower and non-complete reactions these excited state reactions have to be taken into consideration for the calculation of the formation constant. As a first example we have studied the excited state reaction of 2-naphthol. This species undergoes at pH < 7 a deprotonation step in the excited state. Using the time resolved laser induced fluorescence spectroscopy we were able to confirm the kinetics of the deprotonation. We found a value of $4.3*10^7$, which is in agreement with literature data ($6.0*10^7$). Applying such mechanism to the small organic ligands, we deconvolute the measured spectra and can calculate the correct concentrations of the non-complexed ligand in the ground state. (FZR)

Moreover, the complexation of U(VI) with malonate has been studied by TRLFS spectroscopy of the uranyl fluorescence [15] (FZR). Stability constants were determined for the complexes $UO_2C_3H_2O_4°_{(aq)}$ and $UO_2(C_3H_2O_4)_2^{2-}$ from results of spectra deconvolution using a least square fit algorithm (logβ_1°=4.48±0.06, logβ_2°=7.42±0.06 or logK_2°=2.94±0.04).

Complex formation with tetra-valent actinides, M^{4+}

Th^{4+} was used as a model ion and the experimental studies involved α-hydroxy-acetate and 5-sulfosalicylate, *i. e.* model ligands representing aliphatic and aromatic hydroxy acids [16, 17]. Both ligands formed complexes with very similar stoichiometry where ternary di- and tetra-nuclear species are prominent. The complexes with aliphatic hydroxy acids are weak in comparison with the hydrolysis, while the complexes with aromatic hydroxy acids are very strong, the former will not influence the speciation in ground and surface water systems, but ligands of the latter type must be considered. In the pH range 2 to 4 the complex formation is dominated by the formation of binary mononuclear complexes MA_n, $n = 1 – 4$, where A = $HOCH_2COO^-$ and $HOC_6H_3(SO_3^-)COO^-$ at higher pH di- and tetranuclear species are formed. By using NMR techniques we have been able to determine the constitution of the different complexes and to prove that the very strong complexes are formed at pH>4 involve deprotonation of the α-hydroxy group and the aromatic OH-group. The α-hydroxy group can be deprotonated for both ligands resulting in the formation of very stable chelate complexes. This deprotonation takes place in very different pH regions for the two ligands as the aliphatic hydroxy group is a much weaker acid than the aromatic one.

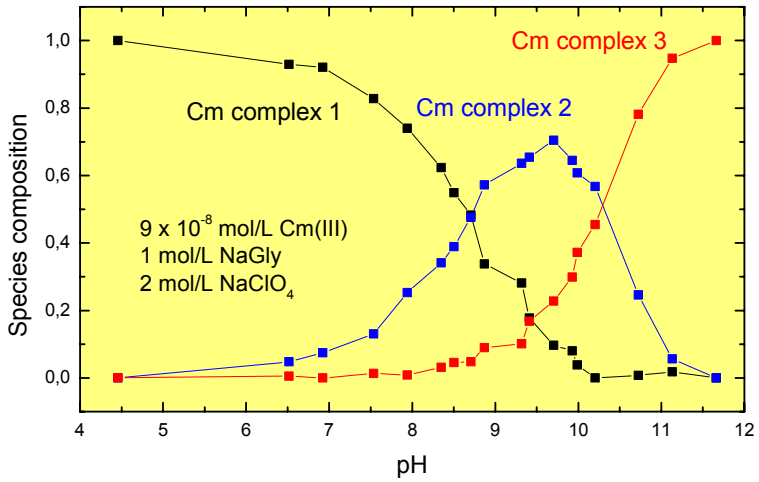

Fig. 1.5: Species distribution of Cm(III) in glycolic acid derived by TRLFS. At high ligand concentration (1.0 M) three different complexes are identified by their spectroscopic properties.

Complex formation with tri-valent actinides, M^{3+}

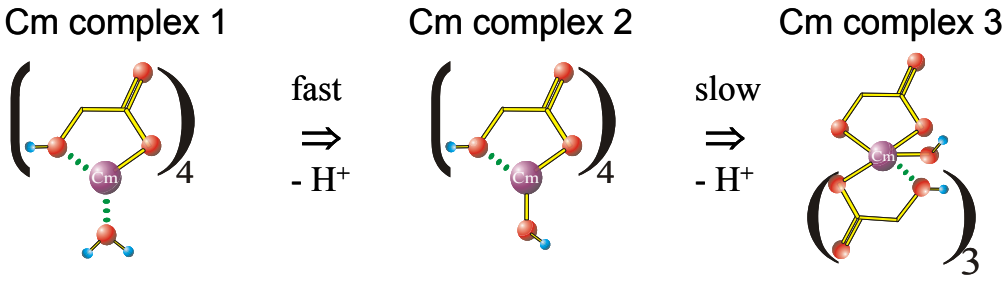

This study has been made by KTH in cooperation with FZR and /FZK. Trivalent lanthanides and Cm(III) were used as model ions and α-hydroxy-acetate as the model ligand [18, 17]. The spectroscopic properties of the Ln(III) and Cm(III) complexes have been studied using fluorescence spectroscopy. Three complex species of Cm(III) have been identified and quantified by TRLFS. In Fig. 1.5 the species distribution is shown as a function of pH. The Cm complexes are assigned to the following species. Whereas the deprotonation of the first complex is a fast reaction, the formation of the chelate at pH above 10 is slow.

The complexes formed are very similar to those formed by Th(IV), a result that can be rationalized by the similar coordination chemistry of tri and tetra-valent actinides; both groups have similar ionic radii and are characterized by high and variable coordination numbers. The rate of equilibration is very slow for the Th(IV) system and also for Cm(III), while the corresponding Eu(III) system is dynamically much more labile. These findings indicate that dynamic phenomena are important when interpreting experimental results; they also indicate a possible method to use dynamic methods for group separations of tri-valent actinides and lanthanides. (KTH, FZR, FZK)

Structure of complexes in solution, identification of isomers

Most solution chemical methods do not provide information on the presence of isomers of a complex with a given stoichiometric composition. Information of this type is very important when using coordination chemistry as a predictive tool and studies of isomer formation have therefore been made within the work package using quantum chemical methods and EXAFS spectroscopy. The financing has largely been made by other sources than the ACTAF program. In section 5.1.5 on Computational Actinide Chemistry it is demonstrated what has been achieved. (KTH)

5.1.3 Complexation with minor ligands

Introduction

The work performed in this task is focussed on the complexation of actinides with phosphate, arsenate and glyphosate. The latter is as an organic ligand with different functional groups as phosphate, carboxylate and amine. Despite the fact that phosphate may influence speciation of actinides in natural groundwaters or in a phosphate containing engineered barrier, the thermodynamic data are insufficient or lacking. Contributions have been made by UPC, EP, FZR, and KTH.

U(IV) complexation with phospate and arsenate

Including the protonation constants for phosphoric and arsenic acid we obtained the formation constants according to the complex formation reaction

$$U^{4+} + 2H^{+} + XO_4^{3-} \leftrightarrows UH_2XO_4^{3+}$$

for X = P with log $ß^0 = 25.23 \pm 0.13$ and for X = As with log $ß^0 = 23.94 \pm 0.08$.

When comparing these data with the corresponding uranium(VI) systems it can be seen that the binding tendency of the dihydrogen arsenate is lower than that of dihydrogen phosphate. Also the binding tendency of the uranium(VI) is lower than that of uranium(IV). This is an expected behaviour. Using the ionic strength dependence of the complex formation of uranium(IV) with arsenate and phosphate we derived the specific ionic interaction coefficients between the formed complex and the perchlorate ion. These coefficients were derived using the data for the interaction coefficients of uranium(IV) and protons with the perchlorate ion given in the NEA TDB [19]. We found for the phosphate system an interaction coefficient of 0.42 and for the arsenate system of 0.46. These values are in good agreement with data in the NEA TDB for other trivalent uranium(IV) species: $U(OH)^{3+}$ with 0.48. (FZR)

As a new result we could confirm the fluorescence properties of uranium(IV). Uranium(IV) shows very intense fluorescence emission bands in the wavelength region from ~300 nm to about 520 nm. The fluorescence lifetime is extremely short (~2.6 ns). During complex formation a dramatic change in the fluorescence emission occurs. (FZR)

Glyphosate is the active substance in the herbicide “Roundup” and might seem a far-fetched ligand to study in a project dealing with nuclear waste. However, the ligand contains three different types of donor groups, carboxylate, phosphate and amino groups, all present in organic material in nature. This study has allowed us to investigate the relative affinity of these donors to U(VI), information that can be directly used to estimate the binding characteristics of other ligands containing these functional groups, and a basis for estimating their influence on speciation, solubility, sorption and transport properties of actinides [20] (KTH).

Uranium minerals

In continuation of the fluorescence spectroscopic measurements on uranium minerals we studied up to now more than 100 uranium minerals. As important minerals with fluorescence properties we found some carbonate and sulphate minerals. The fluorescence properties of well defined uranium minerals can be used to determine solution species. This was shown for example in the case of uranyl hydrogen arsenate where the fluorescence properties of the mineral troegerite ($UO_2HAsO_4 \cdot 4H_2O$) were used to deconvolute the complex fluorescence spectrum of the solution [21]. (FZR)

5.1.4 Redox behaviour of actinides

Introduction

The work performed at UPC has focussed on the influence of oxygen and bicarbonate, as well as of hydrogen peroxide on the dissolution reaction of uranium dioxide and on Redox reactions of U(VI) at Fe(II/III) oxide/hydroxide surfaces. Theoretical methods are applied by KTH to describe the U(VI) reduction to U(V).

Dissolution of UO_2

Dissolved oxygen consumption by UO_2 is independent on HCO_3^- concentration, at bicarbonate concentrations lower than 5 mM, this is the case for most of granitic groundwaters. The rate of oxygen consumption by uranium(IV) dioxide is far larger than the rate of U(VI) dissolution by bicarbonate. This would indicate that in normal disposal conditions the spent fuel constitutes an important sink of oxidants and largely contributes to the Reducing Capacity of the system [22]. The effect of hydrogen peroxide consumption by the UO_2 surface has been studied by a combination of flow-through experiments and AFM and XRD spectroscopies. From these studies it has been possible to determine a rate of uptake of H_2O_2 by the UO_2, surface (see Fig. 1.6).

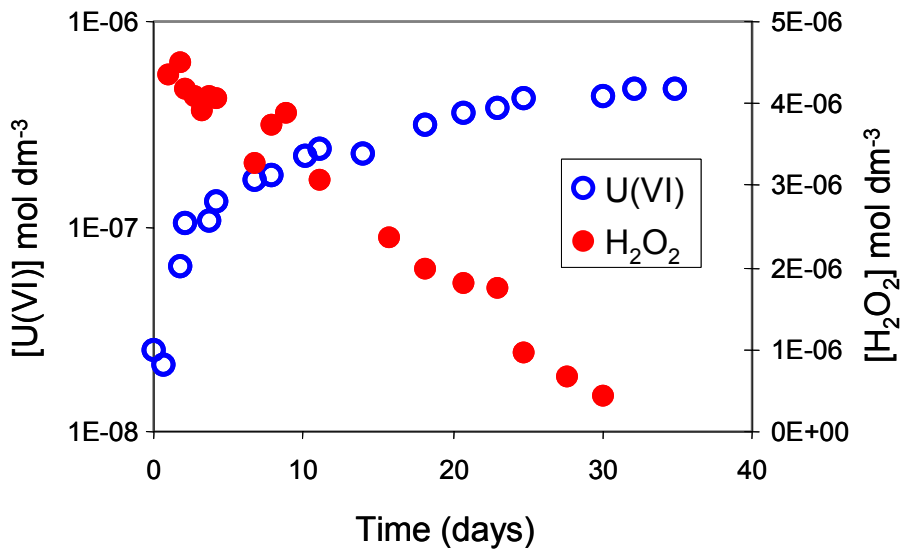

Fig. 1.6: Time dependency of U(VI) formation and H_2O_2 disappearance in the experiments of the kinetics of UO_2(s) oxidation by hydrogen peroxide.

The experiments have been performed with UO_2 powder of particle size (100-320 μm) with varying pH, carbonate and H_2O_2 concentrations. The experiments with varying hydrogen peroxide have been performed at pH: 5.5-6 in the absence of carbonate. The experimental data in the range $-5.5 \leq \log [H_2O_2] \leq -4$ can be approximated by a straight line of slope close to 1 (0.95). The proposed dissolution rate law is given by the equation:

$$r = 3 \cdot 10^{-6} [H_2O_2]^{0.95}$$

At higher H_2O_2 concentration, the dissolution rate seems to reach a constant value of $10^{-9.5}$ $mol \cdot m^{-2} \cdot s^{-1}$. This behaviour is similar to that described previously [23]. The formation of Studtite $UO_4 \cdot 4H_2O$ as secondary product of the hydrogen peroxide mediated alteration of UO_2 could be established by XRD. AFM investigations allowed to derive the rate of Studtite precipitation on the UO_2 surface [24]. (UPC)

U(VI) reduction at solid Iron oxide/hydroxide surfaces.

The mechanism of U(VI) reduction by Fe(II) containing phases, magnetite and olivine has been studied both in the presence of H_2 and N_2 by means of a combination of solution chemical and XAS spectroscopic methods.

The outcome of the investigations indicates that magnetite is an efficient reductant of U(VI) in the presence of hydrogen. The reduction is less efficient in N_2 atmosphere indicating that hydrogen plays a key role in the overall reduction process. The process is clearly mediated by the initial sorption of U(VI) onto the magnetite surface, followed by the reduction of the activated complex by the dissolved hydrogen. There is a clear decrease of the U(VI) concentration with increasing the partial pressure of H_2 as can be seen in the Fig. 1.7.

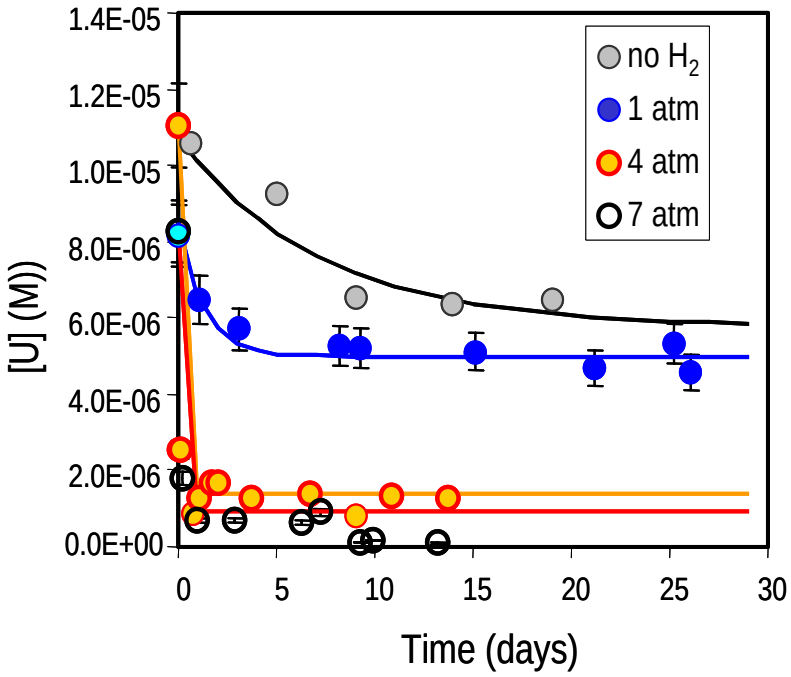

Fig. 1.7: Dependence of U(VI) removal by magnetite on partial pressure of H_2(g).

XANES data have been correlated with the fraction of U(VI) and U(IV) in reference materials for the purpose of calibration. The standards were meta-schoepite as a well characterised U(VI) solid, UO_2 as an end member for U(IV), U_3O_8 with a known proportion of U(VI) and U(IV) and a mixture of 50% schoepite and 50% UO_2. On the basis of the calibration line, the oxidation state of uranium has been determined in various samples, where the Fe-containing solids had been contacted with the uranium for different time periods (1 to 30 days) in anoxic (N_2) or reducing (H_2) atmosphere. The X-Ray absorption studies have been performed at ROBL /ESRF (Grenoble). The data indicate that the highest degree of reduction is attained for sample MH30B, this is with magnetite, under hydrogen atmosphere and reacting for 30 days in batch [25]. (UPC)

The rate and mechanism of redox reactions in the system $ActO_2^{2+} + e^- \leftrightarrows ActO_2^+$

Changes in redox state of the actinides plays perhaps the most important role for estimates of their transport (and sorption characteristics) in ground and surface water systems. We have explored inner-sphere mechanisms for the electron exchange using hydroxide, fluoride and carbonate as bridging ligands by using theoretical methods. The study is still under way but we can conclude that there is a significant decrease in the activation barrier between carbonate and the other two ligands [26]. This is consistent with an earlier observation (Ferri, Salvatore and Grenthe) that the U(VI)/U(V) redox potential in carbonate media is very stable. (KTH)

5.1.5 Computational actinide chemistry

Introduction

The experimental activities in this field were related to a number of EXAFS studies; the structure of U(VI) fluoride, hydroxide, carbonate, acetate, oxalate and malonate complexes in solution, the structure of Np(VII) under alkaline conditions and the structure of ternary Th and lanthanide glycolate complexes at high pH. Experimental studies have been made at ROBL-ESRF (Grenoble) in cooperation between KTH and FZR. The theoretical work is a effort within the KTH – theory network and also by UPC.

Solvent effects and ligand exchange reactions have been studied on U(VI) fluoride and hydroxide complexes by EXAFS and quantum chemical tools [27, 28, 29]. A fivefold coordination in the equatorial plane of UO_2^{2+} is derived from EXAFS for the complexes $UO_2F_n(H_2O)_{5-n}^{2n-}$ with n = 3-5, whereas $UO_2(OH)_4^{2-}$ has a square geometry both in the solid state and in solution. As shown in Fig. 1.8 a Density Functional Theory (DFT) calculation including solvent effects can not only reproduce the experimental bond distances, but also reflects the structural differences between the fluoride and hydroxide complexes very well. (KTH)

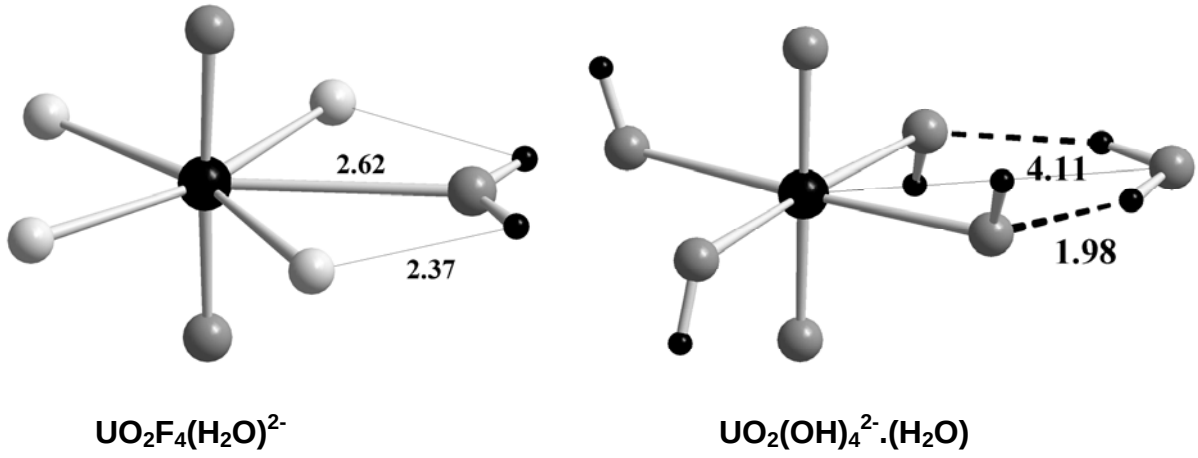

Fig. 1.8 Ab-initio calculation of $UO_2F_4(H_2O)^{2-}$ (left) and $UO_2(OH)_4^{2-}.(H_2O)$ (right). Note the different interaction of the water molecule with both complexes: In the fluoride complex the H_2O is directly coordinated to the U(VI), whereas in the hydroxo complex it is coordinated with reverse orientation to the hydroxo groups [27].

As shown for these systems, precise structural information has been provided by quantum chemical calculations also for U(VI) complexes with oxalate [30, 31] and for the interaction of Np(VI) and Np(VII) with hydroxide [32]. This was used to ascertain the accuracy of theory calculations of the structure of species in solution. The results were excellent, theory is able to predict even complicated structures within experimental accuracy. In addition, theory provides information about structural details that are not accessible by EXAFS, but that are very important for the understanding of chemical properties. In addition these studies have been used to ascertain the relative energy between isomers in solution, an activity that required extensive studies of the properties of different solvent models. We have been able to explain the observed differences in chemistry between hydroxide and fluoride complexes and also the experimental redox data in the Np(VII)/Np(VI) system.

A model has been developed within a cooperation (KTH + Valerie Vallet (TU München) + Ulf Wahlgren (University Stockholm)) that describes solution chemical thermodynamics with a much better accuracy than any method developed so far, the accuracy of our predictions is 10 kJ/mol, or better. The model has been tested on Zn(II) amine and U(VI) oxalate complexes [33].

The solubility of the tetravalent actinides is constant over a very broad pH range from around 4 to 12. The constant solubility means that the soluble species is uncharged and commonly formulated as $M(OH)_4(aq)$. It is well known that the coordination number of the tetravalent actinides is high and variable, for Th(IV) it ranges from 6 to 9 or perhaps even 10. If we assume that $M(OH)_4(aq)$ is a mononuclear species we must have additional coordinated water ligands in order to have a composition that is consistent with the known coordination number. However, in the experiments one cannot determine the number of coordinated water ligands. On the other hand we expect coordinated water ligands to be stronger acids than the bulk water, accordingly complexes with a negative charge should be formed in strongly alkaline solution. This is not found in the experimental studies. In order to resolve the problem we have investigated the system using quantum chemical methods and suggest that "$Th(OH)_4$" is a tetramer "$Th_4(OH)_{16}$" containing six-coordinated Th(IV). Such tetramer structures are known, and two important type structures are Te_4Cl_{16} and $[Al_4(OH)_{16}]Ba_2$. Using quantum chemical methods we have shown that the charge on the water protons in $Th(OH)_4(H_2O)_n$ is positive, supporting our expectation that the protons should dissociate at high pH. We were also able to show that the total energy change for the reaction $4Th(OH)_4 \rightarrow Th_4(OH)_{16}$ is strongly exothermic, an additional support of our hypothesis.

The DFT methods have been applied to predict the structure of uranyl complexes of relative complexity. The aim of this work has been to demonstrate that theoretical chemistry can be used as a complementary tool in determining geometric parameters of a number of uranyl complexes in solution, which are not observable by experimental methods. In addition, a plausible structures with partial geometric data from experimental results was proposed. A gradient corrected DFT methodology with relativistic effects has been used employing a COSMO solvation model. The theoretical calculations show good agreement with experimental X-ray and EXAFS data for the triacetato-dioxo-uranium (VI) and tricarbonato-dioxo-uranium (VI) complexes and are used to assign possible geometries for dicalcium-tricarbonato-dioxo-uranium (VI) and malonato-dioxo-uranium (VI) complexes. The results of this exercise indicate that carbonate bonding in these complexes is mainly bidentate and that hydroxo bridging plays a critical role in the stabilization of the polynuclear uranyl complexes. The calculations performed in this work are in good agreement with experimental EXAFS data for a series of uranyl carboxylate and carbonate complexes [34].(UPC)

The conclusions drawn from all these studies are very important for estimating the accuracy of theory when predicting thermodynamic properties of actinide complexes in solution. Many of these studies are the first of their kind and have received considerable interest from the theory community [35, 36]. We hope that also the waste management community will be able to consider these techniques to supplement experimental studies and to reduce their extent.

5.2 Work-package 2:

Thermodynamics of solid-water interface reactions (sorption phenomena)

Summary of the specific project objectives

To provide a thermodynamic basis for the quantification of sorption reactions of actinide ions onto mineral phases, the reactions at the solid-water interface are being studied by a combination of classical wet-chemistry and direct speciation methods. The species of U(VI), Cm(III) and Ln(III) at the solid-water interface for simple model mineral phases (e.g., alumina, silica, goethite, magnetite, illite, etc) are being characterised and quantified by e.g., laser fluorescence spectroscopy (TRLFS) and X-ray absorption fine structure spectroscopy (EXAFS). Based on this molecular-level process understanding, appropriate thermodynamic sorption models will be developed. A composite approach is generated for the description of U(VI) sorption to natural rock.

Structure of the work-package and contributing partners

5.2.1 Sorption of uranium and plutonium onto iron metal oxides (CIEMAT)

5.2.2 Sorption of Eu(III), Cm(III) and U(VI) onto clay minerals (PSI)

5.2.3 Sorption of U(VI) onto rock-forming mineral phases (FZR)

5.2.4 Spectroscopic study on surface interaction mechanism for actinides (FZK)

5.2.1 Sorption of uranium and plutonium onto iron metal oxides (CIEMAT)

Introduction

The aim of this work was to study the sorption of uranium and plutonium onto two important iron oxides: magnetite and goethite. In particular, the final objective of the work is to understand the sorption mechanisms of the above mentioned radionuclides on these oxides at the canister/bentonite interface.

Magnetite is the most important end member of iron corrosion products under reducing environment, which is the condition expected in a deep geological high level radioactive waste disposal. Apart from magnetite, goethite, hematite and siderite have also been reported as possible corrosion products of steel canisters under repository conditions. In particular, goethite (α-FeOOH) is a ferric hydroxide very common in nature and, since it is one of the thermodynamically most stable at room temperature, it is expected to be the main end member of many iron oxide transformations in a wide range of environmental conditions. Both oxides were synthesised in the laboratory, under controlled conditions, and their main physico -chemical properties (composition, microstructure, surface area and surface charge) were analysed as a previous step to sorption experiments. The stability of the oxides, under the conditions used in sorption studies, was also investigated.

In the first part of the project, the sorption behaviour of the selected radionuclides was studied in a "simple system" (solid + simple electrolyte). The sorption behaviour of the radionuclides onto these oxides was studied under O_2 and CO_2 - free atmosphere and in a wide range of experimental conditions (pH, ionic strength, radionuclide and solid concentration), in order to assess the validity of different surface complexation models, available for the interpretation of sorption data.

In order to study in more realistic conditions the sorption behaviour of radionuclides at the canister/bentonite interface ("complex system"), a simplified water simulating a resaturated bentonite pore water was also produced. The chemical characteristics of this synthetic water are: neutral pH (7), relatively high ionic strength ($I \cong 0.15$) and reduced Eh ($\cong$-100 mV; 100 mV). Calculations for the radionuclides equilibrium in this synthetic water and theoretical studies about the possible influence of the competing ions for sorption have been carried out prior to the experimental work. Furthermore, since the Eh is the most difficult parameter to control in this synthetic water, the possible effects of the Eh variation were studied. It has been found that possible competing ions to sorption are mainly carbonates in the case of uranium and carbonates/sulphates in the case of plutonium.

Uranium (VI) sorption

The kinetics of the adsorption of U(VI) and the kinetics of the actinide reduction to a lower oxidation state, in presence of the oxides, were studied by means of batch sorption techniques and x-ray photoelectron spectroscopy (XPS) analysis. The combination of batch sorption experiments and XPS allowed the differentiation the kinetics of sorption, redox and precipitation processes occurring in the oxide/electrolyte system.

Whereas for the goethite system no evidence was found for a reduction of U(VI) over long time periods [37], in the case of magnetite a partly reduction to U(IV) after 4 months was deduced from the sorption data and XPS results [38, 39]. The sorption process on both mineral surface followed a very fast kinetics (hours). XPS measurements showed that the speciation of uranium at the surface does not show significant changes with time (from 1 day to 3 months), as well as the quantity of uranium detected at the surface Besides U(VI) and U(IV) phases, mixed phases, like U_3O_8, were clearly observed.

The surface speciation depends on the initial pH of the contact solution. The pH-edge of the U sorption onto magnetite is shown in Fig. 2.1 at various ionic strength as a function of equilibration time. Only after 4 month equilibrating time the sorption is strongly increased especially at low pH due to reduction of U(VI) to U(IV).

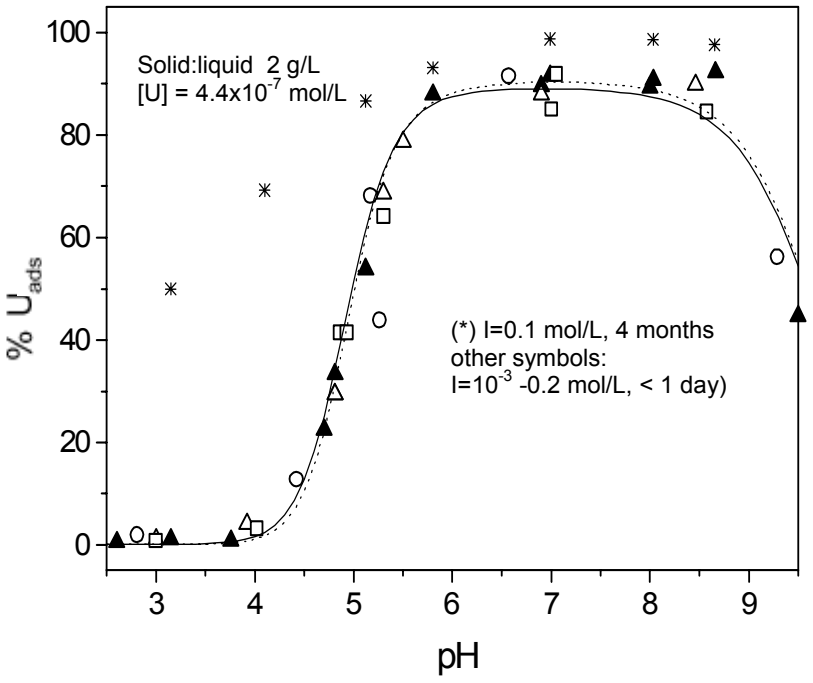

Fig. 2.1: U(VI) sorption on magnetite under anaerobic conditions at various ionic strength and equilibration times. The lines corresponds to the modeling of experimental data at I = 0.1 mol/L: (----) Model 1 and (——) Model 2 (see text) [38].

Considering that the Eh of equilibrium between magnetite and the solution, under our experimental conditions, was slightly positive (between 50 and 100 mV), the uranium reduction would also be possible from thermodynamic reasons within the liquid phase. However, the kinetics of reduction in the liquid occur at a much slower rate which, in turn, depends on the attainment of the magnetite/solution equilibrium. The decrease of uranium in solution, observed after the uranyl adsorption stage, and particularly at acidic pH, is most probably due to the precipitation of U(IV) formed in the solution.

The ionic strength did not significantly affect the uranyl sorption on both oxides. This may indicate the formation of inner sphere complexes. Finally, sorption isotherms showed a Langmuir-type behaviour. Uranium sorption data were fitted considering only one type of surface site and evaluating three simple models. The dominant charged species (UO_2^{2+} and UO_2OH^+), in the region where most of the adsorption takes place (pH<5), were considered to form the surface complexes. Model 1 considered the formation of two single monodentate complexes:

$$SOH + UO_2^{2+} \Leftrightarrow SOUO_2^+ + H^+ \qquad K_c^1$$

$$SOH + UO_2OH^+ \Leftrightarrow SOUO_2OH + H^+ \qquad K_c^2$$

Model 2 considered the formation a binuclear bidentate complex:

$$2SOH + UO_2^{2+} \Leftrightarrow (SO)_2UO_2 + 2H^+ \qquad \beta_c^1$$

the addition of a second complex did not improve at all the fit.

A third model, used in the case of goethite, considered the reactions of Model 1 but the double layer correction (electrostatic term) was not taken into account (Non - Electrostatic model). All the models simulated the sorption isotherms in a similar way. The variation with the pH and the ionic strength could be accounted for with the three models, but Model 2 failed in describing the curve at low solid concentrations. This showed that even if, in a limited data set, different models can be considered equivalent, they have to be validated on the widest range of experimental conditions. In particular, the experimental study of the sorption dependence on the solid to liquid ratio is a very important point to be considered.

To evaluate the "general" applicability of the two models that better fit our experimental data, they were applied to Hsi and Langmuir's (1985) uranium sorption data onto goethite without any change of the model parameters. The models were capable to reproduce the adsorption edges even though they tended to slightly underestimate the sorption in the region where sorption is nearest to 100 % (pH>6).

Complementary HRTEM experiments with natural uranium at high loading indicated that the uptake of uranium affects the internal structure of goethite crystals whereas the same effects is not seen in magnetite.

Plutonium sorption

A large series of preliminary experiments (with and without the solid phases) was carried out to find an adequate methodology for the sorption studies with Pu. These preliminary experiments concerned: a) the sorption behaviour of Pu on various vessel materials; b) the analysis of colloids formation, as a function of pH and different Pu concentrations; c) the optimisation of the conditions for sorption studies in neutral to mildly alkaline solutions (bentonitic environment). An additional experiment for the evaluation of the importance of the actinide colloidal phase onto the shape of the sorption edge was carried out with magnetite, trying to separate the solid phase by a magnetic field instead of ultra-centrifugation.

The results of the experiments in the “simple system” showed that the sorption edge of plutonium (Pu(IV) was initially added as tracer) occurs between pH 3 and 4 when using goethite as a sorbing surface and between pH 4 and 5 when magnetite is used. Sorption seems to be quantitative for pH values above 5. Data were modelled using a simple surface complexation approach, using a non-electrostatic model [40].

In the case of goethite, taking into account the short contact times used for the experiments (hours), a reduction process was considered unlikely and only the sorption of tetravalent Pu was considered. The sorption model for goethite consider the formation of surface complex with $Pu(OH)_2^{2+}$ and $Pu(OH)_4(aq)$. The formation of $Goe\text{-}O\text{-}Pu(OH)_2^{+}$ and $Goe\text{-}O\text{-}Pu(OH)_3$ were able to explain macroscopically the behaviour of the system.[40]

The sorption onto magnetite was also initially modelled by assuming the sorption of tetravalent plutonium; however, the results were not in good agreement with the experimental data. Thus, a reduction process of Pu(IV) to Pu(III) in the presence of magnetite, due to the interaction of the actinide with the ferrous iron present in the solid surface is implemented. $Mag\text{-}OPu(OH)_3$ and $Mag\text{-}OPu^{2+}$ were the species assumed to explain the sorption data.

The modelling was initially done assuming mildly anoxic conditions (Eh = 200-250 mV) but given that a redox sensitive element is used, the sensitivity of the system to the redox potential in solution is of the utmost relevance. For this reason a sensitivity analyses of the behaviour as a function of the Eh was also carried out.

5.2.2 Sorption of Eu(III), Cm(III) and U(VI) onto clay minerals (PSI)

Introduction

Clay minerals are an important component in the argillaceous rock formations being viewed in a number of European waste management programmes as suitable for the deep geological disposal of radioactive waste. (Opalinus Clay, Switzerland; Boom and Ypresian Clay, Belgium; Spanish Reference Clay, Spain; Callovo-Oxfordian and Toarcian, France).

Illite is one important component of argillaceous host rock. In order to allow the quantitative assessment of fission product and actinide migration in such formations, sorption data are of high interest. Following the methodology of recent study on montmorillonite [41], the sorption of Eu(III) as a representative for trivalent actinides and of U(VI) have been investigated. A publication of the results is in preparation [42].

Experimental Details

Illite du Puy, obtained from the region of Le Puy en Verlay, France, was powdered, converted to the Na-form and conditioned to a $NaClO_4$ background electrolyte. The acid/base characteristics of Na-illite suspensions in 0.01, 0.1 and 0.5 M $NaClO_4$ solutions were determined in the pH range between 2.5 and 11.5 by batch back titration experiments under inert atmosphere conditions. To correct for the mineral dissolution the cation concentrations were determined for each pH value in the supernatant of the centrifuged solutions. The conditioning, pH titration procedure and data analysis methodology used for the illite are essentially the same as described previously for montmorillonite (Schulthess & Sparks 1986).

Sorption edge data for Eu at $NaClO_4$ concentrations of 0.5, 0.1 and 0.01 M, and sorption isotherms at 0.1 M $NaClO_4$, pH~7 and 5, were measured. Similar data sets were collected for U(VI): sorption edges at 0.1 and 0.01 M $NaClO_4$ and sorption isotherms at pH= 5.8, 5.3 and 4.9. Sorption times were generally 7 days. Kinetic tests had shown to be sufficient to reach equilibrium. Supernatant solutions were analysed from experiments made under similar conditions to the sorption edge measurements but with no activity added.

Acid base properties of the illite

The modelling of titration results in terms of the protolysis behaviour of edge surface hydroxyl functional groups (>SOH sites) is complicated, especially at pH values below 4 where a number of proton consuming processes are not accounted for in the back titration measurements (see Bradbury & Baeyens 1997) and cannot be properly corrected for. The measurements made in this work and some previous work by Poinssot et al (1999) show clearly that illite is dissolving and that a release of Ca occurs. The inventory of Ca is ~50 mmol/kg and only a few mmol/kg of this are present as exchangeable Ca on the illite after the end of conditioning at 0.1 M $NaClO_4$ and pH=7. This Ca, and the released Al, undergo cation exchange on the illite planar sites, further complicating the chemistry. Also it is unlikely that the proton consumption during the dissolution of the clay in the forward titration is the same as the proton consumption in the back titration because the dissolved clay phase can never be reconstituted. Thus, there are two different processes occurring in the forward and back directions which do not therefore compensate one another. Consequently, though some processes are known in detail and can be quantified (e.g. Al exchange, Bradbury & Baeyens 2003), others cannot. Hence the form of the titration curve below pH=4 is unclear. In contrast, the data measured at high pH seem to be less disturbed by additional processes even though the clay is dissolving.

Eu(III) sorption onto illite

As discussed by Bradbury & Baeyens (1997) the development of a sorption model and the definition of the associated parameters is an iterative process involving the titration data and the sorption edges and isotherms measured under different conditions. Therefore, a modelled curve for the titration data is not just the result of considering the titration data alone but all of the available measured data together.

Montmorillonite and illite have essentially the same structures consisting of a two dimensional array of aluminium-oxygen-hydroxyl octahedra sandwiched between a two dimensional array of silica-oxygen tetrahedra (TOT class of clay minerals). They were considered to be sufficiently structurally similar to justify the premise that essentially the same protolysis and sorption models (with minor variations) could be valid for both systems i.e. the 2SPNE plus cation exchange model, Bradbury & Baeyens (1997).

After a series of iterations a "best set "of parameter values for site capacity and protolysis constants for the two site types, $\equiv S^{W1}OH$ and $\equiv S^{W2}OH$ have been derived (Table 2.1). The approach adopted to model the sorption data on Na-illite was the same throughout. The procedures outlined below are a somewhat simplified version of the iterative process actually used. (Further details can be found in Bradbury and Baeyens, 1997). In the acid region of sorption edges where R_d values were observed to be constant and independent of pH, the uptake of the particular sorbate was generally interpreted as being due to cation exchange on the permanently charged planar sites and was characterised by a derived selectivity coefficient, Table 2.2, following the Gaines and Thomas (1957) approach. Site types, their individual capacities and the protolysis constants associated with them, were considered to be non-adjustable parameters and were fixed in all further calculations at the values given in Table 2.1.

Table 2.1: Summary of site types, site capacities and protolysis constants determined for Na-illite.

Site types:	Site capacities:
$\equiv S^{S}OH$	2.0×10^{-3} mol kg^{-1}
$\equiv S^{W1}OH$	4.5×10^{-2} mol kg^{-1}
$\equiv S^{W2}OH$	4.5×10^{-2} mol kg^{-1}
Surface complexation formation reactions	log K_{int}
$\equiv S^{S}OH + H^{+} \Leftrightarrow \equiv S^{S}OH_2^{+}$	5.5
$\equiv S^{S}OH \Leftrightarrow \equiv S^{S}O^{-} + H^{+}$	-6.2
$\equiv S^{W1}OH + H^{+} \Leftrightarrow \equiv S^{W1}OH_2^{+}$	5.5
$\equiv S^{W1}OH \Leftrightarrow \equiv S^{W1}O^{-} + H^{+}$	-6.2
$\equiv S^{W2}OH + H^{+} \Leftrightarrow \equiv S^{W2}OH_2^{+}$	9.0
$\equiv S^{W2}OH \Leftrightarrow \equiv S^{W2}O^{-} + H^{+}$	-10.5

As an illustrative example consider a metal M of valency Z_M. The initial step was to calculate the aqueous speciation of M in the pH range and for the background electrolyte used in the sorption measurements. In the pH range where the dominant aqueous species was the free M^{z_M+} cation, the first and simplest surface complexation reaction to be considered was:

$$\equiv S^{S}OH + M^{z_M+} \Leftrightarrow \equiv S^{S}OM^{(z_M-1)+} + H^{+} \qquad \text{(Eqn. 2.1)}$$

The situation often arose that the rising edge of the sorption curve and the sorption plateau could not be fitted simultaneously with a single reaction: any approximate fit to the first resulted in a substantial underestimate in the second. In this case the procedure was to find the

best fit for the free metal cation to part of the edge, Eqn. 2.1, and then fix this surface complexation constant in the following modelling steps. Next, a surface reaction with the first hydrolysis species was considered, Eqn. 2, and the process repeated and so on for the second, Eqn. 3 , third, Eqn. 4, etc hydolysis species until a satisfactory fit to the whole sorption edge was obtained.

$$\equiv S^sOH + M^{z_M+} + H_2O \Leftrightarrow \equiv S^sOMOH^{(z_M-2)+} + 2\,H^+ \qquad \text{(Eqn. 2.2)}$$

$$\equiv S^sOH + M^{z_M+} + 2\,H_2O \Leftrightarrow \equiv S^sOM(OH)_2^{(z_M-3)+} + 3\,H^+ \qquad \text{(Eqn. 2.3)}$$

$$\equiv S^sOH + M^{z_M+} + 3\,H_2O \Leftrightarrow \equiv S^sOM(OH)_3^{(z_M-4)+} + 4\,H^+ \qquad \text{(Eqn. 2.4)}$$

An iterative procedure then follows to find the best fit to the data and "fine tune" the surface complexation constants. As in previous cases (Bradbury and Baeyens 1997) it was found that with sorption edges presented in the log R_d versus pH form, the fits to the data are rather sensitive to the surface complexation constants chosen and that fitting by eye worked quickly and well for the stepwise procedures used. Where isotherms or sorption edges at high sorbate concentrations were modeled, a similar modelling procedure to that given above was applied to the weak sites.

A Eu sorption edge and isotherm are given in the Fig. 2.2 (a) and (b). The solid lines are the modelled curves using the Eu-Na selectivity coefficient and the surface complexation reactions and corresponding constants given in Table 2.2.

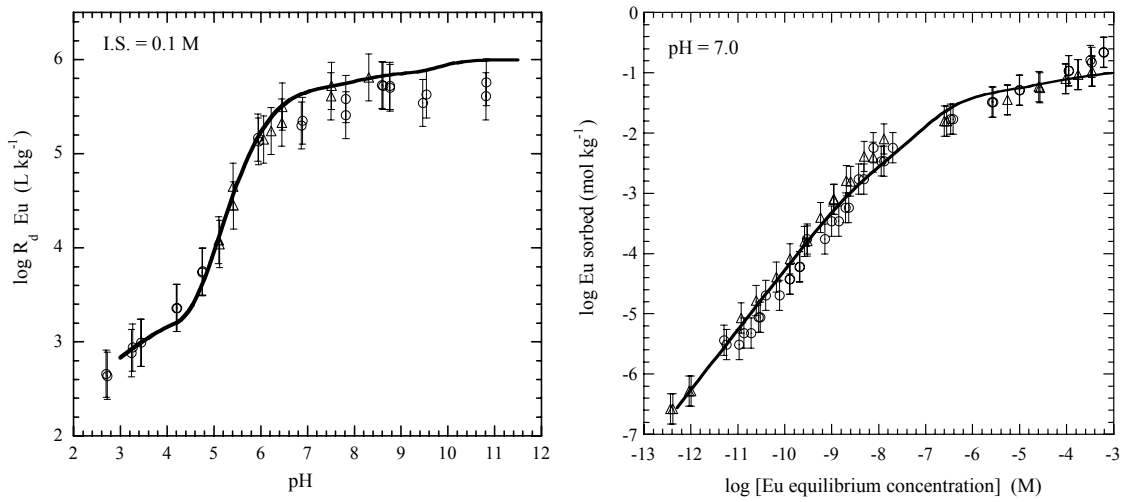

Figure 2.2: Eu sorption (a) edge and (b) isotherm on Na-illite at 0.1 M $NaClO_4$. The solid lines are calculated using the model parameters given in Table 2.1. and 2.2.

TRLFS speciation of Cm(III) sorped onto illite (FZK /PSI)

The sorption study of Cm(III) onto illite du Puy by TRLFS was done as a cooperation between PSI and FZK. By using this spectroscopic method outer-sphere complexation via ionic exchange dominating the Cm(III)/Eu(III) sorption at low pH can clearly be distinguished from inner-sphere complexation. Emission spectra and lifetimes were derived for $2 \cdot 10^{-7}$ mol/L Cm(III) in 0.25 g/L illite and 0.1 M $NaClO_4$ solution between pH 4 and 12. Within this pH range three inner-sphere surface complexes have been identified, which show similar characteristics like the species found at the γ-Al_2O_3 interface. It was concluded that the Cm(III) is bound to monodentate aluminol groups at the edge of the clay layer. With increasing pH ternary hydroxo complexes are formed as in the case of γ-Al_2O_3 (see Fig. 2.3). Good correspondence was found between an Eu(III) sorption edge measured on Na-illite suspended

in 0.1 M $NaClO_4$ and one deduced for Cm(III) from TRLFS measurements under similar conditions.

In the same context, a sorption study of Cm(III) onto montmorillonite was performed in bilateral collaboration between PSI and FZK outside the ACTAF project [43]. Similar results were achieved as obtained for the illite system.

Table 2.2: Summary of surface complexation constants and selectivity coefficients for the sorption of Eu on Na-illite.

Cation exchange reaction	K_c
3 Na-illite + Eu^{3+} ⇔ Eu-illite + 3 Na^+	76
Surface complexation formation reactions on strong sites	**log K_{int}**
$\equiv S^SOH + Eu^{3+} \Leftrightarrow \equiv S^SOEu^{2+} + H^+$	3.1
$\equiv S^SOH + Eu^{3+} + H_2O \Leftrightarrow \equiv S^SOEuOH^+ + 2\ H^+$	-5.0
$\equiv S^SOH + Eu^{3+} + 2\ H_2O \Leftrightarrow \equiv S^SOEu(OH)_2^o + 3\ H^+$	-14.5
$\equiv S^SOH + Eu^{3+} + 3\ H_2O \Leftrightarrow \equiv S^SOEu(OH)_3^- + 4\ H^+$	-24.0
$\equiv S^SOH + Eu^{3+} + 4\ H_2O \Leftrightarrow \equiv S^SOEu(OH)_4^{2-} + 5\ H^+$	-34.5
Surface complexation formation reaction on weak sites	**log K_{int}**
$\equiv S^{W1}OH + Eu^{3+} \Leftrightarrow \equiv S^{W1}OEu^{2+} + H^+$	0.1
$\equiv S^{W1}OH + Eu^{3+} + H_2O \Leftrightarrow \equiv S^{W1}OEuOH^+ + 2\ H^+$	-5.7

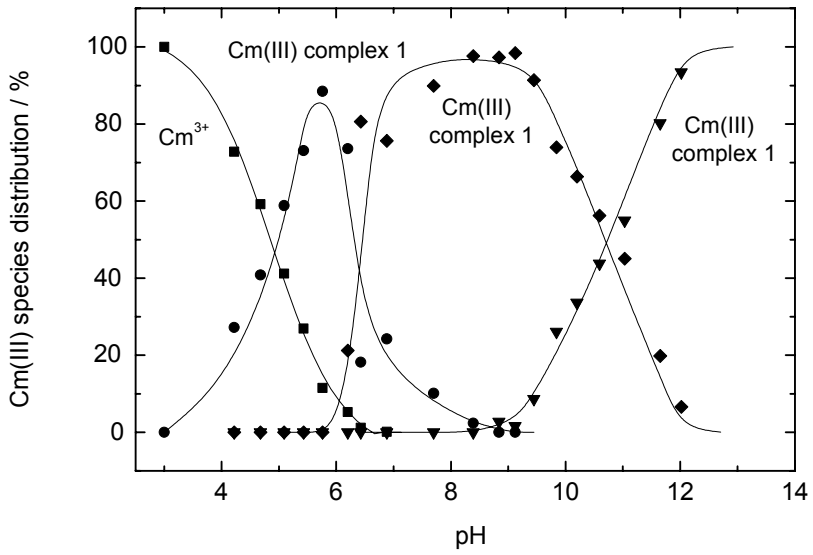

Fig. 2.3: Species distribution for the Cm(III) sorption onto illite; 2 E-7 mol/L Cm(III), 0.25 g/L illite, 0.1 M $NaClO_4$

Sorption of U(VI) onto illite

At the moment only the U(VI) sorption edge at 0.1 M $NaClO_4$ could be modelled, (see Fig. 2.4). Preliminary surface complexation reactions and constants and a selectivity coefficient for UO_2^{2+} exchange on Na-illite are given in the Table 2.3.

Table 2.3: Mass action equations and associated constants used in the modelling of U(VI) on Na-illite.

Cation exchange reaction	K_c(I.S.=0)
2 Na-illite + UO_2^{2+} ⇔ UO_2-illite + 2 Na^+	4.5
Surface complexation formation reactions on strong sites	**log K_{int}**
$\equiv S^SOH + UO_2^{2+} \Leftrightarrow \equiv S^SO\ UO_2^+ + H^+$	2.6
$\equiv S^SOH + UO_2^{2+} + H_2O \Leftrightarrow \equiv S^SO\ UO_2OH^o + 2\ H^+$	-3.9
$\equiv S^SOH + UO_2^{2+} + 2\ H_2O \Leftrightarrow \equiv S^SO\ UO_2(OH)_2^- + 3\ H^+$	-10.3
$\equiv S^SOH + UO_2^{2+} + 3\ H_2O \Leftrightarrow \equiv S^SO\ UO_2(OH)_3^{2-} + 4\ H^+$	-17.5

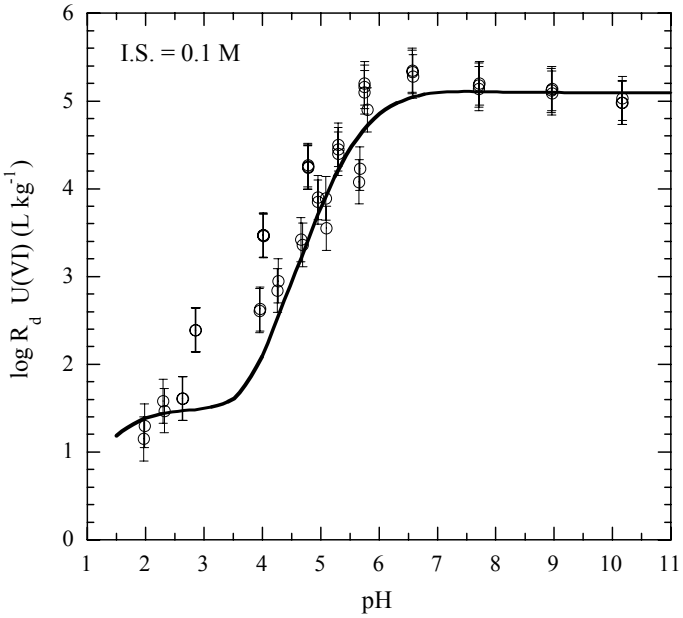

Fig. 2.4: U(VI) sorption pH edge measurements and modelling in 0.1 M $NaClO_4$.

The dominant sorption mechanism relevant for the U(VI) sorption edge measured at 0.01 M $NaClO_4$ is thought to be cation exchange of U(VI), but influenced by competing cations arising from the dissolution of the Na-illite. Modelling of the sorption isotherms measured for U(VI) was not attempted because of step changes in the sorption at certain combinations of concentration and pH. This behaviour was very reproducible but the cause is not yet understood. Further work will be required to explain the sorption edge results at 0.01 M $NaClO_4$ and to understand the form of the isotherms.

EXAFS characterisation of U(VI) sorped onto illite

Four samples of Na-lllite with U(VI) loadings between 750 and 1650 ppm were prepared at pH = 5 and ph = 6 in an 0.1 M $NaClO_4$ background electrolyte with reaction times of 7 days for EXAFS investigations at the Rossendorf beamline (ROBL), ESRF. The radial structure

functions (RSFs, uncorrected for phase shift) of k^3-weighted L_{III}-edge EXAFS spectra of uranyl treated illite are shown below. The figure shows that there are peaks at R + ΔR ~ 1.4 Å and ~ 1.8 Å (peaks A and B), R + ΔR ~ 2.5 Å (peak C), and at R + ΔR ~ 3.0 Å (peak D). The intensity and position of the peaks remain essentially unchanged by varying the pH and initial U(VI) concentration indicating that the uptake mechanism under the chosen experimental conditions is not affected by these parameters.

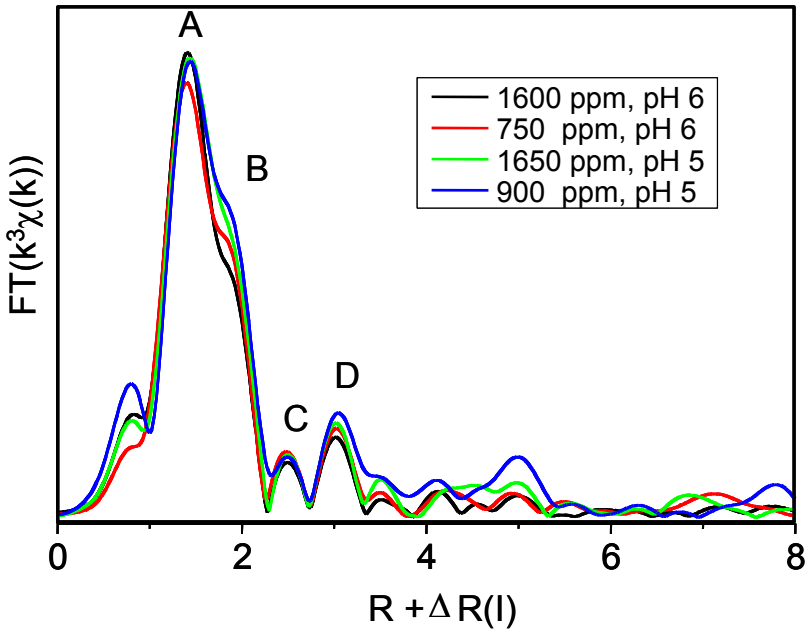

Fig. 2.5: RSFs of k^3-weighted U L_{III}-edge EXAFS spectra for U sorbed onto illite at pH 5 and 6 and various U concentrations.

Data analysis reveals that the uranium atoms in all samples are coordinated by 2 axial oxygen atoms (O_{ax}, Peak A) at a distance of ~1.78 Å. The multiple-scattering (MS) path of the uranyl moiety was linked during data analysis to the U-O_{ax} scattering parameters as described by [Hudson et al. (1996)] without introducing additional variable fit parameters. The distances between the uranium and equatorial oxygen atoms (O_{eq}, Peak B) vary slightly between 2.27 Å and 2.29 Å and the coordination numbers N (U-O_{eq}) are in the range of 4.9 to 5.7. These U-O_{eq} distances are far from values for mononuclear outer-sphere uranyl aquo-complexes with U-O_{eq} distances of 2.41 Å–2.43 Å obtained at lower pH values (this study, Dent et al., (1992), Chisholm-Brause et al. (1994)). The short U-O_{eq} distances indicate that an inner-sphere complexation process dominates the sorption under the experimental conditions used. This finding is supported by analyzing the structural origin of peak D. Data analysis indicates that peak D is caused by U-Al/Si backscattering pairs (1-2 U-Al/Si pairs at 3.35 – 3.38 Å).

The origin of peak C is not yet resolved. Peak C could be fitted equally well with an oxygen shell (2.9 Å) or a carbon shell (2.9 Å). The uranium-carbon distance is typical for bidentate coordinated carbonate, as in ternary U(VI)-carbonato surface complexes [Bargar et al. (2000)]. The experimental conditions, i.e., N_2 atmosphere, pH 5, and 0.1 M $NaClO_4$, make, however, the formation of U(VI)-carbonato surface species unlikely. It is foreseen in the upcoming ROBL beamtime (January 2004) to test this hypothesis by preparing some U(VI)/ illite samples under atmospheric conditions.

Further, it is considered to be unlikely that peak C is caused by a long oxygen shell (2.9 Å), since to the best of our knowledge such long O distances have never been observed for U(VI) sorbed on clay minerals. Typical long U-O distances observed in the literature normally vary from 2.45 to 2.49 Å [Barger et al. (2000); Sylwester et al. (2000); Thompson et al. (2000)].

To verify whether polynuclear species play a role in the U(VI)/illite uptake system two 10^{-2} M U(VI) solutions at pH 2 and 5 were prepared. In the pH 5 sample a peak is present at R + ΔR ~ 3.7 Å which is caused by U-U back scattering pairs. Data analysis reveals that the U-U peak consists of ~0.6 U-U pairs at 3.86 Å. Since this peak is absent in all of the samples of U(VI) sorbed on illite, the formation of polynuclear species and/or the formation of an U(VI) precipitate can be excluded under the chosen experimental conditions. (PSI)

References

Bargar, J.R., R. Reitmeyer, J.J. Lenhart, and J.A. Davis, *Characterization of U(VI)-carbonato ternary complexes on hematite: EXAFS and electrophoretic mobility measurements.* Geochim. Cosmochim. Acta, 2000. **64**(16): p. 2737-2749.

Bradbury, M. H. and Baeyens, B. (1997). A mechanistic description of Ni and Zn sorption on Na-montmorillonite. Part II: Modelling. J. Contam. Hydrol. 27, 223-248.

Chisholm-Brause, C.J., S.D. Conradson, C.T. Buscher, P.G. Eller, and D.E. Morris, *Speciation of uranyl sorbed at multiple binding sites on montmorillonite.* Geochim. Cosmochim. Acta, 1994. **58**: p. 3625-3631.

Dent, A.J., J.D.F. Ramsay, and W. Swanton, *An EXAFS study of uranyl ion in solution and sorbed onto silica and montmorillonite clay colloids.* J. Colloid Interface Sci., 1992. **150**: p. 45-60.

Gaines G. I. and Thomas H. C. (1953). Adsorption studies on clay minerals. II. A formulation of the thermodynamics of exchange adsorption. J. Chem. Phys. 21, 714-718.

Hudson, E.A., P.G. Allen, T. J., M.A. Denecke, and T. Reich, *Polarized x-ray-absorption spectroscopy of the uranyl ion: Comparison of experiment and theory.* Physical Review B, 1996. **54**(1): p. 156-165.

Poinssot, C., Baeyens, B., Bradbury, M.H. (1999). Experimental and modelling studies of caesium sorption on illite. Geochim. Cosmochim. Acta. 63, N019/20, pp. 3217 - 3227.

Schulthess, C.P. and Sparks, D.L. (1986). Back titration technique for proton isotherm modelling of oxide surfaces. Soil Sci. Soc. Am. J., 50: 1406-1411.

Sylwester, E.R., E.A. Hudson, and P.G. Allen, *The structure of uranium (VI) sorption complexes on silica, alumina, and montmorillonite.* Geochim. Cosmochim. Acta, 2000. **14**: p. 2431-2438.

Thompson, H.A., G.E. Brown Jr., and G.A. Parks, *XAFS spectroscopic study of uranyl coordination in solids and aqueous* solution. American Mineralogist, 1997. **82**: p. 483-496.

5.2.3 Sorption of U(VI) onto rock-forming mineral phases (FZR)

Introduction

The sorption of U(VI) onto the rock phyllite was studied by conducting batch sorption experiments with the rock phyllite and with the mineralogical rock constituents of the phyllite, i.e. the minerals quartz, chlorite, muscovite and albite feldspar. The sorption experiments were then used to determine surface complex formation constants between the aqueous uranyl(VI) and the respective mineral phases. The surface complexation model used was the Diffuse Double Layer Model (DDLM). In addition, the phyllite forming minerals were studied in respect to the formation of secondary iron phase. This turned out to be important for the mineral chlorite, because small amounts of ferrihydrite form during the batch sorption experiments. Based on the mineralogical phyllite composition the uranyl(VI) sorption on phyllite was then predicted and compared with the experimental sorption data.

Sorption onto phyllite and its mineralogical constituents

The basis for the successful interpretation of the experimental sorption data of uranyl(VI) on phyllite, which is composed of 48 Vol. % quartz, 25 Vol. % chlorite, 20 Vol. % muscovite, 5 Vol.% albite feldspar, and 2 Vol. % opaque material, mostly rutile, magnetite, and traces of hematite, were:

(1.) the determination of surface complex formation constants of uranyl with quartz, chlorite, muscovite, albite, and ferrihydrite, respectively, in individual batch sorption experiments, shown in Table 2.4.

(2.) the determination of surface acidity constants of quartz, chlorite, muscovite, and albite, obtained from separate acid base titration [44, 45]

(3.) the determination of surface site densities of quartz, chlorite, muscovite and albite evaluated independently of each other with adsorption isotherms and

(4.) the quantification of the secondary phase ferrihydrite, which formed during the batch sorption experiments with phyllite.

The surface complex formation constants and the protolysis constants were optimized by using the experimentally obtained data sets and the computer code FITEQL (Herbelin, A. and Westall, J., 1996). Surface site densities were evaluated from adsorption isotherms at pH 6.5 and a total uranium concentration of 1×10^{-4} M. The formation of ferrihydrite during the batch sorption experiment was identified by Mössbauer spectroscopy, showing a 2.8 percent increase of Fe^{3+} in the phyllite powder. The newly formed ferrihydrite was present as Fe nano-particles or agglomerates with diameters ranging from 6-25 nm.

FITEQL calculations were carried out for a composite phyllite which was assembled from the respective mineral components quartz, chlorite, muscovite, and albite in their relative proportion within the phyllite, and in addition with the newly forming phase ferrihydrite.

Fig. 2.6 shows the modelled sorption curve together with the experimental sorption data of phyllite. It is noteworthy that the predicted sorption curve of the phyllite is based exclusively on surface complex formation and surface acidity constants obtained from individual batch experiments with pure mineral phases. No experimental data of phyllite were used for the optimization procedure. A detailed description of the conducted experiments is given in [44].

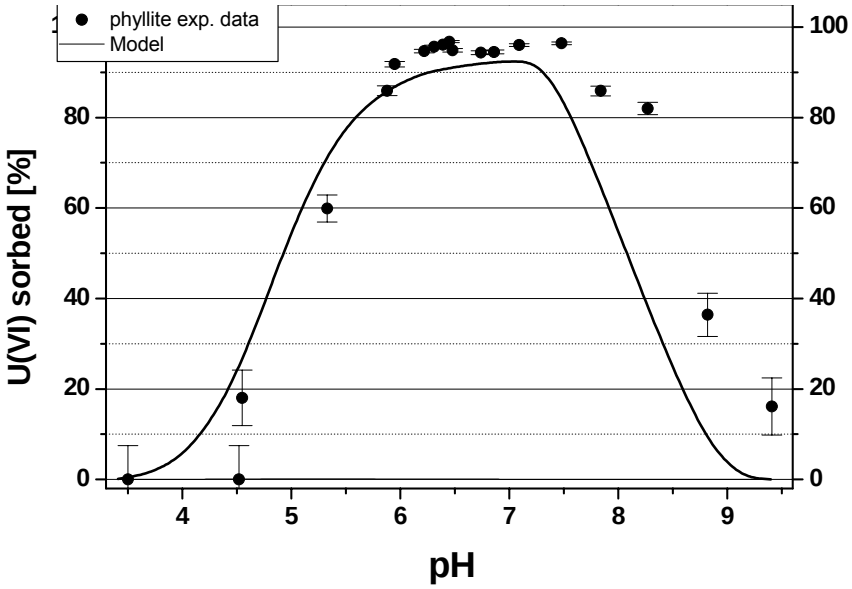

Fig. 2.6: Experimental data of uranium(VI) sorption on phyllite compared with predicted values.

Table 2.4: Surface complex formation constants (I = 0) of uranyl(VI) with mineralogical components of phyllite and granite.

Mineral	Reaction	log K	Ref
Quartz	$X(OH)_2 + UO_2^{2+} = (XO_2UO_2) + 2H^+$	-5.51	[44]
Chloride	$XOH + UO_2^{2+} = (XOUO_2)^+ + H^+$	4.71	[44]
Biotite	$X(OH)_2 + UO_2^{2+} = (XO_2UO_2) + 2H^+$ $XOH + UO_2^{2+} = (XOUO_2)^+ + H^+$	-5.73 2.37	
Muscovite	$X(OH)_2 + UO_2^{2+} = (XO_2UO_2) + 2H^+$ $XOH + UO_2^{2+} = (XOUO_2)^+ + H^+$	-0.55 -5.75	[44] [44]
Orthoclase	$XOH + UO_2^{2+} = (XOUO_2)^+ + H^+$	-0.65	
Albite	$XOH + UO_2^{2+} = (XOUO_2)^+ + H^+$	1.54	[44]
Ferrihydrite	$Fe_s(OH)_2 + UO_2^{2+} = Fe_sO_2UO_2 + 2H^+$ $Fe_s(OH)_2 + UO_2^{2+} = Fe_sO_2UO_2 + 2H^+$ $Fe_s(OH)_2 + UO_2^{2+} + CO_3 = Fe_sO_2UO_2CO_3 + 2H^+$ $Fe_s(OH)_2 + UO_2^{2+} + CO_3 = Fe_sO_2UO_2CO_3 + 2H^+$	-3.18 -6.31 3.67 -0.42	[44] [44] (Waite 1994)

Sorption onto granite and its mineralogical constituents

The granite system was studied analogous to the phyllite rock system by conducting batch sorption experiments with the rock itself and with the main mineralogical rock constituents, i.e. the minerals quartz, albite, orthoclase, muscovite and biotite [46]. Surface site densities were evaluated from adsorption isotherms at pH 6.5 and a total uranium concentration of $1x10^{-4}$ M.In addition, the granite forming minerals were studied in respect to the formation of secondary iron phases.

The sorption of uranyl(VI) on granite was predicted over a pH range from 3.5 to 9.5 and then compared with experimental uranyl(VI) sorption data on granite (see Fig. 2.7). The predictions were obtained by the superpositioning of simultaneously occurring, with each other competing, surface reactions of the mineralogical granite rock constituents (46 Mass % quartz, 25 Mass % orthoclase, 20 Mass % albite, 4.5 Mass % biotite, and 3.5 Mass %

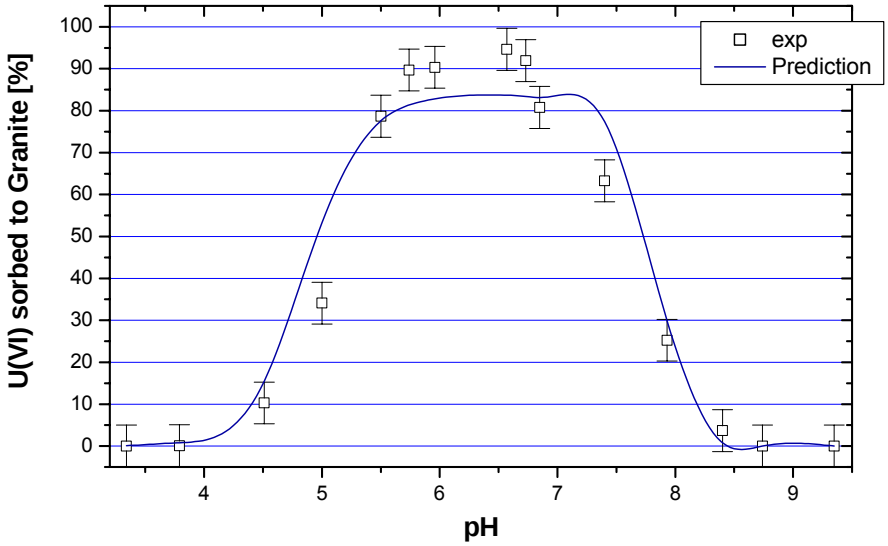

Fig. 2.7: Experimental predicted U(VI) sorption data on granite.

muscovite) and the aqueous metal species, i.e. the same approach was used for the prediction as in the case of phyllite. One modification to the above outlined approach had to be undertaken to obtain a good prediction. This modification arose from the fact that the softer minerals biotite and muscovite in the granite 63 to 200 µm fraction were, as a result of the grinding process, distinctively smaller than the harder grains quartz and albite. Conclusively, the smaller grain size had to be taken into consideration and an appropriate specific surface area for these minerals had to be used in the modelling. In addition, no increase of ferric iron was detected with Mössbauer spectroscopy indicating that ferrihydrite is not a major contributor to the sorption process on granite. Thus, ferrihydrite was not considered in the modelling. The predictions were compared with experimental sorption data and it was found that the predictions were in good agreement with the experimental results, clearly showing the great potential of this approach to model heavy metal sorption on rocks.

The above outlined identical approach applied to two different rocks, i.e. granite and phyllite, using identical surface complex formation constants for quartz, albite, and muscovite, predict that the mineralogical constituents dominates the U(VI) sorption on granite, and that the formation of ferrihydrite dominates the U(VI) sorption on phyllite.

TRLFS speciation of U(VI) sorbed onto muscovite

Spectroscopic evidence for two adsorbed uranium(VI) surface species on edge surfaces of a muscovite platelet were obtained by TRLFS. The mineral is taken as one rock forming mineral constituent. Muscovite platelets of approximately 1 cm^2 and 5 mm height were immersed in 0.1 N $NaClO_4$ solution, and a pH of about 6.3 was adjusted. The sorption experiment was then conducted as described in [47]. Uranyl(VI) was added to set the total uranium(VI) concentration in solution to 1×10^{-5} M. Then the final pH was measured and the uranium concentration in solution was determined by ICP-MS. Species 1 has a fluorescence life time of 1.15 ± 0.02 µs and species 2 a distinctively greater one of 9.65 ± 0.05 µs. The emission bands were in the range of 500 to 600 nm and are shown in Table 2. In contrast, no fluorescence signal was obtained on the basal plane surfaces clearly indicating that U(VI) sorption on muscovite predominantly takes place at the edge surfaces.

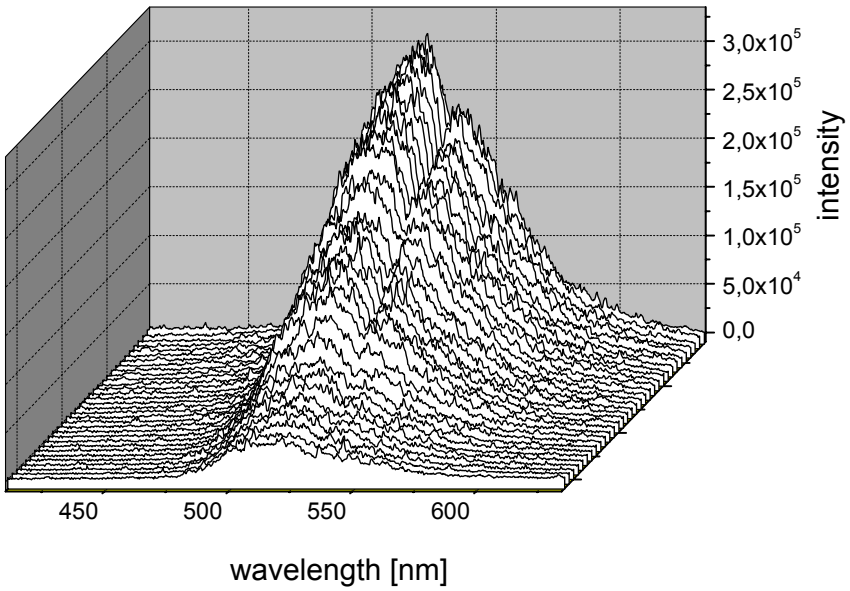

Fig. 2.8: TRLFS of U(VI) adsorbed on the edge surfaces of muscovite platelets.

Table 2.5: Life times and emissions bands of the two U(VI) surface species detected on the edge surfaces of muscovite platelets.

Species	Lifetimes [ns]	Peak centre [nm]				
1	1150±20	502.9	522.1	545.4	569.2	596.4
2	9650±50	502.1	521.7	545.2	569.8	599.4

References

Herbelin, A. and Westall, J. FITEQL Report 96-01, Dep. of Chem., Oregon State University, Oregon (1996).

Waite, T.D., J.A: Davis, T.E. Payne, G.A. Waychunas, and N.Xu (1994) Uranium(VI) adsorption to ferrihydrite: Application of a surface complexation model. Geochimica et Cosmochimica Acta 58 (24), 5465-5478.

5.2. 4 Spectroscopic study on surface interaction mechanism for actinides (FZK)

Introduction

Within this task the speciation of Cm(III) at the mineral-water interface of Al and Si containing minerals was studied by TRLFS to elucidate the sorption mechanism. Sorption reactions have been studied for colloidal minerals and in the case of α-alumina also for single crystals with different orientations. For the single crystal study various spectroscopic and microscopic methods were applied to gain more detailed information on the influence of the surface heterogeneity and of the surface potential on the interaction of the actinides with the surface. The aim of these investigations is to provide process understanding for the validation of presently surface complexation models.

Cm(III) sorption onto colloidal γ-alumina

The surface complexes of Cm(III) onto colloidal pyrogenic γ-alumina have been characterized and quantified by TRLFS based on a previous sorption study of Am(III) and Eu(III) (Rabung et al., 2000) and a previous TRLFS study [48]. Emission spectra and decay rates were measured under Ar atmosphere in a suspension of 0.6 g/L purified γ-alumina in 0.1 M $NaClO_4$ spiked with $2.7 \cdot 10^{-7}$ mol/L Cm-248 in the pH range from 4 to 13 (Fig. 12).

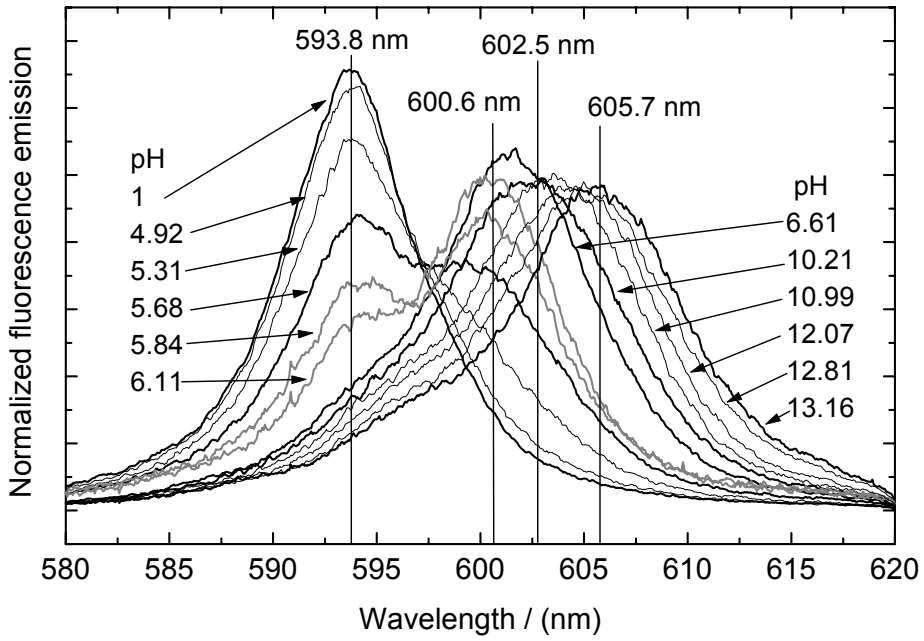

Fig. 2.9: Fluorescence emission spectra of 2.5×10^{-7} mol/L Cm(III) in 0.6 g/L aqueous γ-Al_2O_3 suspension (0.1 M $NaClO_4$) at various pH; spectra are scaled to the same peak area.

By peak deconvolution of the spectra the presence of three Cm/alumina surface complexes can be deduced (Rabung et al, 2001). The species emitting at 600.6, 602.5 and 605.7 nm are most dominant in the pH range 5.3 - 6.3, 6.3 - 11.8 and above pH 11.8, respectively. The lifetime for all the surface complexes is about 110 µs corresponding to 5 H_2O or OH^- ligands in the first coordination shell of Cm(III) [49]. From these results inner-sphere monodentate Cm(III) complexes bound to surface aluminol groups are assumed. With increasing pH ternary hydroxo complexes are formed with the neutral end-member $\equiv AlO\text{-}Cm(OH)_2(H_2O)_3$ above pH 11.8. The distribution of the various sorbed and dissolved Cm(III) species has been fitted as a function of pH by a surface complexation model (Fig. 2.10).

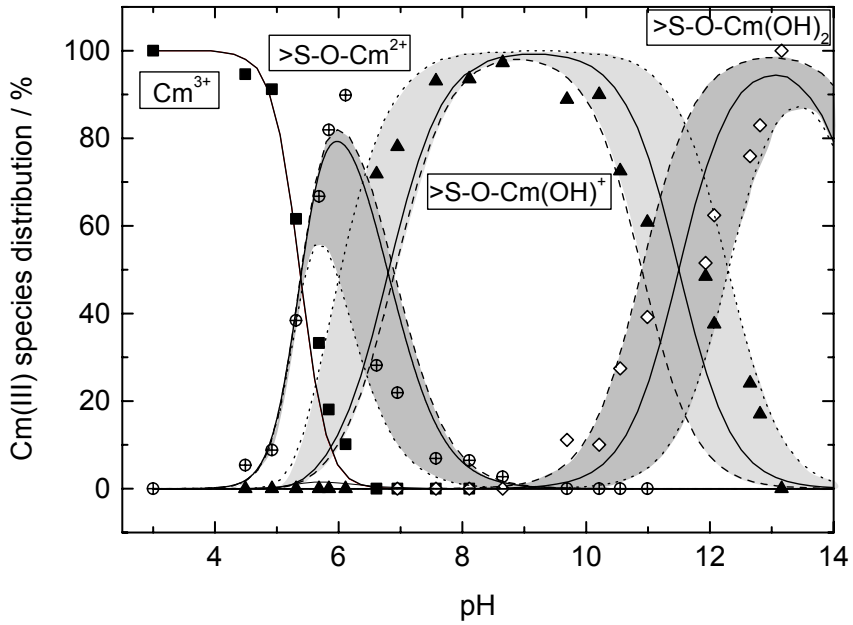

Fig. 2.10: Thermodynamic modeling of the calculated Cm(III) species distribution using log K values from Table 2.6

Table 2.6: Sets of surface complexation constants used to describe the calculated Cm(III) species distribution (see Fig. 2.10).

Reaction	log K		
	dotted line	solid line	dashed line
≡Al-OH + Cm^{3+} ⇔ ≡Al-O-Cm^{2+} + H^+	2.5		
≡Al-OH + Cm^{3+} + H_2O ⇔ ≡Al-O-$Cm(OH)^+$ + $2H^+$	-3.5	-4.3	-4.4
≡Al-OH + Cm^{3+} + $2H_2O$ ⇔ ≡Al-O-$Cm(OH)_2$ + $3H^+$	-15.8	-15.8	-15.3

Spectroscopic speciation of sorption process on α-alumina single crystals

To elucidate the sorption reactions on clear defined mineral surfaces Cm(III) sorption experiments onto sapphire single crystals with different crystal faces (001, 110, 012, 018 and 104) were started. The 1 x 1 cm epi-polished sorption samples prepared at pH 4.5, 5.1 and 6.0 exhibit very low Cm(III) concentrations at the surface (between 0.015 and 0.40 atoms/nm^2 or 2E-12 – 7E-11 mol/cm^2) and were studied with TRLFS [50]. It comes out that the 001 surface with a peak maximum at 601.2 nm and a fluorescence lifetime of 110 µs behaves different compared to the 4 other faces with almost identical peak positions of 603.4 nm and fluorescence lifetimes between 160 and 190 µs. From the spectroscopic properties the 001 surface looks very similar to the first sorption species of the γ-alumina system derived from peak deconvolution (Fig. 2.11). An explanation for this observation could be the relaxation of the 001 surface in contact with water and formation of a Gibbsite (γ-$Al(OH)_3$) similar surface layer which was already described in the literature and which is also expected for the γ-alumina system. Furthermore, the quantification of the Cm(III) sorption with α-spectroscopy shows very strong differences in the sorbed amounts of Cm(III) for the different faces under

identical experimental conditions. The lowest Cm(III) content was found for the 018 surface, the highest for the 001 surface with a sorption increase up to a factor of 25. Within the limits of resolution autoradiography shows a homogeneous Cm(III) distribution on the plan surface. Compared to the results of the γ-alumina sorption study the Cm(III) sorption onto sapphire single crystals is enhanced by 2 –3 orders of magnitude at pH 4.5 which possibly can be ascribed to a shift in the point of zero charge to lower pH values in case of single crystals as already described in the literature. (FZK)

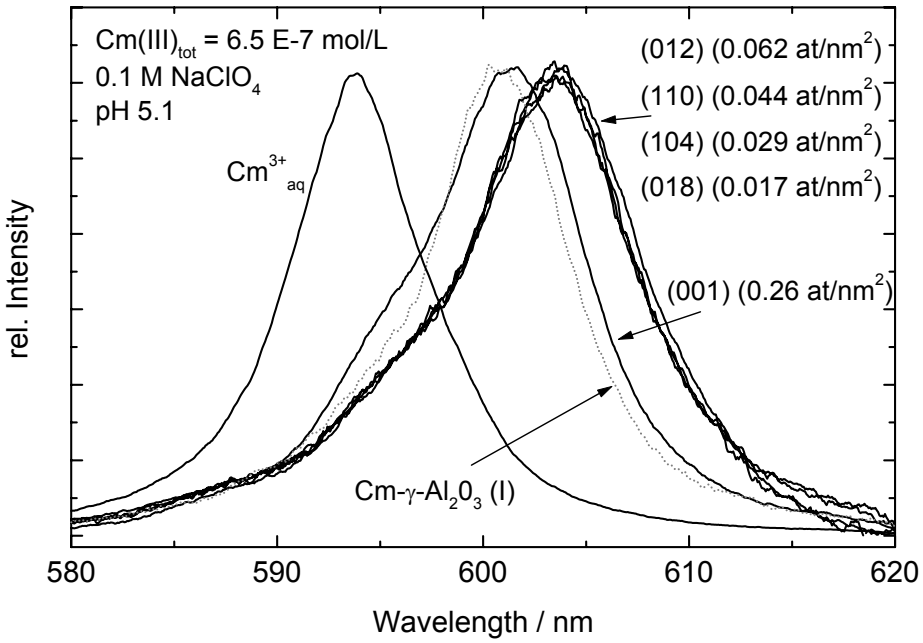

Fig. 2.11: TRLFS spectra for the Cm(III) sorption onto different sapphire single crystals (001), (110), (012), (104) and (018) at pH 5.1 and 0.1 M $NaClO_4$ normalized to the same peak height. Cm(III) surface concentrations measured by α-spectrometry are added in brackets in atoms/nm^2. Also the spectra for the unsorbed free Cm^{3+} aquo ion and for the first Cm(III) sorption species onto γ-Al_2O_3 derived by peak deconvolution at similar pH are included.

XAFS spectra have been measured at the U L3 edge by polarized gracing incidence excitation of less than a monolayer of U(VI) sorbed onto the (110) surface of α-Al_2O_3. [51]. A remarkable polarization dependency of the EXAFS spectrum was found under two orthogonal orientations of the wafer, by which a differentiation between the axial and the equatorial coordination shell of oxygen is possible. Because of this polarization dependency, monodentate binding sites and surface imperfections as reactive surface sorption sites may be excluded. The two possible candidates for bidentate sorption on the (110) α-Al_2O_3 surface are AlO_6 octahedra edges and bridging two adjacent AlO_6 apices. From the present spectra a differentiation between edge and apices sites is not possible. Future measurements are underway to record XAFS spectra of uranyl sorbed onto other specific α-Al_2O_3 surfaces and at several relative angles of orientation.

Sorption of Cm(III) onto silica

Contrary to the alumina system in which the formation of inner-sphere surface complexes was deduced, earlier studies on the sorption of Cm(III) onto amorphous pyrogenic silica colloids by TRLFS indicated a different sorption mechanism (Chung, et al., 1998). From lifetime measurements is derived that the two Cm(III) species found to be bound to the silica have only two or no coordinated water molecules. It was rationalised that the Cm(III) does not form a surface complex but the non-hydrated ion will enter the bulk silica structure. To prove this hypothesis and understand the sorption mechanism, within the ACTAF project Eu(III) and Cm(III) has been incorporated into silica by using the sol-gel process [52]. The doped

silica (350 and 35 ppm Eu and 15 ppb Cm) was stepwise annealed between 50 and 800 °C to remove the water from the silica gel. From the TRLFS lifetime the hydration number of Eu(III) and Cm(III) were determined to decrease from 9 at 25 °C to 5 at about 300 °C annealing temperature. Complete removal of coordinated water needs temperatures of 800 °C. However, the emission spectra above 300 °C showed a much stronger red shift compared to the Cm(III) sorbed onto silica. Thus the Cm(III) incorporated into the low and high temperature silica gel phases does not present a model for the Si-O- coordination of Cm(III) sorbed onto colloidal silica. (FZK)

Outside the ACTAF project, an indication of the sorption process of Cm(III) onto silica has been obtained by a study on the interaction of trivalent actinides with hydroxyaluminosilicate (Kim, MA, et al., 2003, Panak et al., 2003). Colloidal hydroxyaluminosilicates were prepared by co-precipitation of acidic Al(III) and alkaline silicate solution in the presence of Cm(III) under various conditions. The amounts of colloids, their average size and their stability were determined by LIBD as a function of pH. The Cm(III) interaction with the hydroxyaluminosilicate was characterized by TRLFS. Two complexes with peak maxima at 598.5 nm (Cm-HAS(I)) and 601.8 nm (Cm-HAS(II)) in the pH region from 4 to 9 were observed. Using oversaturated silicate solution (0.02 mol/L), containing more reactive oligomeric silicates, a further Cm(III) species with a peak maximum of 605.2 nm (Cm-HAS(III)) was formed even in the absence of Al. Lifetime measurements of Cm-HAS(III) have proven that the Cm(III) looses its primary hydration sphere and is imbedded into the structure of the hydroxyaluminosilicate colloids. In another study outside the ACTAF project the sorption of Cm(III) onto synthetic quartz was studied by TRLFS (S. Stumpf, 2004). Normal sorption behaviour with a hydration sphere of 5 H_2O was found. Due to the lower solubility of quartz compared to amorphous silica, the concentration of orthosilicilic acid is not high enough to bury the Cm(III) in the silica bulk structure. These results are in perfect agreement with the results obtained for the sorption of Cm(III) onto silica colloids.

References

Chung, K.H., Klenze, R., Park, K.K., Paviet-Hartmann, P., Kim, J.I., A study of the surface sorption process of Cm(III) on silica by time-resolved laser fluorescence spectroscopy (I), Radiochim. Acta **82**, 215-219 (1998)

Kim, MA; Panak, PJ; Yun, JI; et al., Interaction of actinides with aluminosilicate colloids in statu nascendi, Part I: generation and characterization of actinide(III)-pseudocolloids, Colloid Surface A 216, 97 (2003)

Panak, PJ, Kim, MA; Yun, JI; et al. Interaction of actinides with aluminosilicate colloids in statu nascendi. Part II: spectroscopic speciation of colloid-borne actinides(III) Colloid Surface A 227, 93 (2003)

Rabung, Th., Stumpf, Th., Geckeis, H., Klenze, R., Kim, J.I., Sorption of Am(III) and Eu(III) onto γ-alumina: experiment and modelling, Radiochim. Acta 2000, **88**, 711-716

Rabung, Th., Geckeis, H., Kim, J.I., Solid-water interface reactions of actinides and lanthanides with mineral surfaces, Migration '01, 8th Internat.Conf. Bregenz, A, September 16-21, 2001, Abstracts p.185

Stumpf, S., PhD thesis, (Heidelberg), in preparation

5.3 Work-package 3:

Thermodynamics of secondary phase formation

Summary of the specific project objectives

The formation of secondary solid phases is considered to be one of the key processes for the immobilisation of radionuclides in the environment. The mechanisms by which a radionuclide is bound to a mineral are of fundamental importance and at present, not well understood. To develop basic process understanding and data for the impact of secondary solid phase generation, the study is focussed on calcite. Surface sensitive spectroscopic and nanoscopic techniques are being used in combination with wet-chemistry and radioanalytical methods. In a addition other relevant secondary phases such as barite, phosphates and hydrated Ca-silicate phases (CSH) have been included in this study.

Structure of the work-package and contributing partners

5.3.1 Formation of solid solutions of actinides with calcite (KU, FZR, PSI))

5.3.2 Formation of solid solutions of radionuclides with barite, phosphate minerals and CSH phases (UPC, Enterpris, FZR / PSI)

5.3.1 Formation of solid solutions of actinides with calcite (KU, FZR, PSI))

Introduction

Calcite is a widespread secondary and primary phase in planned radioactive disposal systems. In cementitious environments, large amounts of calcite are expected to precipitate as a result of the interaction of concrete with carbonated water or organic waste (Curti, 1998). The precipitated calcite is expected to incorporate considerable fractions of the dissolved radionuclides, particularly trivalent lanthanides and actinides (Curti, 1999). Moreover, it is reactive even at low temperature and thus suitable for laboratory experiments. Finally, calcite has a relatively simple structure with a single cationic site. These properties make calcite a suitable material for both solid solution experiments and modelling. As a representative for trivalent actinides, Eu(III) has been chosen as inactive chemical homologue and both Cm(III) and Eu(III) because of their favourite spectroscopic properties.

The general purpose of task was: a) to improve the fundamental geochemical understanding of reactions between calcite and actinides and b) to develop a conceptual model of processes at the molecular level through coupling of experiment and theory. Such information fortifies the scientific database for predictive modelling, decreases uncertainty in risk assessment and promotes safer design and lower cost for waste recycling, treatment and disposal.

The work of this task has been performed in close collaboration between KU, FZR and PSI. KU contributed detailed experimental experience on the calcite system, FZR performed speciatiation of the incorporated metal ion by laser spectroscopy, PSI performed extended modeling on the experimental results using the GEM code.

A) Experimental and theoretical studies on the incorporation of Eu(III) into calcite (KU)

The specific aim of the work was to investigate the processes involved in uptake of a trivalent cation, namely Eu(III), by calcite and to gain a fuller understanding of the behaviour of the calcite surface from a theoretical perspective. To do this, we combined three approaches: *experimental studies* i) at a macroscopic level, ii) surface analysis at the nanometer scale and iii) *theoretical studies* using molecular modelling. We used classical geochemical methods combined with state-of-the-art surface analytical and computational techniques. Eu concentrations were analysed using Inductively Coupled Plasma Mass Spectometry (ICP-MS) in collaboration with the Danish Lithosphere Center (DLC).

I) Organic carbon on commercial calcite powder and a treatment method for its removal

In order to establish a standard set of calcite substrates to insure data consistency between the various partners of ACTAF, preliminary studies were carried out on a number of natural and synthetic samples. Natural Iceland spar calcite from Chihuahua, Mexico, another unknown location in Mexico and Breivik calcite mine in Norwary were tested. The Mexican calcite from the unknown location was selected because it had the lowest concentration of trace metals. Commercial powders from Merck, Sigma and Aldrich were tested but all were found to contain significant amounts of adventitious carbon, used as a growth inhibitor during production. A treatment method was developed, which consisted of aging the powder in freshly deionised water at 65°C under 100% bubbling CO_2, which removed most of the organic contamination and restored surface behavior to something much closer to that of natural single crystals. This information is important for any geochemical research made with synthetic powders.

II) Eu adsorption and its effects on calcite dissolution and precipitation

Atomic Force Microscopy (AFM) allows observation of surface morphology of minerals at resolution of micrometers or nanometers which allows one to watch what happens, in situ. Samples of calcite exposed to pure water and to solutions of various concentrations of Eu(III) demonstrate that Eu is quickly and effectively adsorbed, even under conditions favouring dissolution, and that its presence changes the behaviour of the surface [53]. Dissolution and precipitation rates are certainly affected.

III) Eu(III) co-precipitation with calcite.

A set of macroscopic experiments investigated the uptake capacity of calcite for Eu as a model for trivalent, f-orbital elements. The preliminary studies used a closed system approach [54]. More in-depth experiments used the constant composition method [55]. We now know that partitioning of Eu(III) to calcite is highly favoured ($K_d \sim 800$) meaning that Eu is removed from solution and immobilised in the solid. The stoichiometry of the relationship suggests that the charge for substitution of Eu(III) for Ca(II) is balanced by a vacancy for every two Eu substituted. Compensation of charge by Na or OH does not fit the data.

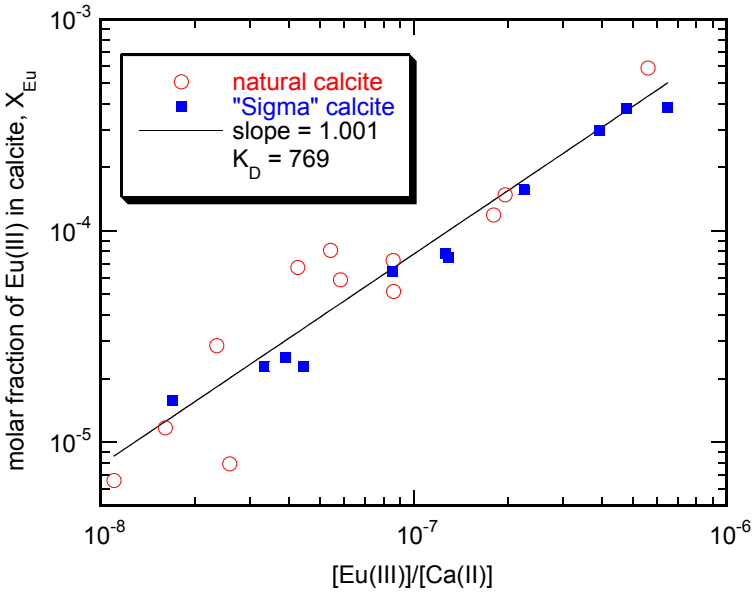

Fig. 3.1 Eu molar fraction in calcite, X_{Eu}, as a function of the steady-state concentration ratio, [Eu]/[Ca] in the solution The straight line corresponds to a constant partitioning coefficient, K_D of 769. Open symbols denote results from natural calcite, closed symbols the commercial powder.

V) Eu incorporation by solid state diffusion

Previous work in our group has shown that some adsorbed divalent cations move into the solid by diffusion through the bulk. Other studies have shown diffusion of monovalent elements out of the bulk to the surface. This sub-project investigates the uptake behaviour of Eu(III), as an example of a trivalent element, using X-ray Photoelectron Spectroscopy (XPS) and Time-of-Flight Secondary Ion Mass Spectroscopy (TOF-SIMS). These techniques are sensitive to the chemical composition of the top atomic layers of a sample. Some first experiments suggest that movement is slow or negligible on the time scales of radioactive waste disposal (10^6 years), but serious instrumental problems have hindered progress in obtaining absolutely trustworthy data so far.

II) Eu concentrations in natural calcites

As a result of the findings of subproject (I), a suite of more than a hundred calcite samples has been collected from all over the world, from a variety of geological environments, including Iceland spar, limestone, chalk and biologically produced material. They are being analysed for rare Earth element (REE) concentration by ICP-MS. A systematic study of the trends in REE distribution will offer valuable information to petrologists who use such relationships to interpret rock genesis but for comparison with the experiments of subproject (I), the distribution of Eu(III) in the natural samples provides a window onto uptake conditions of f-orbital behaviour in nature. The Eu concentrations found in all of the samples analysed to date is at maximum only a couple of ppm. Experimental evidence [**Fehler! Textmarke nicht definiert.**, 55] demonstrates that at least 100 times that amount can be accommodated by solid solution within the calcite structure. This means that in natural systems, the availability of Eu(III) (and trivalent actinides) in solution is the limiting factor to calcite sequestration. Immobilisation is not limited by the solid's ability to include it, until concentrations reach very high levels. Preliminary results were presented as poster [56].

VI) Theoretical Studies: Determination of the fundamental behaviour of calcite surfaces.

State-of-the-art techniques that can provide observations at the nanometer scale now allow us to investigate mechanisms at molecular level. Sometimes interpretation of these observations is ambiguous. Calculations made from theory can predict behaviour at molecular level and give clues for the interpretation of experimental data. Furthermore, questions arising from modelling studies can be tested by experiment. The combination of experiment and theory has much to offer to the understanding of solid/liquid interactions. We have investigated the structure of steps and kinks on the calcite surface and determined the relative energies within the set of active sites. Several observations with AFM have been reproduced in our calculations such as (2x1) surface reconstruction , a preference for production of obtuse steps during cleavage, and the relatively higher reactivity of some sites during dissolution or precipitation. Accounting for the dipole created when atoms are removed to make steps and kinks was a time-consuming problem but it was eventually overcome. For results see [57].

However, modelling adsorption of Eu(III) remains to solved. It includes solving another problem with the dipole created by adding a trivalent ion in a divalent site.

Time-resolved Laser Fluorescence spectroscopy of Cm(III) and Eu(III) in calcite (FZR)

I) Cm(III)/Calcite system

Fluorescence emission spectra of Cm(III) (9×10^{-8} mol/L) in calcite suspension are measured at different contact times between 24 hours and 6 month [58]. All measured spectra can be deconvoluted with just two pure spectra. In contradiction to the peak maximum of the Cm^{3+} aquo ion at 593.8 nm, the peak maxima of the Cm/calcite species are 607.5 nm (1) and 618.0 nm (2). The spectrum of complex 1 is very similar to the spectrum of the Cm(III) tetracarbonato complex $Cm(CO_3)_4^{5-}$ in solution (Fanghänel et al., 1998). To show that curium is sorbed onto the calcite and not a Cm-carbonato complex in solution is detected, the suspension was centrifuged (15000 rpm; 15 min) and the supernatant was measured by ICP-MS and TRLFS.

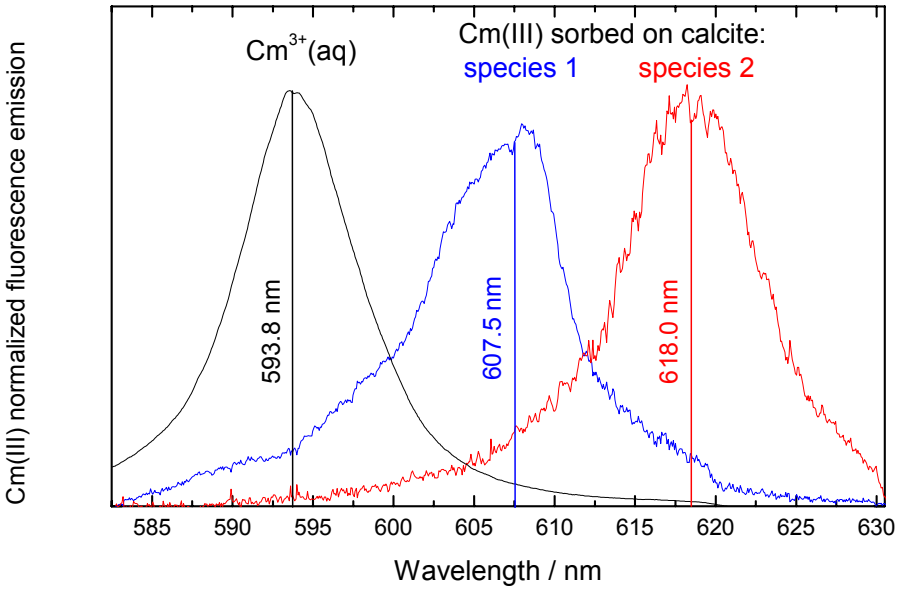

Fig. 3.2: Fluorescence spectra of Cm(III) sorption species in calcite suspension in comparison to the Cm^{3+} aquo ion.

The extraordinary red shift of the second Cm species (peak maximum at 618.0 nm) indicates an extremely change of the ligand field of the actinide ion. With longer contact time the fluorescence intensity of the Cm/calcite complex 1 decreases and the intensity of complex 2 increases.

To get more information about the structure of the Cm/calcite complexes, the fluorescence emission lifetime are was measured. A linear correlation between the decay rate and the number of H_2O molecules in the first coordination shell of Cm(III) complexes exists (Kimura & Choppin, 1994). A lifetime of 68 µs, determined for the Cm(III) aquo ion, corresponds to 9 water molecules and a value of 1.3 ms corresponds to zero H_2O molecules in the first coordination shell of Cm(III). For the fluorescence emission decay of Cm(III) in calcite suspension two different lifetimes of Cm(III) species are found. For complex 1 314 ± 6 µs and for complex 2 1302 ± 75 µs. The second value is very close to the above calculated radiative lifetime for Cm(III) without any water in the first coordination sphere.

Fluorescence spectra of the same Cm/calcite sample at different delay times are also analysed. With increasing delay time the ratio of the intensity of complex 1 and complex 2 changes. That proves that the extremely red shifted peak of complex 2 is the one with the long fluorescence lifetime of 1.3 ms.

Using the correlation between the fluorescence lifetime and the number of water molecules in the fist coordination sphere of Cm(III), we calculated 1.2 water molecules for surface complex 1 and 0 for complex 2.

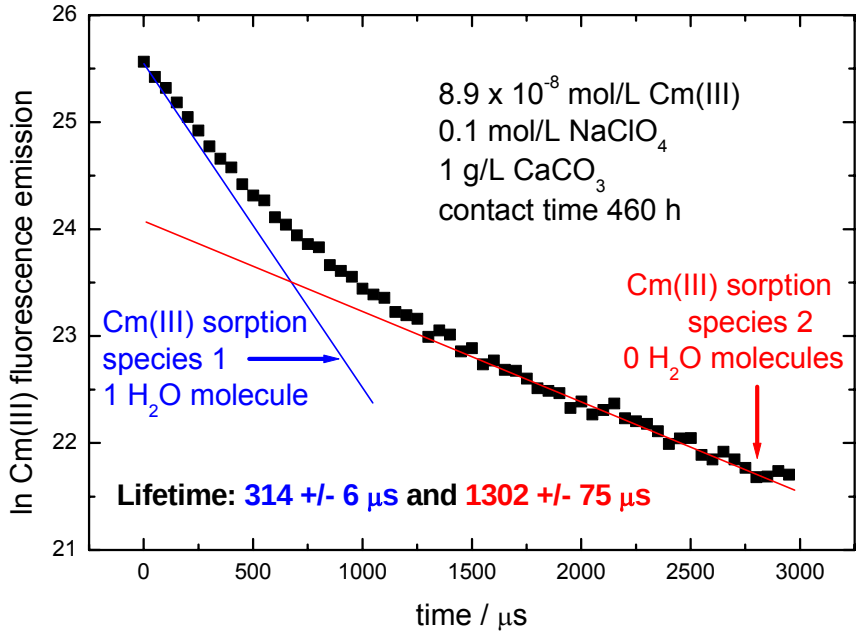

Fig. 3.3: Fluorescence spectra and lifetimes of the aqueous Cm^{3+} ion and its two species formed with calcite in 0.1 mol/L $NaClO_4$ at room temperature.

In summary we conclude:

- TRLFS enables the speciation of Cm (III) for the sorption process onto calcite in the trace concentration range.
- With increasing Cm/calcite contact time two Cm(III)/calcite sorption species are formed.
- The second sorption Cm(III) species has lost its complete hydration sphere and is incorporated into the calcite bulk structure.- The first Cm(III) species is coordinated to about 1 H_2O or OH^- and could represent a surface complex.

II) Eu(III)/Calcite system

A natural calcite (from Creel/Mexico) with relatively high concentration of incorporated europium (307 ppm) is studied by TRLFS. The position of the europium fluorescence emission bands are almost independent of the chemical environment of the metal ion. Only the intensity of the $^5D_0 \rightarrow {}^7F_2$ transition changes significantly when Eu(III) is complexed. This is a consequence of the so-called "hypersensitive effect". The ratio of the emission intensity obtained for the $^5D_0 \rightarrow {}^7F_1$ (λ = 594 nm) and $^5D_0 \rightarrow {}^7F_2$ (λ = 619 nm) transitions together with the lifetime of the fluorescence emission provide valuable information on the europium(III) speciation. For Eu(III) incorporated into natural calcite two different $^7F_1/^7F_2$ ratios dependent on the delay time are found, indicating that two Eu(III)/calcite species in the calcite lattice exist. The decay of the fluorescence signal, shown in figure 20, follows a bi-exponential decay law confirming the existence of two different Eu(III)/calcite species with two different lifetimes derived above from the analysis of the delay time spectra. A fit of the decay curve gives lifetimes of 552 ± 35 µs for the first Eu(III)/calcite species and a lifetime of 2216 ± 114 µs for the second species. According to the Horrocks equation (Horrocks &

Sudnick, 1979), a lifetime of 552 ± 35 μs corresponds to 1.3 water/OH^- molecules in the first coordination sphere of Eu(III) whereas a lifetime of 2216 μs indicates the total loss of the hydration sphere of the second Eu(III)/calcite species. The number of europium species found in natural calcite and their hydration status is in good agreement with the results of TRLFS investigations of Cm(III) incorporation into calcite. From this we suggest that the same sorption and incorporation mechanism applies for both metal ions.

Modelling of solid solution formatation of trivalent f-elements with calcite (PSI)

The reactivity and simple structure of calcite also facilitate the study of heterovalent substitutions, where the charges of replacing and replaced cations differ (e.g. Ln^{3+} or An^{3+} for Ca^{2+}). In heterovalent substitution processes one has to consider the problem of local charge balance. For instance, isomorphic substitution of Eu^{3+} for Ca^{2+} in calcite would imply a local excess of one positive charges, which must be compensated. Two possible local charge balance mechanisms are coupled ionic substitution and substitution adjacent to vacancies. The first mechanism can be exemplified by substitution of two Ca^{2+} sites by an Eu^{3+} and a Na^+ ion. The second mechanism would require two Eu^{3+} ions and a vacant cation site replacing three adjacent Ca^{2+} ions. Alternative mechanisms are conceivable. For instance, substitution of the hydroxylated group $EuOH^{2+}$ for Ca^{2+} would also satisfy charge-balance requirements. Another possibility is the simultaneous substitution of a Ca^{2+} and a CO_3^{2-} by the electrically neutral $Eu(OH)_3^o$ group. However, the last two mechanisms require considerable accommodation of the calcite structure.

From the point of view of thermodynamics, it is possible to make predictions for ideal solid solutions representing all of the mentioned substitution mechanisms (listed in Table 1). In the course of this project, we performed systematic calculations with the code GEMS/PSI in order to model the Eu coprecipitation experiments at pH 6 and 1 atm CO_2, carried out by our partners of the Copenhagen University. Details of the experiments are given elsewhere in this report. Here, we focus on the results obtained by our thermodynamic modelling.

A major aim of our work was to find a thermodynamic explanation for the observed data trends. Specifically, the coprecipitation data define a linear trend with slope close to +1 in a logarithmic plot of equilibrium Eu molality, m_{Eu} , vs. mole fraction, x_{Eu}. From simple thermodynamics, it could be demonstrated that the slope in such a plot is inversely proportional to the stoichiometric coefficient of Eu in the corresponding end-member, provided the experiments are carried out under constant conditions. That is, for the solid solution defined by the end-members $Eu_2(CO_3)_3$-$Ca_3(CO_3)_3$ one expects a slope of + ½ as a "fingerprint" of the postulated substitution mechanism (2 Eu^{3+} + 1 vacancy for 3 Ca^{2+}). In contrast, for the other end-members listed in Table 3.1, a slope of +1 results, which is consistent with the data.

Figure 3.4 shows the experimental data and predicted Eu concentrations at equilibrium with the calcite ideal solid solutions as a function of cation mole fraction of Eu, for all four end-member pairs listed in Table 1. All speciation calculations were carried out using the thermodynamic data specified in Hummel et al., (2002) and Davies' approximation for the calculation of ion activity coefficients. Each dot indicates a single GEMS/PSI calculation. Dots belonging to the same line define the isotherm for a specific solid solution model. The calculations within an isotherm differ only by the total amount of Eu added to the system, while all other compositional parameters remained fixed.

Table 3.1: Selected end-members for Eu-calcite solid solution calculations, with solubility products and corresponding literature references. All solubility products are defined as dissociation into free aqueous ions ($BCX \Leftrightarrow B^{+ZB} + C^{+ZC} + X^{-ZX}$).

Eu end member	Ca end-member	substitutions	log K^o_{sp} (Eu solid)	References
$Eu_2(CO_3)_3$	$Ca_3(CO_3)_3$	$2\ Eu^{3+} + \square \Leftrightarrow 3\ Ca^{2+}$	-35.0 ± 0.3	1 , 2
$EuNa(CO_3)_2$	$Ca_2(CO_3)_2$	$Eu^{3+} + Na^{+} \Leftrightarrow 2\ Ca^{2+}$	-20.5 ± 0.7	3 , 4
$EuOHCO_3$	$CaCO_3$	$EuOH^{2+} \Leftrightarrow Ca^{2+}$	-21.7 ± 0.1	1 , 2
$Eu(OH)_3$	$CaCO_3$	$Eu^{3+}+3OH^{-} \Leftrightarrow Ca^{2+}+CO_3$	-27.1 ± 0.3	1 , 5

[1]Hummel et al. (2002); [2]Runde et al., (1992); [3]Fannin (1999) [4]Fannin et al. (2002); [5]Bernkopf (1984).

As expected, a slope of + ½ results from the model calculations with the $Eu_2(CO_3)_3$ end-member. Therefore, incorporation of two contiguous Eu^{3+} ions adjacent to a vacant octahedral site can be ruled out, considering that the data define a slope close to unity (0.97 ± 0.06). The other three models define a slope of +1, consistent with the data. However, the $Eu(OH)_3$-$CaCO_3$ solid solution model must be discarded due to the unreasonably large non-ideality corrections required to fit the experimental data.

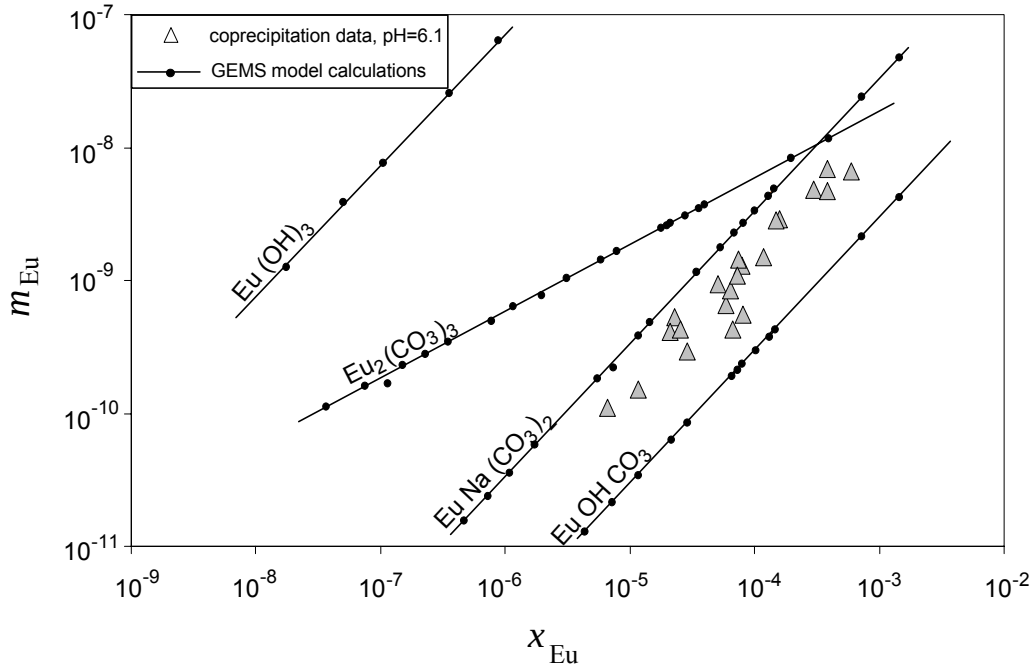

Figure 3.4: Comparison of ideal solid solution model calculations with the data of Stipp and Lakshtanov (2003) from Eu coprecipitation experiments with calcite carried out in a 0.025-0.1 m $NaClO_4$ medium (pH 6.1). Each line represents the model calculations for an end-member pair defined in Table 1. GEMS/PSI calculations are represented by dots on the model lines.

The degree of non-ideality is smaller for predictions based on the $EuNa(CO_3)_2$ as well as $Eu(OH)CO_3$ end-members. The model results are close to the experimental data (within one order of magnitude). Particularly, for the $EuOHCO_3$-$CaCO_3$ solid solution, the non-ideality

correction would require a reasonable Margules parameter ($a_o \sim 2$; see Glynn, 2000). In contrast, a coupled $Eu^{3+} + Na^{+}$ substitution mechanism, though appealing, can be excluded due to the fact that the results seem to be insensitive to the Na concentration in solution. The coprecipitation experiments were carried out at different background Na concentrations (0.025, 0.05 and 0.1 mol kg^{-1}). This spread of one order of magnitude in Na solution concentrations should be reflected in a dispersion of the data in Fig. 18, but this is not observed.

In summary, our thermodynamic analysis favors a solid solution with a substitution of $EuOH^{2+}$ for Ca^{2+}. However, this result is in contradiction with Cm(III) and Eu(III) laser fluorescence data by our partners (FZK/FZR), which unequivocally point to loss of the entire hydration shell during Cm incorporation in calcite. This result apparently excludes the presence of hydroxyl groups in the first shell of Eu^{3+} in calcite. Either there is a "disruption" of the $EuOH_2^{+}$ group during incorporation, with migration of the OH^{-} group in interstitial sites, or other substitution mechanisms must be called for. The main lessons learned from our three-year work in this project can be summarised as follows. First, we had to recognize that solid solution formation with ions of different charge (heterovalent substitution) is far more complex than the usual homovalent solid solutions, where ions of equal charge substitute for each other. In the case of Eu(III) substitution in the calcite lattice, we could not find a definitive solution to this puzzle even considering 4 different end-member pairs. At least, a number of specific substitution mechanisms can be ruled out. Further, we realized the importance of combining the thermodynamic analysis with independent spectroscopic data. TRLFS on Cm(III) was a powerful tool, allowing us to restrict the choice of possible end-members. Finally, we must acknowledge that even spectroscopic methods have their limitations. For instance, TRLFS does not yield any geometric information; on the other hand, an EXAFS analyses cannot distinguish between O^{2-}, OH^{-} and H_2O neighbours.

Therefore, our recommendation is to extend the investigation methods. Essential complementary information could be provided by quantum mechanical calculations (molecular modelling). This method could serve either as a test for the feasibility of proposed substitution mechanisms, or even for ab initio calculations to determine the coordinative environment of trace radionuclides incorporated in the calcite lattice. We therefore propose looking in this direction when planning future work on heterovalent solid solution formation.

Recent analysis of the Eu(III) /calcite system (PSI)

A new attempt has been made by PSI recently to find a consistent model for both experimental sorption data and spectroscopic results. A paper was submitted to Geochim Cosmochim Acta by PSI at November 2003 [59]. Three sets of Eu(III) uptake experiments, two of which taken from the literature, were considered: (a) recrystallization tests in synthetic cement pore water at pH ~ 13 in the absence of CO_2 (this work); (b) coprecipitation tests in 0.1 M NaClO4 at pH ~ 6 and $pCO_2 \sim 1$ bar [54]; (c) coprecipitation tests in synthetic seawater at pH ~ 8 and pCO_2 ranging from 3 x 10-4 to 0.3 bar (Zhong and Mucci, 1995).

Solid solution formation was modelled using the Gibbs energy minimization (GEM) method. It was found that the three datasets can be reproduced simultaneously only by the ternary ideal solid solution $EuHCO_3 – EuO(OH) – CaCO_3$, with G*$EuHCO_3$ = □1733 kJ mol-1 and G*EuO(OH) = -955 kJ mol-1 while all other considered end-member combinations failed. Our results are consistent with time-resolved laser fluorescence data indicating two distinct species for Cm(III) and Eu(III) incorporated in calcite, one partially hydrated, the other completely dehydrated.

According to the model, at low pH, the coupled substitution $H^{+} + Eu^{3+} = 2\ Ca^{2+}$ prevails, while at high pH the substitution of a $CaCO_3$ group by an Eu-oxyhydroxide complex prevails.

References

Fanghänel, Th., Weger, H. T., Könnecke, Th., Neck, V., Paviet-Hartmann, P., Steinle, E., Kim, J. I, Radiochim. Acta 82, 47-51 (1998)

Beitz, J. V., Hessler, J. P., Nucl. Techn. 51, 169-177 (1980)

Kimura, T., Choppin, G. R., J. Alloys Comp. 213/214, 313-317 (1994)

Horrocks Jr., W. D.; Sudnick, D. R. J. Am. Chem. Soc. 101, 334-340 (1979)

Curti E. (1998) Coprecipitation of radionuclides during cement degradation: a preliminary modelling study for the Swiss L/ILW repository. Scientific Basis for Nuclear Waste Management XXI, 313-320.

Curti E. (1999) Coprecipitation of radionuclides with calcite: estimation of partition coefficients based on a review of laboratory investigations and geochemical data. Applied Geochemistry 14, 433-445.

Fannin C., Edwards R., Pearce J., and Kelly E. (2002) A study on the effects of drying conditions on the stability of NaNd(CO3)2.6H2O and NaEu(CO3)2.6H2O. Applied Geochemistry 17, 1305-1312.

Fannin C. A. (1999) The rare earth elements as natural analogues for the actinides. Ph.D., Liverpool John Moores University.

Glynn, P.D. (2000). Solid-solution solubilities and thermodynamics: sulfates, carbonates and halides. In: Sulfate minerals: crystallography, geochemistry and environmental significance. C.N. Alpers, J. L. Jambor and D. K. Nordstrom, eds., Washington, D.C., Mineralogical Society of America and Geochemical Society. 40: 481-510.

Hummel W., Berner U., Curti E., Pearson F. J., and Thoenen T. (2002) Nagra/PSI Chemical Thermodynamic Data Base 01/01. Nagra Technical Report NTB 02-16, Nagra, Wettingen, Switzerland; and Universal Publishers/uPublish.com, Parkland, Florida, ISBN 1-58112-620-4.

Runde W., Meinrath G., and Kim J. I. (1992) A study of solid-liquid phase equilibria of trivalent lanthanide and actinide ions in carbonate systems. Radiochimica Acta, 58/59, 93-100.

5.3.2 Formation of solid solutions of radionuclides with barite, phosphate minerals and CSH phases (UPC, Enterpris, FZR / PSI)

Introduction

The incorporation of radionuclides into phosphate minerals is being studied by solubility measurements on synthesized REE phosphates (UPC) and by analysis of U series elements in secondary mineral phases (Enterpris). Initially, co-precipitation of divalent radionuclides in barite was studied as this represents the closest approach to ideal solid-solution behaviour. These investigations have been extended and new work has commenced on the uranyl phosphate system. Eu(III) and Cm(III) interaction with the cement corrosion product calcium silicate hydrate (CSH) is investigated by laser spectroscopy (FZR/FZK, PSI).

A) Contribution by UPC:

The objective of this work has been to study the reaction mechanisms and thermodynamics of the interaction of La(III) and Y(III) with hydroxoapatite, as a model for general Ln(III) and Ac(III) behaviour. The work has been divided in two phases, in the first one the surface interaction of La(III) and Y(III) has been investigated; in the second phase, Ln(III) phosphate phases have been synthesised and their solubility measured.

REE interaction with phosphates

The surface interaction of La(III) and Yb(III) with a carefully prepared hydroxoapatite has been studied in batch experiments with low Ln(III) initial concentration (on the order of 10^{-6} M) at constant 0.1 M $NaClO_4$, room temperature and under N_2(g) atmosphere to avoid carbonate complexation with the aqueous and solid phases. The initial kinetic experiments indicated that a short contact time is needed to reach equilibrium or steady state in the system (<5 hours). The data indicates that there is a certain exchange of Ca(II) by La(III) during the surface interaction, at the same time there is a decrease on the aqueous phosphate concentration. This would indicate that the reaction mechanisms implies an exchange of Ca(II) by La(III) at the surface together with the formation of a phosphate surface precipitate. AFM investigations are currently undergoing in order to back up these observations.

In order to study the thermodynamics of the La(III), Yb(III), phosphate system in aqueous media, we have synthesised the solid phases: $LaPO_4 \cdot nH_2O$, where a $0.83<n<1.6$ and $YbPO_4 \cdot nH_2O$ with $1.78<n<3.4$. The solubility of these phases has been studied by potentiometric titration at 25ºC in 0.5 M $NaClO_4$ medium and under N_2(g) atmosphere. The experimental solubility data (see fig. 1) have been explained by assuming the formation of: $LaH_2PO_4^{+}$ and $LaPO_4$(aq) in the case of lanthanum, while a more complex speciation scheme appears in the case of Yb(III), with the formation of the following set of complexes: $YbH_2PO_4^{2+}$, $YbHPO_4^{2+}$, $Yb(HPO_4)_2^{-}$ and $Yb(PO_4)_2^{3-}$ [60]. The system is still under investigation and more data will be required before a definitive speciation scheme is achieved.

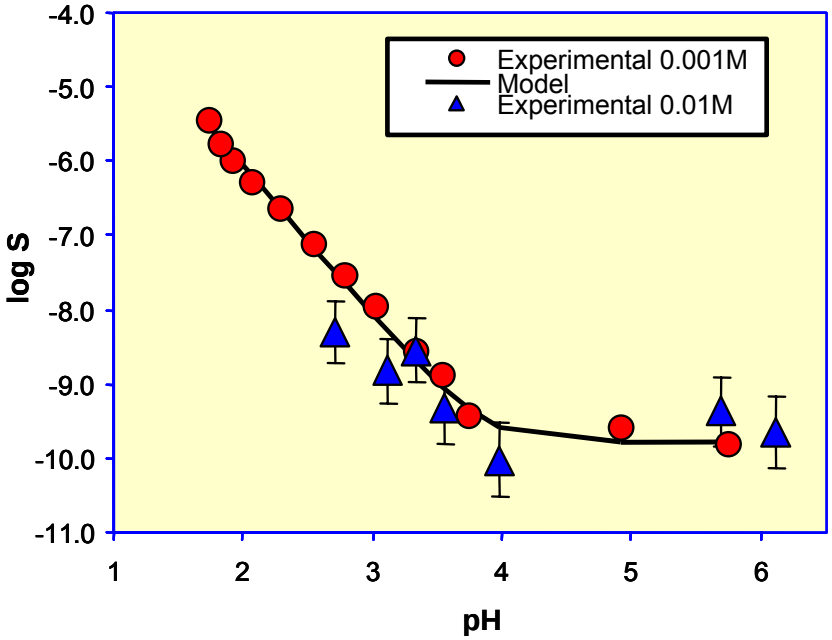

Fig. 3.5: Solubility data and model fit for $LaPO_4(s)$ in two different total phosphate concentrations, 0.01 and 0.001 M respectively

Incorporation of actinides into hydroxoapatite

This work has been mainly focused on the potential incorporation of uranyl in hydroxoapatite $Ca_5(PO_4)_3OH$, whixh is a very common phosphate phase in subsurface environments. The hydroxoapatite was duly characterised and the incorporation of uranium (VI) followed in batch experiments under well controlled conditions. The resulting phase was analysed by means of EXAFS. The preliminary interpretation of the spectra would indicate that there is some U-P bonding at 3.024 and 3.633 Å, respectively.

B) Contribution by Enterpris

In order to perform meaningful performance assessment calculations, solubility data are required for situations where:

sufficient mass concentrations of radioelements are present to form discrete solid phases in which the contaminant species is an essential constituent.

trace concentrations are incorporated in the lattice sites of mineral phases where the contaminant is not an essential constituent. These mineral phases may or may not display high selectivity for the radioelement in question.

For the vast majority of disposal environments, the first case is restricted to uranium and possibly, thorium solids. In the current project, it was investigated by studying the incongruent degradation of natural uraniferous minerals and their alteration to secondary phases that show marked enrichment in uranium. These data were supplemented by controlled laboratory experiments on the alteration of uranium metal in phosphate and silicate media. The uranyl phosphates are among the most important uranyl species in nature but not only do they suffer from a lack of reliable thermodynamic data, the governing reaction sequences and the rates of reversion from one phase to another are largely unknown.

The incorporation of trace quantities of a radioelement into a crystal lattice was addressed by carefully controlled radium substitution into barite. This has furnished detailed mechanistic data for a system of major radiological concern.

Geochemical migration and secondary enrichment of U and Th

The behaviour of U and Th during low temperature alteration of natural monazite (ideally $LREEThPO_4$, where LREE denotes the light rare earths) was studied on an ultra-high grade ore body containing 45% rare earths, 9% thorium (expressed as weight % oxide) and 600ppm uranium [61]. The findings were correlated with those from experiments on synthetic phosphate-based waste forms incorporating the transuranics [62].

Monazite is known to be extremely stable in most geochemical environments but is susceptible to prolonged attack by acid or alkali solutions. Weathered crystals from a number of sources were examined by electron probe and shown to display similar features. Petrographical evidence points to preferential mobilisation of the heavy rare earths from the margins of altered grains accompanied by incongruent dissolution of U and Th [61]. The results demonstrate that, for this system, uranium is substantially more mobile than the rare earths, which in turn show greater mobility than thorium. Thorium is re-deposited locally (micrometre scale) in cracks as secondary silicates and oxides, containing up to 50% by weight ThO_2 Although also enriched to around 8% in some silicate and phosphate alteration products, a significant proportion of the original uranium present was lost on weathering. It was concluded that monazite-like ceramics designed for containment of HLW may retain tetravalent actinides but are likely to release uranium in response to natural degradative processes.

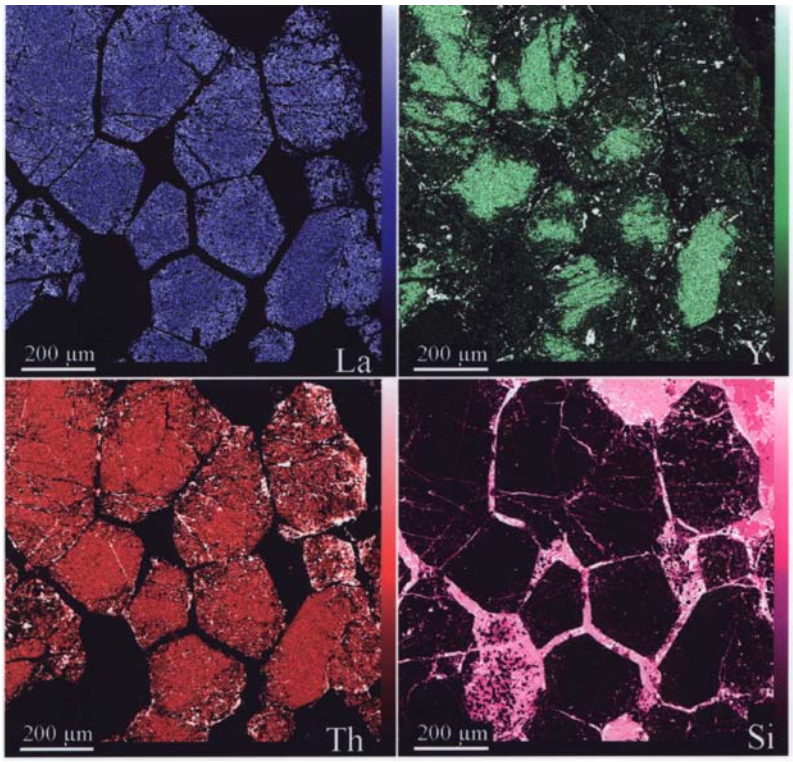

Fig. 3.5: Elemental maps of La (a), Y (b), Th (c) and Si (d) are showing the distribution in altered monazite. Observations indicate that U is substantially more mobile than the rare earths, which in turn show greater mobility than Th, which is re-deposited locally in cracks as secondary silicates and oxides, containing up to 50% by weight ThO_2. It seems likely that a significant proportion of the original U present is lost. [61]

Development of secondary phosphates and silicates on uranium metal

Dissolution experiments focussed on depleted metallic uranium in both powder form and as manufactured discs. The latter allowed more detailed characterisation of surface features and so were favoured for quantitative work. Analyses were conducted on pristine metal using gamma spectrometry and Inductively Coupled Plasma Mass Spectrometry (ICP-MS). The material was supplied by BAe Systems (Royal Ordnance Speciality Metals) in the form of 25 mm diameter discs, 0.5 mm in thickness, cut from whole penetrators.

A protocol was developed for analysis of trace constituents. Details of the analytical methods are provided in [63]. Depleted uranium used in munitions contains transuranic elements owing to the mixing of tails depleted and reprocessed uranium (Table 1). Activity levels for the radiologically significant transuranic elements are sufficiently low at <10 Bq g^{-1} for ease of handling but high enough to investigate dissolution and re-incorporation in the form of secondary precipitates [63]. This is a major advantage over spent fuel.

Table 1 Radiochemical analysis of depleted uranium [63]

Radionuclide	*Specific Activity (Bq g^{-1})*	*Uncertainty ± Bq g^{-1}*
^{238}U	12,343	0.916
^{235}U	156.6	0.461
^{234}U	2,382	1.161
^{236}U	7.113	0.113
^{237}Np	5.002	0.267
$^{239+240}Pu$	2.195	0.098
^{238}Pu	1.059	0.055
^{243}Am	6.678	0.117
^{241}Am	2.166	0.085
^{99}Tc	78.97	0.795

Uncertainties are 2σ counting statistics.

Discs of uranium metal from unfired penetrators were artificially weathered over a year, in order to quantify dissolution rates and to investigate the development of secondary alteration products on the corroding surface. The solutions employed were Ultra High Quality (UHQ) water, as a control, calcium phosphate and a silica-rich solution. The samples were examined by X-ray diffraction (XRD), SEM/EDAX and the Atomic Force Microscope (AFM).

The first phase formed in UHQ water is UO_2 followed by higher oxides, schoepite ($(UO_2)_8O_2(OH)_{12}(H_2O)_{12}$) and, after four months, studtite ($UO_4{\cdot}4H_2O$). Surface alteration is accompanied by a steady increase in uranium concentration from which rate constants for dissolution have been derived [64].

Analysis of uranium alteration in the silica-rich solution also detected a range of uranyl oxides ranging from UO_2 to UO_3, but to date no silicate minerals have been observed, although phases such as uranophane are abundant in nature. Corrosion in the silica solution was much more rapid than in water and after one year most of the original mass had been lost.

In contrast, samples placed in calcium phosphate solution became discoloured but otherwise displayed little sign of corrosion. The mass did not change significantly during the experiment implying passivation by a surface film. This was confirmed by aqueous concentrations, which

remained very low (≤ 10^{-8} mol dm^{-3}) throughout. Surface analysis detected a uranyl phosphate hydrate, tentatively identified as chernikovite or 'H-autunite' ($[(H_3O)(UO_2)(PO_4)]_2 \cdot 4\text{-}8H_2O$).

Despite the presence of calcium in the solution, autunite ($Ca[(UO_2)(PO_4)]_2(H_2O)_{10}$) was not detected. Again, this phase is abundant in nature though attempts to synthesise it directly in the laboratory have not been successful. It is suggested, therefore, that chernikovite and schoepite may be important percursor phases in the formation of the more common U(VI) phosphates and silicates [65].

Formation of solid solutions incorporating trace radionuclides

The characteristics of the radium-barium sulphate system are relatively well known and therefore ideal for parameterising a numerical solid-solution model in preparation for application to more complex situations involving the transuranics.

A static system allowing slow crystallisation from aqueous solutions in a porous medium (Prieto et al., 1997). was used to prepare radium-substituted barite crystals. The protocol uses silica hydrogel as a diffusion medium between two reservoirs containing ^{226}Ra-spiked $BaCl_2$ and Na_2SO_4. The crystals were characterised by WAXS-XRD, SEM/EDAX and AFM. Activity levels were measured by gamma spectrometry.

The first series of tests, examining the effect of initial concentration on solid-solution composition, indicated quantitative uptake of Ra by the crystallising barite with negligible sorption loss on the gel. Radium is abstracted from the point of nucleation and throughout the crystal growth period (1 month). Although relatively low activities were employed in these experiments for ease of handling, parallel studies on industrial barite scales demonstrate that the linear substitution relationship can be extrapolated to crystals containing several thousand Bq/g (Read et al., 2004).

A second series of tests examined the effect of a competing cation (Sr^{2+}) on radium incorporation. Variable concentrations of $SrCl_2$ (0.5 – 0.05 mol dm^{-3}) were added to the $BaCl_2$ reservoir and each experiment run for four weeks. A linear dependence between the Ba-Sr solid solution composition and the characteristic d spacing of the 021 and 121 peaks (deduced from the 2θ value) was obtained (Ceccarello et al., 2003, 2004).

The particle size, morphology and activity (hence radium uptake) of the crystals are a function of the initial [Sr]/[Ba] molar ratio of the starting solution. Systems richer in strontium produce smaller sized crystals and clusters characterised by a lower degree of order. Activity profiles highlight the relationship between the initial solution composition and the radium content of the synthesised crystals. Uptake of ^{226}Ra during formation of the crystals ($SS_{barite\text{-}celestite}$) is inhibited by the introduction of a competing ion (Sr^{2+}). Thus, the higher the initial [Sr]/[Ba] molar ratio of the starting solution, the lower the intensity of the activity peak in the crystals. However, this trend may be attributed to competition for lattice sites, the smaller unit cell dimensions of celestite-rich members of the series or both. Further work is required to deconvolute the two contributing factors.

C) Actinide sorption on CSH phases

The presence of cementitious material in a nuclear waste repository has a strong influence on the chemical environment when groundwater has access. The study of radionuclide behavior within the corroding cement system is, thus, of high relevance. This work studies the influence of calcium silicate hydrates (CSH) phases generated as secondary phases during cement corrosion on radionuclide retention [66, 67].

The interaction of the two trivalent metal ions (Cm(III) and Eu(III)) with calcium silicate hydrates (CSH phases) at pH 13.3 has been investigated in batch-type sorption studies for Eu(III) and complemented with time-resolved laser fluorescence spectroscopy (TRLFS) for Cm(III). The sorption data for Eu(III) reveal fast sorption kinetics and a strong uptake by CSH phases with distribution ratios of $(6\pm3)\cdot10^5$ L kg^{-1}. Three different Cm(III) species have been identified: A non-fluorescing species, which was identified as a curium hydroxide (surface) precipitate, and two fluorescing Cm(III)/CSH sorbed species. The fluorescing sorbed species have characteristic emission spectra with main peak maxima at 618.9 nm (F1) and 620.9 nm (F2) and fluorescence emission lifetimes of 289 ± 11 µs and 1482 ± 200 µs, respectively. From the fluorescence lifetimes it was calculated that the two fluorescing Cm(III) species have one to two and no water molecules left in their first coordination sphere suggesting that these species are incorporated into the CSH structure.

A structural model for Cm(III) and Eu(III) incorporation by CSH phases was developed based on a defect 11Å Tobermorite structure (figure 24). The crystal structure of 11Å Tobermorite was reported by Hamid [9]. It consists of layers of Ca octahedra ("stable Ca") linked through non-bridging oxygens to chains of silicate tetrahedra on either side, forming Ca-silicate layers. In the interlayers between the Ca-silicate sheets, variable amounts of Ca atoms may be located ("labile" Ca). Thus, the Tobermorite structure contains Ca atoms at three different types of sites: The "labile" Ca in the interlayers (labelled 1 in Figure 24) is coordinated with 7 oxygen atoms of which 2 originate from H_2O molecules. In the second type of sites (labelled 2 in the figure) Ca is coordinated with 6 oxygen atoms originating from Si tetrahedra, and one oxygen from H_2O (stable Ca) and in the third type of sites (labelled 3 in the figure), Ca is coordinated with 7 oxygen atoms originating from Si tetrahedral (stable Ca). The fluorescing Cm(III) species, F1 corresponds to Cm(III) substituting for Ca in the interlayer (type 1 Ca) or Ca bound in the type 2 sites of the Ca octahedral layers, whereas the fluorescing Cm(III) species, F2, can be interpreted as being a Cm(III) substituting for Ca in the type 3 sites of the

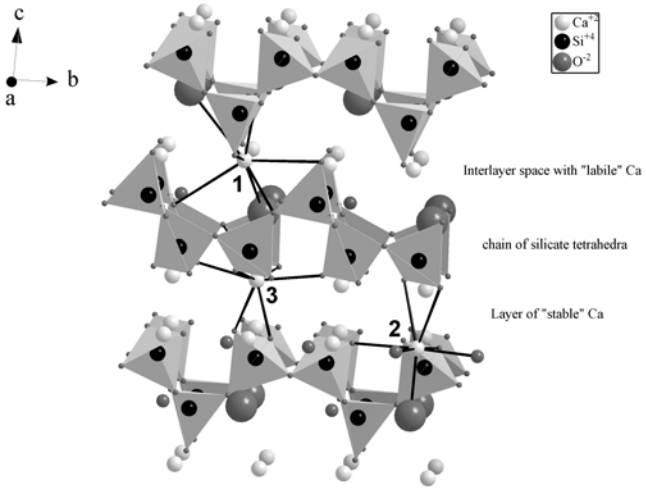

Fig. 3.6: Tobermorite structure indicating Ca-ions at different positions Ca octahedral layers.

Publications

Ceccarello, S., Black. S., Read, D. and Hodson, M. (2003). Suppression of radium uptake in barite crystals by introduction of competing ions (e.g. Sr). Geochim. Cosmochim. Acta, 67, A55.

Ceccarello, S., Black. S., Read, D. and Hodson, M. (2004). Suppression of radium uptake in barite crystals by introduction of competing ions. Min. Eng. (in press).

Prieto, M., Fernandez-Gonzalez, A., Putnis, A. and Fernandez-Diaz, L. (1997). Nucleation, growth and zoning phenomena in crystallising $(Ba,Sr)CO_3$, $(Ba,Sr)SO_4$, and $(Cd,Ca)CO_3$ solid solution from aqueous solutions." Geochim. Cosmochim. Acta, 61, 3383-3397.

Hamid, S. A. Zeitschrift für Kristallographie 154, 189 (1981)

Curti E. (1998) Coprecipitation of radionuclides during cement degradation: a preliminary modelling study for the Swiss L/ILW repository. *Scientific Basis for Nuclear Waste Management XXI*, 313-320.

6. Assessment of Results and Conclusions

The objectives of the ACTAF project was to improve the geochemical basis for the performance assessment of nuclear waste and spent fuel disposal by experiments and model development. The project was aimed to provide two kinds of geochemical knowledge: filling up serious gaps in the thermodynamic database for relevant reactions in solution and with mineral phases, and secondly to improve the understanding of relevant processes, such as colloid formation, sorption mechanism, solid solution formation. Basic process understanding is indispensable for application of models available already, but also for the development of new models appropriate to include a quantitave description of that process in PA codes.

In the following, the results achieved by the ACTAF project are discussed with respect to completion of databases and to process understanding for the three working-packages. The discussion on the WP2 and WP3 is combined within one section.

Thermodynamics of aquatic actinides (WP1)

The work was focussed on reactions of actinides controlling the solubility in aqueous solution, such as solid/liquid equilibria, hydrolysis, complexation but also formation of colloidal species. The most important success of the ACTAF project has been achieved in providing reliable data for tetravalent actinides on solubility and hydrolysis reactions. However, not only serious gaps have been closed, the results also open the doors to solve other questions. As it has been demonstrated by the identification and quantification of ternary hydroxo-carbonate complexes, stability constants for complexation reactions may be derived from solubility measurements, if no other solid phase is formed. Another problem are colloidal amorphous An(IV) hydroxides, which dominate the solubility of actinides over a broad pH-range in the absence of complexing agents. How these colloids are stabilised over long times even in strong brine solutions? Based on the ACTAF results on An(IV), in future redox reactions of actinides could be tackled, particularly of Pu. The necessary solid/liquid equilibria and hydrolysis reactions are now completely known for all oxidation states from III to VI with sufficient accuracy.

The successful elucidation of ternary hydroxo-carbonato complexes and the identification of only very few relevant complexes out of the manifold of possibilities shows the way how to deal with other complexation reactions. Theoretical or semi-empirical approaches could be calibrated by the present results to estimate dominant ternary species for other reactions. The investigations on the complexation of actinides with organic ligands, especially under alkaline conditions was another attempt to improve our understanding on the formation of ternary complexes. These experimental studies were intended directly to provide structural and thermodynamic data for quantum chemistry calculations on the complex formation.

The task on complexation with minor ligands was focused on the phosphate complexation of actinides. Phosphate is an important ligand in natural groundwaters but is also considered in the form of minerals, such as apatite and Th phosphates as a backfield material with strong retardation of radionuclides. However, due to the formation of sparingly low soluble solid phases, the complexation chemistry is poorly known, not only for the tetravalent actinides. As the uncertainty on the aqueous actinide phosphate chemistry solution thwarts partly the benefits of the immobilising properties of phosphate minerals, the envisaged study is considered as an important task. Despite the interesting results obtained within the ACTAF project, it must be admitted that the critical mass in this field was not sufficient to achieve a breakthrough. The same is true for the efforts to elucidate mechanism of redox reactions. As for the phosphate complexation study, important single results including a quantum chemistry calculation have been obtained. As explained above however, the foundations have been laid

within the ACTAF project for a promising endeavour on actinide redox reactions in the near future.

The improvement and application of computational tools for actinides developed rapidly during the ACTAF project time, essential pushed by I. Grenthe and the group of U. Wahlgren at University of Stockholm. Although the computational study was not funded by the EC, the established link with theoretical groups had an important impact on experimentally working researcher, recognising the high potential for future actinide research. Other groups of the ACTAF consortium, entered this field actively already (UPC), have started to build-up a theoretical group (FZK) or plan to enter this field in future time (PSI).

Radionuclide retention by interaction with mineral phase (WP2 and WP3)

Reactions of radionuclides at the mineral/water (WP2) and incorporation of radionuclides in secondary phases (WP2) present the most important retention mechanism. In general the sorption and desorption kinetics at the interface are considered to be fast, whereas the radionuclide forming a solid solution with the mineral phase will only be released if the matrix is dissolved. Thus the latter irreversible process seems to be the favourable case for long-term radionuclide retention. However, it must be noted that the secondary phase could also be formed in colloidal form. These mobile species would transport the radionuclides with the groundwater flow without any retardation. Thus a profound knowledge on the secondary phase formation seems to be indispensable, not only to take advantage of this process for a long-term safety analysis but also to rule out a possible colloidal transport.

Interface reactions of radionuclides are considered to be reversible, thus they will cause a retarded radionuclide transport or in the case of colloids a partially enhanced transport with respect to the groundwater flow. Interface reaction may be the first step for the incorporation of the radionuclide into the secondary phase. Thus from an experimental point of view, the differentiation between both processes may be difficult.

Within the commonly used Kd approach all the various processes with different kinetics are lumped together. For a sound geochemical description it must be distinguished between the various sorption mechanism, such as ionic exchange, specific adsorption, surface precipitation, incorporation etc.. This may be achieved by spectroscopic methods, such as XAFS, which provides additional structural information. TRLFS on sorbed Cm(III) has been proven within the ACTAF project as a versatile tool to perform the differentiation between various mechanism at trace level concentrations.

Specific sorption at functional groups at the interface presents the most common sorption mechanism and is described by a surface complexation model (SCM). Within this project the sorption data of actinides have been quantified with a state-of-the-art SCM, yielding high-quality sorption data.

It should be mentioned however, that presently a variety of SCMs exists, which use different ways to describe the electrostatic field at the interface. This ambiguity makes it difficult to compare results analysed by different approaches or to build up a sorption database. Another problem arises from the unsufficient experimental data often used to parameterise the SMC. Hypothetical surface complexes are introduced to fit the isotherms and pH-edges, without any justification of their existence except the goodness of the fit. This kind of information could be supplied by spectroscopic methods, which allow to study the sample in contact with the aqueous phase and provide sub-monolayer sensitivity, but in general are not available. Within the ACTAF project, XAFS has been applied for the speciation of surface species yielding valuable structural information. The lack in sensitivity was overcome using grazing-incidence measurement on single crystals. The other spectroscopic method used within the ACTAF

project was TRLFS on Cm(III) and U(VI). Except for Fe oxide/hydroxides, which quench the emission, this method has been successfully applied to all studies performed on sorption and solid solution formation.

Especially TRLFS on Cm(III), which has been used before for speciation in aqueous solution at FZK and at only a very few laboratories worldwide, is unique in the periodic table. Its high sensitivity and selectivity makes it a favourite subject, not only to derive sorption data on trivalent actinides, but to test the applicability of the SCM to highly charged metal ions and to validate the various SCMs. This kind of basic study was the objective of the FZK contribution to WP2. Meanwhile the work has been focused on single crystal of sapphire with different orientations studied by various spectroscopic and microscopic methods.

The objective of this approach is to improve our knowledge on interface reactions. It does not mean that all sorption reaction should be studied on the same level. For PA purposes even the SCM approach is probably too complex to be included in numerical codes. Thus an objective of the ACTAF project was to provide simplified sorption models, such as a composite model, which was successfully studied in WP2 by FZR for rocks. However, any simplification of the models must be justified on the base of fundamental understanding of the relevant processes. We have gained much insight into these processes, but many questions are still open and the development of simplified sorption models adapted to the demands by PA will be a future topic.

Good progress in understanding interface reactions, not only for actinides, but in general has been made in the last years. By contrast, the knowledge on the formation of secondary phases and the incorporation of radionuclides is still very poor. Due to the slow kinetics of secondary phase formation generally observed, mechanistic studies on synthetic phases are rare and mostly the leaching behaviour of trace constituents from natural mineral samples has been studied. This approach yield important information on the stability of radionuclide homologues incorporated into the matrix and was used also in the ACTAF project to study solid solution formation of phosphate and other minerals. However, to deduce thermodynamic and kinetic information on the reaction mechanism, calcite was chosen as a model mineral with sufficient fast precipitation and dissolution kinetics, good crystallinity and with favourite spectroscopic properties. Calcite has been subject to many sorption studies with divalent metals, furthermore it also a relevant mineral component of clays and cement corrosion products.

The study on the incorporation of Eu(III)/Cm(III) in calcite was performed in fruitful collaboration between KU, FZR and PSI. Based on precise coprecipitation experiment and TRLFS speciation of Cm(III) indicating the incorporation of two species into the bulk, attempts have been made to model the results. The key issue was to identify the charge compensation mechanism to replace Ca(II) by Cm(III). Even if a final model, consistent with the sorption and spectroscopic results has not been found during the run-time of the ACTAF project, this work presents a breakthrough for our understanding of the incorporation of trivalent metal ions into calcite.

Conclusions

In the broad range of research topics covered by the ACTAF project, many of the ambitious objectives have been achieved. In some areas even breakthroughs have been made. As discussed above, many new important questions have been raised, together with the unsolved problems, this will build the basis for a future research programm. Further it should be noted, that the research structure of the ACTAF project, bringing together research facilities at large institutions with expertise in various field at universities, corresponds to network structure envisaged for actinide sciences within the 5th frame work programme.

7. ANNEX

7.1 List of contact persons of the partner organisations

FZK: Dr. Reinhardt Klenze
Institut für Nukleare Entsorgung
Forschungszentrum Karlsruhe GmbH
P.O. Box 3640
D-76021 Karlsruhe, Germany
Tel.: +49 7247 82 4602; FAX: +49 7247 82 4308; e-mail: klenze@ine.fzk.de

FZR: Dr. Vinzenz Brendler,
Institut für Radiochemie
Forschungszentrum Rossendorf,
P.O.Box 510119,
D-01314 Dresden, Germany
Tel.: +49 351 260 2430; FAX: +49 351 260 3553; e-mail: v.brendler@fz-rossendorf.de

PSI: Dr. Michael Bradbury
Waste Management Laboratory (LES)
Paul Scherrer Institut (PSI)
CH-5232 Villigen, Switzerland
Tel.: +41 56 310 2290; FAX: +41 56 310 2205; e-mail: mike.bradbury@psi.ch

KTH: Prof. Dr. Ingmar Grenthe
Dep. of Inorganic Chemistry
Kungl. Tekniska Högskolan, KTH, (Royal Institute of Technology)
Teknikringen 26
S-10044 Stockholm, Sweden
Tel.: +46 8 7908 144; FAX: +46 8 212 626; e-mail: ingmarg@inorg.kth.se

UPC: Prof. Dr. Jordi Bruno
Universitat Politecnica Catalunya (UPC)
E-08028 Barcelona, Spain
Tel.: +34 93 582 44 10; FAX: +34 93 582 44 12; e-mail: jbruno@quantisci.es

KU: Assoc. Prof. Dr. Susan L.S. Stipp
Geologisk Institut (GI)
Kobenhavn Universitet
Øster Voldgade 10
DK-1350 Copenhagen, Denmark
Tel.: +45 3532 2480; FAX: +45 3532 2499; e-mail: stipp@geo.geol.ku.dk

Enterpris: Prof. Dr. David Read
Enterpris Ltd
Philip Lyle Building
University of Reading
Whiteknights
Reading RG6 6BX, United Kingdom
Tel.: +44 118 986 8250; FAX: +44 118 986 1894; e-mail: enterpri@readinguni.u-net.com

Ciemat: Dr. Tiziana Missana
Centro de Investigaciones Energéticas, Medioambientales y Tecnológicas (Ciemat)
Technicas Geologicas. Edif. 20 a
Ave. Complutense 22
E-28040 Madrid, Spain
Tel.: +34 91 346 6185; FAX: +34 91 346 6185; e-mail: tiziana.missana@ciemat.es

7.2 Glossary

AFM: Atomic Force Microscopy
DDLM: Diffuse Double Layer Model
EXAFS: Extended X-ray Absorption Fine Structure Spectroscopy
LIPAS : Laser-Induced Photoacoustic Spectroscopy
LPAS: Laser-Induced Photoacoustic Spectroscopy
LREE: Light Rare Earth Elements
REE: Rare Earth Elements
SEM: Scanning Electron Microscopy
TEM: Transmission Electron Microscopy
TRLFS: Time-Resolved Laser Fluorescence Spectroscopy
fs-TRLFS: Femtosecond TRLFS
HREE: Heavy Rare Earth Elements
XPS: X-rayPhotoelectron Spectroscopy
XANES: X-Ray Absorption Near Edge Fine Structure Spectroscopy
HRTEM: High Resolution Transmission Electron Microscopy

7.3 List of ACTAF publications

The following list of references cited in the Scientific and Technical Description of this report are related to publications generated within the context of the ACTAF project. The notable high number and quality of the publications are considered as the main part of the scientific deliverables of the ACTAF project. The following list sorted according to the Work Packages includes original conference contributions, reports and peer reviewed publication. Out of the 67 ACTAF publications listed below, 30 original publications, which are indicated by bold citation index have been selected, which represent the main scientific output of the ACTAF project up to now. A compilation of these papers is printed as an Annex to the present Final Report in a separate volume.

Work-package 1: **Thermodynamics of aquatic actinides: Experiments to improve the database of unknown or uncertain data**

[1] Neck, V., Kim, J.I.; Solubility and hydrolysis of tetravalent actinides, Radiochim. Acta **89**, 1-16 (2001).

[2] Neck, V., Kim, J.I.; An electrostatic approach for the prediction of actinide complexation constants with inorganic ligands - application to carbonate complexes, Radiochim. Acta **88**, 815-822 (2000).

[3] Neck, V., Solubility of tetravalent actinides: General trend, specific phenomena and experimental studies with Thorium(IV), Migration '03, 9th Internat.Conf. Gyeongju, ROK, September 21-26, 2003

[4] Neck, V., Müller, R., Bouby, M., Altmaier, M., Rothe, J., Denecke, M.A., Kim, J.I., Solubility of amorphous Th(IV) hydroxide - application of LIBD to determine the solubility product and EXAFS for aqueous speciation, Radiochim. Acta **90**, 485 - 494 (2002).

[5] Rothe J., Denecke, M.A., Neck, V., Müller, R., Kim, J.I.;XAFS investigation of the Structure of Aqueous Th(IV) Species, Colloids, and Solid Th(IV) Oxide/Hydroxide, Inorg. Chem. **41**, 249-258 (2002).

[6] Bitea, C., Müller, R., Neck, V., Walther, C., Kim, J.I.; Study of generation and stability of Th(IV) colloids by LIBD combined with ultrafiltration. Colloids and Surfaces A: Physicochem. Eng. Aspects **217**, 63 - 70 (2003).

[7] Neck, V., Altmaier, M., Müller, R., Bauer, A., Fanghänel, Th., Kim, J.I., Solubility of crystalline thorium dioxide. Radiochim. Acta **91**, 253 - 262 (2003).

[8] Bundschuh, T., Knopp, R., Müller, R., Kim, J.I., Neck, V., Fanghänel, Th; Application of LIBD to the determination of the solubility product of thorium(IV)-colloids. Radiochim. Acta **88**, 625-629 (2000).

[9] Neck, V., Kim, J.I., Seidel, B.S., Marquardt, C., Dardenne, K., Jensen, M.P., Hauser, W.; A spectroscopic study of the hydrolysis, colloid formation and solubility of Np(IV), Radiochim. Acta **89**, 439-446 (2001).

[10] Altmaier, M., Neck, V., Müller, R., Fanghänel, Th.; Solubility and Ternary Hydroxo-Carbonate Complexes of Thorium, Abstract submitted to NRC 6, Aachen (2004)

[11] Moll, H., Geipel, G., Reich, T., Bernhard, G., Fanghänel, Th., Grenthe, I., Uranyl(VI)

complexes with alpha-substituted carboxylic acids in aqueous solution. Radiochim. Acta **91**, 11, (2003 33a

[**12**] Geipel, G., Acker, M., Vulpius, D., Bernhard, G., Nitsche, H., Fanghänel, Th., An Ultrafast Time-Resolved Fluorescence Spectroscopy System for Metal Ion Complexation Studies with Organic Ligands, Spectrochimica Acta A 60 , 417 (2004)

[13] Geipel, G., Bernhard, G., Vulpius, D., Excited state reactions in studies of complex formation between actinides and organic ligands with laser induced methods, Migration '03, 9th Internat.Conf. Gyeongju, ROK, September 21-26, 2003

[14] Geipel, G., Nagasaki, S., Bernhard, G., Complex formation of uranium with 2,5-dihydroxybenzoic acid, Migration '03, 9th Internat.Conf. Gyeongju, ROK, September 21-26, 2003

[15] Brachmann, A., Geipel, G., Bernhard, G., Nitsche, H., Study of uranyl(VI) malonate complexation by time resolved laser-induced fluorescence spectroscopy (TRLFS), Radiochimica Acta, **90**, 147 (2002)

[**16**] Toraishi, T., Grenthe, I., Potentiometric and 1H and 19F NMR studies of the Th(IV) – 5-sulfosalicylate – OH^- - F^- system. J. Chem. Soc. Dalton Trans. **2003**, 1634.

[**17**] Toraishi, T., Farkas, I., Szabó, Z., Grenthe, I., Complexation of Th(IV) and various lanthanides(III) by glycolic acid; potentiometric, ^{13}C NMR and EXAFS studies. J. Chem. Soc. Dalton Trans. **2002**, 3805

[**18**] Stumpf, T., Fanghänel, T., Grenthe, I., Complexation of trivalent actinide and lanthanide ions by glycolic acid: a TRFLS study, J. Chem. Soc. Dalton Trans. **2002**, 3799.

[19] Geipel, G., Bernhard, G., Brendler, V., Complex Formation of Uranium(IV) with Phosphate and Arsenate, in B.-J. Merkel, B. Planer-Friedrich, Chr. Wolkersdorfer (editors), Uranium in the Aquatic Environment, Springer Verlag Berlin, Heidelberg, 2002, p. 373

[20] Szabó, Z., Structure, equilibrium and ligand exchange dynamics in the binary and ternary dioxouranium(VI) – glyphosate – fluoride system. J. Chem. Soc. Dalton Trans. **2002**, 4242.

[21] Geipel, G., Bernhard, G., Rutsch, M., Brendler, V., Nitsche, H., Spectroscopic properties of Uranium(VI) Minerals studied by time-resolved laser-induced Fluorescence Spectroscopy (TRLFS), Radiochimica Acta, **88**, 757 (2000)

[22] Giménez, J., Clarens, F., Casas, I., Rovira, M., de Pablo, J., Bruno, J., Oxygen Consumption in Uranium(IV) Dioxide Dissolution Experiments in Bicarbonate Medium, presented at Migration 01

[23] Bruno, J., Summary of UPC Contribution to the WP 1, ENRESA, Internal Technical Report, March 2002, 11 pages

[24] Clarens, F., de Pablo, J., Díez, I., Casas, I., Giménez, J., Rovira, M., The formation of studtite during the oxidative dissolution of UO_2(s) by hydrogen peroxide. An AFM study. Chem. Geol., accepted

[25] Duro, L., Grivé, M., Bruno, J., de Pablo, J., Hennig, C., Experimental determination of the redox state of uranium in Fe containing solid surfaces by using XAS. Environ. Sci. Tech., submitted

[26] Privalov, T., Schimmelpfennig, B., Wahlgren, U., Grenthe, I., Reduction of Uranyl(VI) by Fe(II) in solutions: An Ab initio study, J. Phys. Chem. A **107**, 587,(2003)

[27] Vallet, V., Wahlgren, U., Schimmelpfennig, B., Moll, H., Szabo, Z., Grenthe, I., Solvent Effects on Uranium(VI) Fluoride and Hydroxide Complexes Studied by EXAFS and Quantum Chemistry, Inorg. Chem., **40**, 3516 (2001)

[28] Toraishi, T., Privalov, T., Wahlgren, U., Grenthe, I., Mechanism of Exchange Reactions, A Quantum Chemical Study of the Reaction $UO_2^{2+}(aq) + HF(aq) \rightleftharpoons UO_2F^+(aq) + H^+(aq)$. J. Phys. Chem. A. **107**, 9456, (2003)

[29] Vallet, V., Wahlgren, U., Szabó, Z., Grenthe, I., Rates and mechanism of fluoride water exchange in $UO_2F_5^{3-}$ and $[UO_2F_4(H_2O)]^{2-}$ studied by NMR spectroscopy and wave function based methods. Inorg. Chem. 41, 5626, (2002)

[30] Vallet, V., Wahlgren, U., Schimmelpfennig, B., Szabó, Z., Grenthe, I., The Mechanism for Water Exchange in $[UO_2(H_2O)_5]^{2+}$ and $[UO_2(oxalate)_2(H_2O)]^{2-}$, as studied by Quantum Chemical Methods, J. Am. Chem. Soc. **123**, 11999, (2001)

[31] Vallet, V., Moll, H., Wahlgren, U., Szabó, Z., Grenthe, I., Structure and Bonding in Solution of Dixouranium(VI) Oxalate Complexes: Isomers and Intramolecular Ligand Exchange. Inorg. Chem. **42**, 1982 (2003)

[**32**] Bolvin, H., Wahlgren, U., Moll, H., Reich, T., Geipel, G., Fanghänel, T., Grenthe, I., On the Structure of Np(VI) and Np(VII) Species in Alkaline Solution Studied by EXAFS and Quantum Chemical Methods, J. Phys. Chem. A, **105**, 11441, (2001)

[**33**] Vallet, V., Wahlgren, U., Grenthe, I., The Chelate Effect and Thermodynamic Data for Metal Complexes in Solution; A Quantum Chemical Study, J. Am. Chem. Soc., **125**, 14941, (2003)

[**34**] Vazquez, J., Bo, C., Poblet, J.M., de Pablo, J., Bruno, J., DFT studies of uranyl acetate, carbonate and malonate complexes in solution, Inorganic Chemistry, **42**, 6136 (2003)

[35] Grenthe, I., Ferri, D., The High Level Radioactive Waste Problem and the Role of Science. Talk given by I. G. at the conference "E. Fermi and Nuclear Energy", Pisa October 15-16, 2001.

[36] Vallet, V., Quantum chemistry: a modeling tool for a better understanding of the chemistry of actinide compounds, Migration '03, 9th Internat.Conf. Gyeongju, ROK, September 21-26, 2003

Work-package 2: **Thermodynamics of solid-water interface reactions (sorption phenomena)**

[**37**] Missana, T., Maffiotte, C., García-Gutierrez, M., Experimental and modelling study of the U(VI) sorption onto goethite, Journal of Colloids and Interface Science, **260**, 291-301 (2003)

[**38**] Missana, T., García-Gutierrez, M., Fernandez, V., U(VI) sorption on colloidal magnetite under anoxic environment: experimental study and surface complexation modelling, Geochimica et Cosmochimica Acta, **67**, 2543-2550 (2003)

[**39**] Missana, T., Maffiotte, C., García-Gutierrez, M., Surface reactions kinetics between nanocrystalline magnetite and uranyl, Journal of Colloids and Interface Science, **261**, 154-160 (2003)

[40] Duro, L., Missana, T., Ripoll, S., Grivé, M., Bruno, J., Modelling of Pu sorption onto the surface of goethite and magnetite as steel corrosion products, E-MRS proceedings "Scientific Bases for nuclear waste management 27", submitted

[41] Bradbury M. H. and Baeyens B., Sorption of Eu on Na- and Ca-montmorillonite: Experimental investigations and modelling with cation exchange and surface complexation, Geochim. Cosmochim. Acta **66**, 2325, (2002)

[42] Bradbury, M. H., Baeyens, B., Modelling titration data and the sorption of Sr(II), Ni(II), Eu(III), Am(III) and U(VI) on Na-illite, PSI Bericht / Nagra NTB, (2003), in preparation

[43] Pierret, M.C., Rabung, Th., Bauer, A., Geckeis, H., Klenze, R., Kim, J.I., Bradbury, M.H., Baeyens, B., Interaction of Cm(III) and Eu(III) with Ca-montmorillonite: surface complexation modeling and spectroscopic studies, Migration '01, 8th Internat.Conf. Bregenz, A, September 16-21, 2001

[**44**] Arnold, T., Zorn, T., Zänker, H., Bernhard, G., Nitsche, H., Sorption Behavior of U(VI) on Phyllite: Experiments and Modeling. J. of Contaminant Hydrology **47**, 219-231 (2001)

[45] Zorn, T., Untersuchungen der Sorption von U(VI) an das Gestein Phyllit zur Bestimmung von Oberflächenkomplexbildungskonstanten. PhD. Thesis, TU Dresden (2000)

[46] Arnold,T., Krawczyk-Bärsch, E., Bernhard, G., Sorption of U(VI) on granite: comparison of experimental and predicted U(VI) sorption data. Annual Report FZR – 343, 21 (2002)

[47] Arnold, T., Geipel, G., Brendler, V., Bernhard, G., Detection of adsorbed U(VI) surface species on muscovite with TRLFS. Annual Report FZR – 373, 15 (2003)

[**48**] Stumpf, Th., Rabung, Th., Klenze, R., Geckeis, H., Kim, J.I., A spectroscopic study of the Cm(III) sorption onto γ-Alumina, J. Colloid Interface Sci. **238**, 219-224, (2001)

[49] Geckeis, H., Rabung, Th., Solid-water interface reactions of polyvalent metal ions at iron oxide/hydroxide surfaces, in Encyclopedia of Surface and Colloid Science" (A. Hubbard, Ed.), Dekker, 2002

[50] Rabung, Th., Geckeis, H., Schild, D., Klenze, R., Fanghänel, Th., Cm(III) sorption onto sapphire single crystals: a time resolved laser fluorescence spectroscopy study, Migration '03, 9th Internat.Conf. Gyeongju, ROK, September 21-26, 2003

[51] Denecke, M.A., Rothe, J., Dardenne, K., Lindqvist-Reis, P., Grazing incidence (GI) XAFS measurements of Hf(IV) and U(VI) sorption onto mineral surfaces, Phys. Chem. Chem. Phys.5, 939 (2003)

[52] Klenze, R., Chung, K.H., Park, K.K., Parviet-Hartmann, P., Lindqvist-Reis, P., Kim, J.I., Incorporation of Eu (III) and Cm(III) in silica studied by time-resolved laser fluorescence spectroscopy, Migration '01, 8th Internat.Conf. Bregenz, A, September 16-21, 2001, Abstracts p.56

Work-package 3: Thermodynamics of secondary phase formation

[53] Stipp S.L.S., Lakstanov L.Z., Christensen J.T., Eu(III) uptake in calcite: A model for actinide retardation by a secondary phase, Goldschmidt Geochemistry Conference, Japan September 2003, Geochimica et Cosmochimica Acta Abstract Volume accepted abstract- talk (2003)

[**54**] Stipp S.L.S., Lakshtanov L.Z., Jensen J.T., Baker J.A., Eu^{3+} uptake by calcite: Preliminary results from coprecipitation experiments and observations with surface sensitive techniques. Journal of Contaminant Hydrology 61, 33-43 (2003)

[**55**] Lakshtanov L.Z., Stipp S.L.S., Experimental study of Europium (III) coprecipitation with calcite, Geochimica et Cosmochimica Acta 68, 819 (2004).

[56] Jensen J.T., Harstad A.O., Waight, T.E. and Stipp S.L.S. Rare Earth Elements in Natural Calcite. EGS-EUG-AGU Geosciences Joint Assembly, Nice, France, 6-11 April 2003 abstract-poster.

[57] Kristensen R., Stipp S.L.S., Refson K., Hedegaard P., Modelling kinks and steps on the calcite cleavage surface, Physical Chemistry, Chemical Physics, to be submitted

[**58**] Stumpf Th., Fanghänel, Th., A Time-Resolved Laser Fluorescence Spectroscopy (TRLFS) Study of the Interaction of Trivalent Actinides (Cm(III)) with Calcite, J. Colloid Interface Sci., **249**, 119-122 (2002)

[59] E. Curti, D.A. Kulik and J. Tits : Solid solutions of trace Eu(III) in calcite : Thermodynamic evaluation of experimental data in a wide range of pH and pCO_2 (submitted to Geochimica et Cosmochimica Acta)

[60] Seco, F., de Pablo, J., Bruno, J., Interactions between Ln(III) elements and hydroapatite. presented at Geochemistry of crustal surfaces, Seefeld, 2002

[61] Read, D., Andreoli, M., Knoper, M. Williams, C.T. and Jarvis, N. (2002). The degradation of monazite: Implications for the mobility of rare earth and actinide elements during low temperature alteration. Eur. J. Mineral, 14, 487-498.

[62] Read, D., Willams, C.T., Degradation of phosphatic waste forme incorporating long-lived radioactive isotopes, Min. Magazine, 65, 589 (2001)

[63] Trueman, E.R., Black, S., Read, D., Characterisation of depleted uranium (DU) from an unfired CHARM-3 penetrator, Scienc. Tot. Environm. (2003), in press

[**64**] Trueman, E., Black, S. Read, D. and Hodson, M. (2003b). Alteration of depleted uranium metal. Geochim. Cosmochim. Acta, **67**, A493.

[65] Trueman, E., Black, S. Read, D. and Hodson, M. (2003c). Alteration of depleted uranium metal. Proc. Int. Conf. "Actinides 2003", Prague, April 2003

[**66**] Tits, J., Stumpf, Th., Rabung, Th., Wieland, E., Fanghänel, Th., Uptake of Cm(III) and Eu(III) by Calcium Silicate Hydrates: A Solution Chemistry and Time-Resolved Laser Fluorescence Spectroscopy (TRLFS) Study. Environ. Sci. Technol., 37, 3568 (2003)

[67] Stumpf, Th., Tits, J., Fanghänel, Th., Uptake of trivalent actinides (Cm(III)) by calcite, calcium silicate hydrates and cement: a time-resolved laser fluorescence spectroscopy (TRLFS) study, Migration '03, 9th Internat.Conf., Gyeongju, ROK, September 21-26, 2003